HARMONIA CA21119

Deliverable 1.5

Photometry from day to night in Europe: solar, lunar and stellar. Historical approach new methods and synergies

Authors: Lionel Doppler[1], Angelos Karanikolas[2], Meritxell Garcia Suñer[3], Veijo Aaltonen[4], África Barreto Velasco[5], Monica Campanelli[6], Thomas Carlund[7], Jan Ebr[8], Victor Estellés[3], , Philippe Golloub[9], Celia Herrero del Barrio[10], Stelios Kazadzis[2], Axel Kreuter[11,12], Mauro Mazzola[13], Jorge Muñiz Rosado[14], Christoph Ritter[15], Roberto Román Diez[10], Carlos Toledano Olmeda[10], Kerstin Stebel[16], Benjamin Torres Rodríguez[9], Stéphane Victori[17], Vito Vitale[13],Frank Wagner[18]

Date: 31 October 2026

[1] Meteorologisches Observatorium Lindenberg - Richard-Aßmann-Observatorium, Deutscher Wetterdienst (MOL-RAO, DWD), Lindenberg (Tauche), Germany

[2] Physikalisch-Meteorologisches Observatorium Davos / World Radiation Center (PMOD/WRC), Davos, Switzerland

[3] Facultat de Física, Universitat de València Estudi General (UVEG), Burjassot (Valencia), Spain

[4] Finnish Meteorological Institute (FMI), Helsinki, Finland

[5] Izaña Atmospheric Research Center, Meteorological State Agency of Spain (IARC-AEMET), Tenerife, Spain

[6] Istituto di Scienze dell'Atmosfera e del Clima, Consiglio Nazionale delle Ricerche (ISAC-CNR), Rome, Italy

[7] Swedish Meteorological and Hydrological Institute (SHMI), Norrköping, Sweden

[8] FZU - Institute of Physics of the Czech Academy of Sciences, Prague

[9] Laboratoire d'Optique Atmosphérique (LOA), Université de Lille-I, Villeneuve d'Ascq (Lille), France

[10] Grupo de Óptica Atmosférica, Universidad de Valladolid (GOA-UVa), Spain.

[11] Department für Physiologie und Medizinische Physik, Medizinische Universität Innsbruck, Innsbruck, Austria

[12] LuftBlick, Innsbruck, Austria

[13] Istituto di Scienze Polari, Consiglio Nazionale delle Ricerche (ISP-CNR), Bologna, Italy

[14] Andalusian Institute for Earth System Research (IISTA-CEAMA), Granada, 18071, Spain

[15] NILU, Kjeller, Norway

[16] Alfred-Wegener-Institut, Helmholtz-Zentrum für Polar- und Meeresforschung (Alfred-Wegener-Institut – AWI), Potsdam, Germany

[17] Cimel Electronique, Paris, France

[18] Meteorologisches Observatorium Hohenpeißenberg, Deutscher Wetterdienst (MOHP-DWD), Hohenpeißenberg, Germany

Table of Content

Table of Content 4

1. Introduction 8

2. From yesterday to today - AOD from day to night: Principles, history, status 9

2.1 AOD retrieval with the sun: Solar photometry 9

2.1.1 Main principles 9

2.1.2 First developments 11

2.1.3 Current state of the art of the main networks 12

2.2 AOD retrieval with the stars: Stellar photometry 14

2.2.1 Main principles 14

2.2.2 Different methods for stellar photometry 16

2.2.3 Current state of the art 21

2.3 AOD retrieval with the moon: lunar photometry 22

2.3.1 Main principles 23

2.3.2 First developments 25

2.3.3 Current state of the art 25

3. From instruments to networks: Developments of techniques and methods 29

3.1. From CIMEL CE318 development to AERONET network 29

3.1.1. The Birth of CIMEL Photometer (CE 318) 29

3.1.2. The birth of AERONET 31

3.2 From PFR to GAW-PFR network 34

3.3 From Prede-POM to SKYNET network 35

4. Development of historical stations in Europe 39

4.1. In Germany instrumental development and stations 39
4.1.1 At Observatory Lindenberg since 1977 39
4.1.2 in Buckow with Carl-Heinz Schulz 47
4.1.3 At DWD Hohenpeißenberg since 1993....49
4.1.4 The "*Zu-Zi Trasse*" (Zugspitze - Zingst Trail) 51
4.1.5 German Polar research about Aerosols: AWI Potsdam and Ny-Ålesund station 55
4.2. In Spain: In Izaña and Valladolid 55
4.2.1 In Izaña at AEMET/IARC observatory 55
4.2.2 At University of Valladolid: The GOA-UVa group....61
4.3. In Switzerland: Davos (PMOD/WRC) and associated stations....63
4.3.1 PMOD/WRC at Davos....63
4.3.2 Station Jungfraujoch (3580 m asl)....64
4.3.3 The world in Davos, HARMONIA and PMOD/WRC....66
4.4. In Italy: From the peninsula to the poles 68
4.4.1 The Genesis of Atmospheric Photometry in Bologna (1970s–1980s)....68
4.4.2 National and International Collaborations (1990s–2010s) 70
4.4.3 Early Antarctic Fieldwork for CNR Bologna and current State at the Institute of Polar Sciences (ISP-CNR) 71
4.4.4 And also in Rome (ISAC-CNR and partners)....72
4.5. In the nordic Europe 74
4.5.1 Photometry in Norway in the past and today: 75
4.5.2 Photometry in Sweden in the past and today: 79
4.5.3 Photometry in Finland in the past and today:....84
4.6. Photometry in France today and in the past:....88
4.6.1. Historical foundations and satellite observations 88
4.6.2. Retrieval methods and polarimetry....89
4.6.3. AERONET and the PHOTONS National Observation Service....89
4.6.4. Calibration, metrology and traceability....91
4.6.5. ACTRIS and photometer-lidar networks 92
4.6.6. Mobile photometry and synergies at sea 92
4.6.7. AGORA-Lab and LOA-CIMEL cooperation....93
4.6.8. Next steps....94
4.7. Photometry in Austria, Pandora and Pandonia network....94

4.7.1 The Innsbruck Atmospheric Observatory (IAO-MUI) 94
4.7.2. Pandora and the Pandonia Global Network (PGN)....95
5. The specificity of Polar regions 96
5.1 Historical approach of AOD retrieval in Polar regions 96
5.1.1 Polar-AOD: Long-term observations and advances in Polar aerosol research 96
5.1.2 Development of the programme and scientific achievements....97
5.2 AOD in Polar regions today 102
5.2.1 Today in the Arctic 102
5.2.2 Spanish contribution....105
5.2.3 The AWIPEV station 106
5.2.4. Italian contribution....107
5.2.5. Norwegian and Swiss contributions....108
5.3 In Antarctica today....108
5.3.1. Spanish contribution....109
5.3.2. Italian contribution....110
5.3.3 Norwegian contribution....112
6. Harmonisation of the different systems: Recent studies on synergies 113
6.1 Synergies and comparisons for lunar and stellar systems 113
6.2 Synergies photometer - ceilometers....116
6.2.1 The GRASP approach 116
6.2.2 CAECENET Study: a photometer - ceilometer synergy....120
6.2.3 Validation of ceilometers with help of Photometers and radiosoundings AOD measurements synergy study: 121
6.3. Synergies Stellar - Lidar: AWIPEV Station at Ny-Ålesund....125
7. From today to tomorrow: Recent innovations in the systems 127
7.1 AOD retrieval from the stars with all-sky cameras 127
7.1.1 Main principles 128
7.1.2 Stations and status....131
7.2 AOD retrieval with wide-field stellar photometry....132

7.2.1 Main principles 133

7.2.2 Stations current status, results, comparisons, validations 135

8. Summary 137

References 139

Table of acronyms 155

Acknowledgements 161

1. Introduction

The quantification of aerosol loading is crucial for two main reasons. First, it is essential for understanding climate evolution, particularly in light of the already dramatic changes in global meteorological conditions caused by climate change. Second, it is important for assessing air quality and air pollution, which are major public-health concerns. Fine aerosols and particulate matter (PM) can seriously damage the human respiratory system.

With regard to the interpretation and quantification of climate change, all reports of the Intergovernmental Panel on Climate Change (IPCC), including the latest report, the Sixth Assessment Report (AR6; IPCC, 2021), point out that the cooling effects of aerosols partly mask the warming of the Earth–atmosphere system caused by the anthropogenic increase in atmospheric greenhouse-gas concentrations, particularly carbon dioxide (CO_2) and methane (CH_4).

The quantification of aerosol loading or concentration in the atmosphere, at both global and local scales, remains a challenging task for the scientific community. One approach—adopted by the scientists and institutions participating in the COST Action HARMONIA—is to focus on the optical properties that govern the absorption and scattering of solar radiation. The main parameter considered is the **Aerosol Optical depth (AOD)**. In general, greater aerosol loading corresponds to a larger AOD, although the relationship between the two is not necessarily proportional. AOD is a column-integrated optical property of atmospheric aerosols. It can be retrieved using remote-sensing techniques based on measurements of solar irradiance at specific wavelengths. These measurements account for the attenuation of radiation as it passes through the atmosphere, as described by the Beer–Bouguer–Lambert law. The total optical depth (TOD) of the atmosphere at the measurement site is first determined (here, “total” refers to the combined contribution of all atmospheric constituents to the optical depth). The AOD is then derived as the aerosol contribution to the TOD. The radiometers used for this type of AOD remote sensing are called **photometers**. The retrieval of aerosol optical and radiative properties—such as AOD—using photometers is the focus of COST Action HARMONIA. At present, aerosol optical depth (AOD) and other aerosol optical and radiative properties are retrieved during the daytime from measurements of direct solar and diffuse-sky radiation conducted by photometer networks worldwide. The principal networks are AERONET, SKYNET, and GAW-PFR. At night, some photometers can retrieve AOD from measurements of lunar or stellar radiation. One of the principal objectives of COST Action HARMONIA is to harmonise the different networks, advance instrumentation and retrieval methods, and promote synergies with other types of instrumentation. Working Group (WG) 1 of COST Action HARMONIA focuses on improving retrieval methods. WG 2 has similar, and in some cases overlapping, objectives, but focuses more specifically on improving aerosol products and instrumentation, including calibration procedures.

In November 2024, WG 2 published Deliverable D2.2 (Campanelli, Estellés et al., 2024), which addresses improvements in the quality of solar, lunar, and stellar photometry. The present report

can be considered a complement to Deliverable D2.2. Whereas D2.2 focuses primarily on improving measurement techniques (focused on the European contribution), particularly calibration, as well as on low-cost instrumentation and synergies with airborne and other radiation measurements for analysing aerosol effects, this deliverable explains the main principles of solar, stellar and lunar photometry, give historical indications and explain the current state of them (part 2). Part 3 traces the development of the observing networks and their main instruments. Part 4 takes the reader on a journey across Europe and through time, focusing on notable sites, stations, companies, and institutions. Part 5 highlights AOD measurements in the polar regions. Part 6 presents selected applications that combine stellar, lunar, and other observational techniques. Finally, Part 7 examines novel approaches to nighttime AOD remote sensing.

2. From yesterday to today - AOD from day to night: Principles, history, status

This part presents the main principles of photometry, beginning with solar photometry (section 2.1), followed by stellar photometry (section 2.2), and concluding with lunar photometry (section 2.3). It outlines the underlying physical principles, traces the history of these methods and techniques back to their origins, and concludes with an overview of the current state of the art in each of the three areas.

2.1 AOD retrieval with the sun: Solar photometry

2.1.1 Main principles

The basic principles of photometry are clearly presented by Toledano et al. (2023) in Chapter 7 of the Elsevier book “Field Measurements for Passive Environmental Remote Sensing”. In this section of the deliverable, we summarise only the main principles.
Photometry is based on the Beer–Lambert–Bouguer law (Equation E2.1), which describes, at a given wavelength (λ), the attenuation of solar irradiance as it passes through the atmosphere, from the top of the atmosphere ($I_0(\lambda)$) to the surface ($I(\lambda)$), as illustrated in Figure 2.1.1,

$$I(\lambda) = I_0(\lambda) \times e^{-m\tau} \quad , \qquad \text{(E2.1)}$$

where (I) is the direct solar irradiance on the ground at a particular wavelength λ, (I_0) the direct solar irradiance at the top of the atmosphere at the same wavelength (extraterrestrial irradiance), (m) the optical airmass (a general approximation of the airmass is the geometric optical airmass:

m ≈ m_{geom} = 1/cos(SZA) with SZA the Solar Zenith Angle), and (τ) the total optical depth (TOD) of the atmosphere. TOD is the sum of all individual optical depths of each atmospheric component (gases and aerosols, absorption and scattering).



Figure 2.1.1: Principles of solar photometry, for a solar beam at the wavelength (λ), when the Sun is at a given solar zenith angle (SZA)

We can express the Beer-Lambert-Bouguer law in a logarithm form replacing (τ) with (TOD):

$$TOD = [\ln(I_0) - \ln(I)] / m \ . \qquad (E2.2)$$

Equation (E2.2) demonstrates that if we know the extraterrestrial irradiance (I_0), and measure the irradiance (I) with the filter radiometer, and calculate the airmass (m), then we can consequently retrieve the total optical depth (TOD).

There are two methods for estimating the ratio (I/I_0):

1) The first method involves measuring precisely the absolute value of the irradiance (I) with a well-calibrated radiometer and using the very precise tabulated value of the extraterrestrial irradiance (I_0). This approach is used for AOD retrieval from spectroradiometer measurements, and explained in detail in deliverable D1.4 (Karanikolas et al., 2026).
2) The second method used for photometers (filter radiometers) does not require measuring the absolute value of the irradiance (I) in $W \cdot m^{-2}$. Instead, it is sufficient to have a stable instrument and take the raw signal of the radiation measurement (we name it (V), since

the raw signal is typically a voltage), provided that the relative value of the solar radiation that the instrument would measure if placed at the top of the atmosphere is known. This hypothetical extraterrestrial raw signal is denoted as (V_0). The technique to retrieve (V_0), called the Langley Plot calibration, is detailed in part 2. Of deliverable D1.3 (Doppler et al., 2026). Shaw (2007) and Toledano et al. (2018; 2023) also present a good discussion about Langley Plot calibration.

Focusing on the second method, the Equation (E2.2) would be (for non spectroradiometer photometers):

$$TOD = [\ln(V_0) - \ln(V)] / m \quad . \qquad \text{(E2.3)}$$

Deliverable D1.3 (Doppler et al., 2026) detailed how to extract the AOD from the TOD. We obtain the following equation (In deliverable D1.3 it is the equation E2.7 in the beginning of part 2):

$$\begin{aligned} AOD = (m_{TOD} \times TOD - m_{Ray} \times CoeffRay(\lambda) \times P - \\ m_{O3} \times CoeffO3(\lambda) \times O3DU - \\ m_{No2} \times CoeffNO2(\lambda) \times NO2DU\ ) / m_{aer} \ . \end{aligned} \qquad \text{(E2.4)}$$

Equation (E2.4) involves, in addition to TOD (obtained with radiation measurement, Beer-Lambert-Bouguer and calibration information), eleven coefficients or parameters:

- Five airmasses coefficients (m_{aer}, m_{TOD}, m_{Ray}, m_{o3}, m_{NO2})
- Three coefficients of molecular scattering or gas absorption (CoeffRay(λ), CoeffO3(λ), CoeffNO2(λ))
- Three quantities of atmospheric components (P, O3DU, NO2DU)

These eleven coefficients or parameters are defined or obtained differently. The definition of them are explained in the following reference papers or manuals:

- For AERONET, ($AOD_{AERONET}$) in Giles et al. (2019).
- For CÆLIS, (AOD_{CAELIS}) in González et al. (2020).
- For GAW-PFR, (AOD_{PFR}) in Wehrli (2009).
- For SKYNET, (AOD_{SKYNET}) in Nakajima et al. (2020).

2.1.2 First developments

The most comprehensive account of the origins of photometry is Shaw (2007), “Genesis of Sun Photometry.” In brief, photometry began with Pierre Bouguer’s *Essai d’optique sur la gradation de la lumière* (1729) and Johann Heinrich Lambert’s *Photometria* (1760). Later, in 1852, August Beer described the exponential attenuation of light through an absorbing medium, laying the groundwork for the concepts of optical depth and exponential attenuation. In recognition of these three contributions, the fundamental relationship is known as the Bouguer–Lambert–Beer law (Equation E2.1).

In the United States, Samuel Pierpont Langley (1834–1906) observed that atmospheric attenuation varies with wavelength. He developed the bolometer and made measurements at high-altitude sites. By measuring solar radiation at different solar elevations, he demonstrated the

logarithmic dependence of measured radiation on air mass. The later calibration method based on this relationship became known as the “Langley Plot method” (Shaw, 2007; Toledano et al., 2018; 2023).

In the twentieth century, solar-irradiance measurements, spectral analyses of solar radiation, and studies of atmospheric turbidity were advanced in Sweden by members of the Ångström family. Anders Jonas Ångström (1814–1874) contributed to the study of the solar spectrum; his son Knut Johan Ångström (1857–1910) conducted irradiance measurements and developed pyrheliometers; and Knut Johan’s son, Anders Knutsson Ångström (1888–1981), studied atmospheric turbidity. Their work (Ångström, 1929; Ångström, 1961, 1970) extended the theoretical approaches of Bouguer, Lambert, and Beer, as well as Langley’s measurement methods. By then, the theoretical foundations, equations, and measurement methods of photometry had been established. The next challenge was technological: to develop a “narrow band pyrheliometer” (an oxymoron: pyrheliometer are designed to be as wide band as possible to capture the whole solar energy) with a spectral band as narrow as possible, so that the Bouguer–Lambert–Beer law would apply to the measured solar radiations.

The first instruments of this kind were developed in the United States in the early 1970s. Glenn Edmond Shaw, John Reagan, and Ben Herman developed a multiwavelength filter radiometer at the Institute of Atmospheric Physics, University of Arizona (Shaw et al., 1973; Shaw, 1983). In Europe, the first photometers appeared toward the end of the 1970s. One example was the East German–Soviet INTERKOSMOS programme (Leiterer and Weller, 1985, 1988), which led to the development of the BAS, ABAS and ROBAS photometers in Lindenberg (section 4.1.1).
Fully automatic photometers with performance comparable to that of today’s instruments first appeared in the late 1980s, with the first Prede POM prototypes (section 3.1.3). In the early 1990s, the SP1A photometer developed by *Dr. Schulz und Partner* followed (sections 4.1.1 and 4.2.2). The first operational CIMEL CE318 photometers were developed around 1991–1992 (section 3.1.1). Finally, the PMOD/WRC Precision Filter Radiometer (PFR) was introduced in the mid-1990s (sections 3.1.2 and 3.2.3).
The development of the networks followed a different timeline. AERONET (Aerosol Robotic Network), which uses CIMEL instruments, officially began on 15 May 1993 (section 3.1.1). The GAW-PFR (Global Atmosphere Watch - Precision Filter Radiometer) network was established in 1996, alongside the founding of the World Optical Depth Research and Calibration Center (WORCC) (section 3.1.2). SKYNET (Sky Measurements Network), which uses Prede instruments, came later: Following a milestone meeting in Granada in 2003, SKYNET was officially launched in Tokyo in 2006 (section 3.1.3).

2.1.3 Current state of the art of the main networks

AERONET status

AERONET (Aerosol Robotic Network) acquires direct-beam solar radiation measurements at eight wavelengths, ranging from 340 to 1640 nm. The current solar aerosol optical depth (AOD)

dataset includes observations from approximately 500 active stations—defined as stations that have reported data within the past six months (see the map in Figure 2.1.2). The AERONET solar AOD product is available in Version 3; equations, methods and parameters are described by Giles et al. (2019). Three data quality levels are available: Level 1.0, Level 1.5, which uses more stringent cloud screening, and Level 2.0. Level 2.0 data are available only for measurement days up to the most recent calibration and use different calibration values (V_0); (section 2.1.1) from those used for Levels 1.0 and 1.5.



Figure 2.1.2: Global distribution of active AERONET stations for solar AOD Level 1.5. © AERONET Website: https://aeronet.gsfc.nasa.gov/new_web/draw_map_display_aod_v3.html

GAW-PFR status

GAW-PFR (Global Atmosphere Watch - Precision Filter Radiometer) acquires direct-beam solar radiation measurements at four wavelengths, ranging from 368 to 862 nm. The current solar aerosol optical depth (AOD) dataset includes observations at about 12 core sites away from local and regional pollution sources and additionally 14 associated stations (see the map in figure 3.2.1). The equations used for GAW-PFR AOD retrievals are listed in Wehrli (2009).

SKYNET status

SKYNET (Sky Measurements Network) acquires direct-beam solar radiation measurements at eleven wavelengths, ranging from 315 to 2200 nm. The current solar aerosol optical depth (AOD) dataset includes observations at about 100 stations worldwide and 16 stations for the regional subnetwork -the European SKYNET Radiometers network (ESR)-; see the maps in figures 3.3.3 and 3.3.4. The equations used for SKYNET AOD retrievals are listed in Nakajima (2020).

2.2 AOD retrieval with the stars: Stellar photometry

2.2.1 Main principles

Stellar photometry requires a telescope because the stars whose radiation is measured appear as point sources from Earth, with angular diameters below 0.01°; by comparison, the Sun and Moon each subtend about 0.5°. Unlike a photometer, which can be installed in an all-weather enclosure, a telescope requires a dome for protection from the weather. An operator must coordinate dome opening with the telescope's azimuth and select suitable target stars. Each site has a pool of approximately 8–20 candidate stars; if the preferred targets are poorly positioned for observation, another must be selected. Figure 2.2.1 shows the dome, operator, and telescope infrastructure at the DWD Lindenberg station.

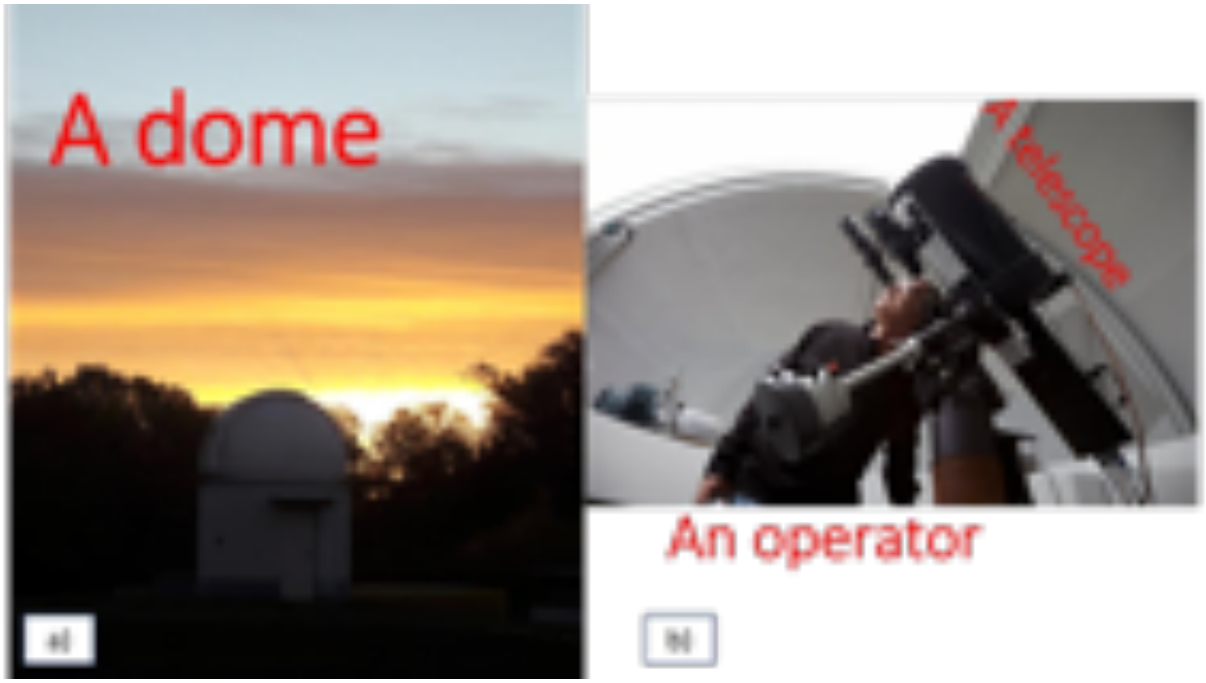


Figure 2.2.1: Stellar Photometer SPST at DWD Lindenberg a) The dome from outside; b) the dome with DWD technician André Knöfel (DWD) setting the telescope of DWD stellar photometer SPST7.

As demonstrated in Leiterer et al. (1995), the principles of stellar photometry do not differ from those of solar photometry (section 2.1). The key difference is that, for stellar photometry, the "photometer" refers to the combined telescope–radiometer system (Figure 2.2.1). In addition, stellar photometry traditionally uses stellar magnitudes -(M) and (M_0)- rather than irradiances -(I) and (I_0)-. Figure 2.2.2 adapts Figure 2.1.1, which illustrates solar photometry, for stellar photometry.

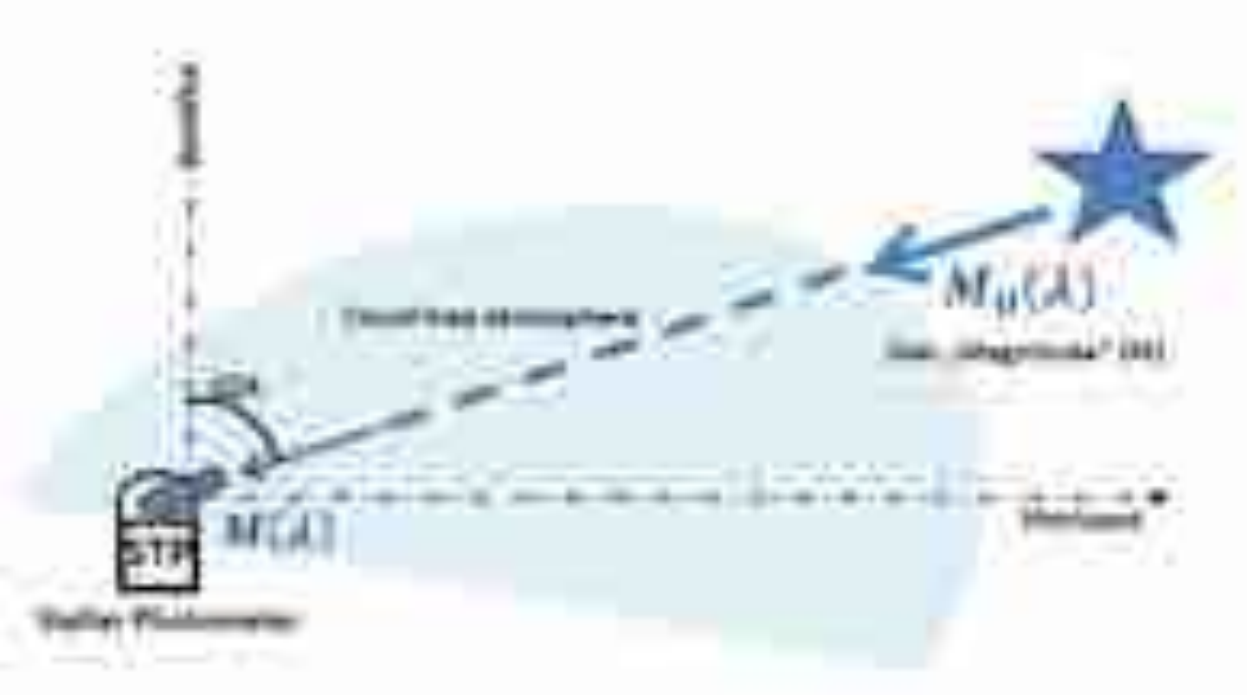


Figure 2.2.2: Principles of stellar photometry, for a stellar beam at the wavelength (λ), when the star is at a given solar zenith angle (SZA).

The Beer-Lambert-Bouguer law (E2.1) becomes, for stellar photometry:

$$M(\lambda) = M_0(\lambda) \times e^{-m\tau} \quad , \qquad \text{(E2.5)}$$

where (M) is the magnitude of the star as measured on the ground at a particular wavelength λ, (M_0) the extraterrestrial magnitude of the star at the top of the atmosphere (well tabulated), (m) the optical airmass ($m \approx m_{geom} = 1/\cos(SZA)$ with SZA is the Star Zenith Angle) and (τ) the total optical depth (TOD) of the atmosphere.

The very simple formulation of TOD of equation (E2.2) is now:

$$TOD = [\ln(M_0) - \ln(M)] / m \; . \qquad \text{(E2.6)}$$

Following the photometry method, we consider the raw signal of the measurement (we name it (U)), and must find through a calibration procedure the relative value of the star magnitude that the instrument would measure if placed at the top of the atmosphere. This hypothetical extraterrestrial raw signal is denoted as (U_0). The technique to retrieve (U_0) depends on the stellar photometer type and will be explained in section 2.2.2. Note that the calibration value (U_0) is only valid for the star with which the calibration has been realised. We need therefore to calibrate the stellar photometer with all the stars we want to use for photometry and build a catalog of calibration values ($U_{0,1}$, $U_{0,2}$, $U_{0,3}$, $U_{0,4}$, …) for each star (1, 2, 3, 4, …).

The total optical depth formulation depending on the measured raw signal in equation (E2.3) for solar photometry is, for stellar photometry:

$$TOD = [\ln(U_0) - \ln(U)] / m \; , \qquad \text{(E2.7)}$$

and the formula that relates (AOD) to (TOD) is the same as (E.2.4):

$$AOD = (m_{TOD} \times TOD - m_{Ray} \times CoeffRay(\lambda) \times P - m_{O3} \times CoeffO3(\lambda) \times O3DU - m_{No2} \times CoeffNO2(\lambda) \times NO2DU) / m_{aer} \quad \text{(E2.8)}$$

2.2.2 Different methods for stellar photometry

Stellar photometers are of different types. The most used in the world (four stations of five) is the stellar photometer of the German company *Dr. Schulz und Partner* (section 4.1.2) and the principles and method of calibrations and measurements are developed here (subsection 2.2.2.1). An alternative stellar photometer is EXCALIBUR of the University of Granada. It is presented in subsection 2.2.2.2.

2.2.2.1 The SPST method (*Schulz und Partner* photometer)

Schulz und Partner Sternphotometers (SPST) are instruments developed by *Dr. Schulz und Partner GmbH* in Buckow (Beeskow), Germany (section 4.1.2). Leiterer et al. (1995) describe their basic operating principle.

The SPST can measure total optical depth (TOD) and, from it, retrieve aerosol optical depth (AOD) with equation (E2.8).

To obtain the (TOD) there are two methods possible: The One-Star Method (OSM), which assumes that the system is calibrated for the observed star; and the Two-Star Method (TSM), which estimates the calibration values for the two observed stars while simultaneously retrieving the optical depth. Figure 2.2.3 illustrates the principles of these two techniques, with the TSM shown on the left and the OSM on the right.

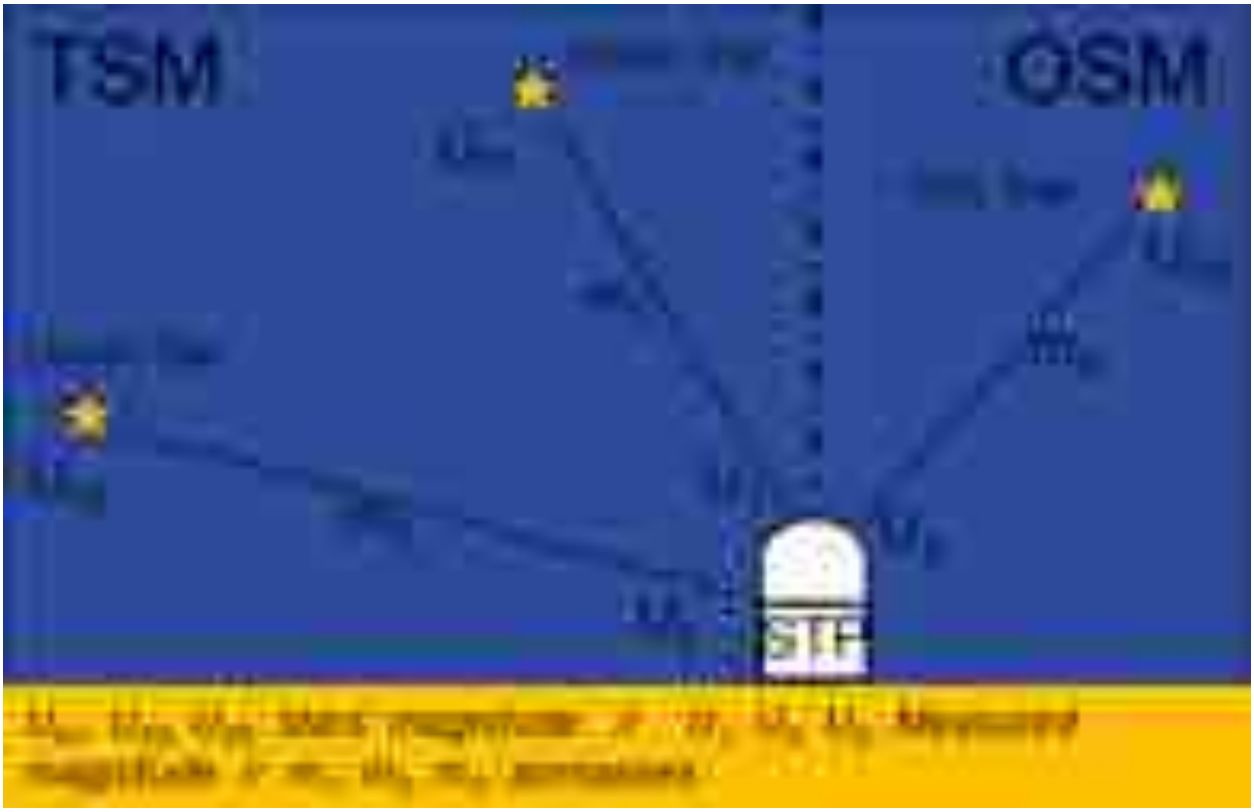


Figure 2.2.3: Principles of measurements with *Schulz und Partner* stellar photometers: TSM (Two Stars Method) and OSM (One Star Method) methods.

The One Star Method (OSM)

The OSM is the classical photometry method. We already have a calibration value (U_{0S}) for the star S and can apply equations (E.2.7) to retrieve the total optical depth (TOD):

$$TOD = [\ln(U_{0S}) - \ln(U_S)] / m_S \qquad \text{(E2.9)}$$

… and then retrieve AOD with (E.2.8).

The challenge here is to have the knowledge of the calibration values (U_{0S}) for the star S. The classical Langley Plot method of solar photometry (Shaw, 2007; Toledano, 2018; 2023) usually does not work, since the excursion of the stars in airmass is much slower than for the Sun, especially in the Polar areas where the stellar photometry is usually used. An alternative is to use the Two Stars Method (TSM) to obtain the calibration values (U_{0S}).

The Two Stars Method (TSM)

For the TSM, we adapt the photometry equations (E2.9) to $\log_{10}$ (this is because of the definition of the magnitudes and their unit; details in Leiterer et al., 1995 and Ivanescu et al. 2021) to each star:

$$U_s = U_{0S} + \alpha \times m_S \quad , \qquad \text{(E2.10)}$$

with α = TOD / 1.086 (1.086 comes from the $\log_{10}$ conversion: $2.5/\ln(10) \simeq 1.086$). (U_{0S}) is the star's extraterrestrial magnitude as would be measured by our instrument outside of the

atmosphere. We name it Star Extraterrestrial Magnitude Instrumental (SEMI): $U_{0S} \equiv SEMI_S$. Notice that the SEMI differs from the “absolute” (an oxymoron for a magnitude that is an attenuated logarithmic parameter) Star Extraterrestrial Magnitude (SEM).
We have precise tabulated values of the SEM of the stars we use taken from the catalog of Pulkovo observatory Sankt Petersburg (Alekseeva et al. 1996).
For a star S, we have the relation between SEM and SEMI:

$$SEMI_S = SEM_S + C_S \ , \qquad \text{(E2.11)}$$

with (C_S) the correction factor of the instrument. This correction factor is not star dependent as long as the wideness of the spectral channel is narrow enough to apply the monochromatic approximation. Then, we have (C), a common correction factor for every star: $C_S = C$.
(E2.10) can be expressed:

$$U_s = SEM_S + C + \alpha \times m_S \qquad \text{(E2.12)}$$

We make (U_s) measurements for two stars: an upper star (1) and a lower star (2). The atmospheric total optical depth (TOD) should be the same for both stars. This requires

(1) a spatially homogeneous atmosphere

(2) similar azimuth angles for the two stars

(3) bright stars (because we have low signals with the stars in comparison to the Sun and we need the best signal/noise ratio as possible) that have a large magnitude.

(E2.12) applied to these two stars gives two equations, but with the same α = TOD / 1.086 (hypothesis of spatial homogeneity of the optical depth):

$$U_1 = SEM_1 + C + \alpha \times m_1 \quad \text{and} \quad U_2 = SEM_2 + C + \alpha \times m_2 \qquad \text{(E2.13)}$$

(U_1) and (U_2) are measured successively. The time between the two measurements should be short, since the optical depth is not supposed to change. For TSM measurements we choose stable nights in order that a time gap up to 5 minutes stays acceptable. For practical reasons (moving the telescope, adjusting the star pointing and focusing with the telescope) it is not possible to be faster than two minutes between low and high star measurement.
We can combine the two equations of (E2.13) and extract the (TOD):

$$\mathbf{TOD = \alpha / 1.086 = 1/1.086 \times [(U_1 - U_2) - (SEM_1 - SEM_2)] / (m_1 - m_2)} \qquad \mathbf{(E2.14)}$$

With (U_1) and (U_2) measured by the stellar photometer; (SEM_1) and (SEM_2) known from the catalogue; and the airmasses (m_1) and (m_2) computed with the star zenith angles (SZA).
Note that the larger is ($m_1 - m_2$), the most precise is the TOD retrieval. Therefore we look at a high elevation star for the upper star (1) and a low elevation star for the lower star (2).
Using equations of (E2.13) and (E2.14), we can compute the calibration parameter (C) and therefore the SEMIs ($SEMI_1$) and ($SEMI_2$) of the stars (1) and (2), which are calibration values (U_{0S}) of both stars involved in the TSM measurements. Then, we can proceed with stellar photometry by using the One Star Method (OSM) with these two stars.

The TSM method is very powerful because we obtain the calibration values for the stars. But since we need a stable atmosphere, for every day monitoring of the AOD, we prefer using the OSM. Nevertheless, every night with a stable atmosphere, the TSM should be used to calibrate the instrument for as many stars as possible.

2.2.2.2 Method for Granada stellar photometer EXCALIBUR

The EXCALIBUR (EXtinction CAmera and LumInance BackgroUnd Register, Astronomica S.L.) star photometer was developed to perform continuous measurements of AOD at nighttime by observing the light emitted by stars. Unlike earlier designs based on semiconductor photon counters, EXCALIBUR used a CCD camera as a detector. The instrument consists of a Celestron CGE 1100 telescope based on a Schmidt–Cassegrain optical system, a filter wheel, and an SBIG ST-8XME CCD camera. The filter wheel was equipped with seven narrow-band filters centered at 380, 436, 500, 670, 880, 940, and 1020 nm, with full widths at half maximum (FWHM) ranging from 7.66 to 11.23 nm (see Figure 2.2.4). This configuration enables stellar irradiance measurements at different wavelengths, supporting the characterization of atmospheric aerosol properties.

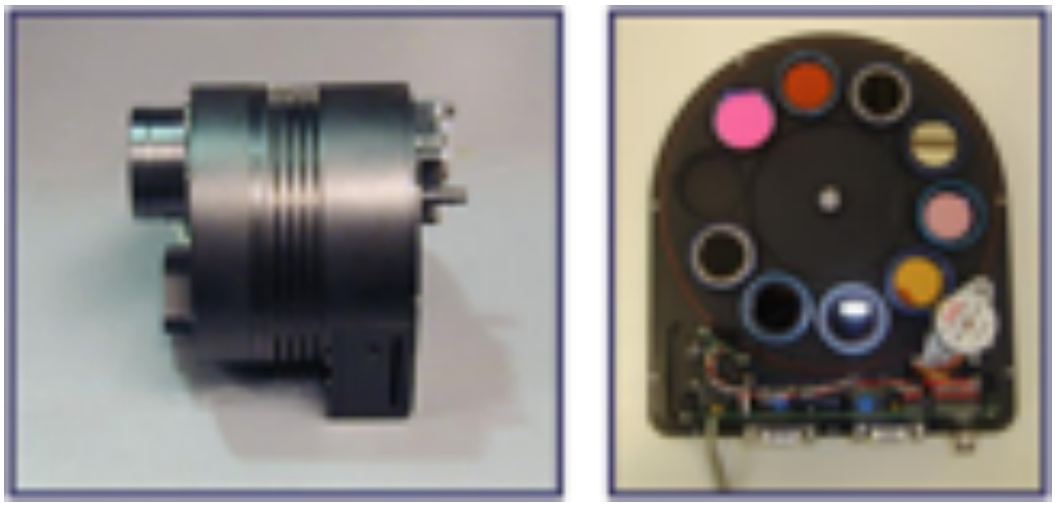


Figure 2.2.4: EXCALIBUR star photometer CCD sensor (left) and filter wheel (right).

The system also incorporated an external wide-field CCD camera, aligned with the telescope, which uses a centering routine to ensure that the target star remains within the field of view of the main detector. To ensure the reliability and accuracy of the photometric measurements, several sources of instrumental error were corrected. These include background signal subtraction using a median-pixel technique, dark current and electronic bias correction through exposures acquired with the shutter closed at different exposure times and temperatures, and pixel-to-pixel sensitivity variations corrected using the flat-field procedure. Appropriate focusing and selection of the CCD sub-frame were also essential to ensure that the stellar signal was accurately recorded. EXCALIBUR was periodically calibrated in the facilities of the German-Spanish Astronomical Centre at Calar Alto.

The instrument design and its operating principles are described in detail by Pérez-Ramírez et al. (2008a,b; 2011, 2012). The instrument has been operating in Granada (Spain) since 2006 within

a dome to protect the system from outdoor conditions (see Figure 2.2.5). It has also been operating during field campaigns in other locations such as in Izaña (Spain) as shown in Figure 2.2.6 (Barreto et al., 2019). This instrument has been used for comparison between star and moon photometry (Barreto et al., 2016, 2019; Román et al., 2020). This instrument has not been operational since the late 2010s.



Figure 2.2.5: EXCALIBUR star photometer operating in Granada (Spain) in the rooftop of the "Instituto Interuniversitario de Inv. del Sistema Tierra en Andalucía (IIsta)" . This instrument belongs to the Group of Atmospheric Physics of the University of Granada (GFAT-UGR).



Figure 2.2.6: EXCALIBUR star photometer operating in the Observatory during the first multi-instrument nocturnal intercomparison campaign in Izaña (Spain) in 2017.

2.2.3 Current state of the art

Stellar photometry request bulky infrastructure like a dome (for the non mobile systems) and manpower: For the mobile systems as EXCALIBUR can be used (like in the Izaña campaign, see Figure 2.2.6) the instrument must be transported outside before every measurements sequence and setted up. For the non transportable systems like SPST systems, manpower present during the night of measurement is desired especially for the Two Star Method in order to supervise the movements of the system from one star to the other.
These are restrictions and this explains why only four stations worldwide and one mobile instrument (EXACALIBUR of university of Granada) has been setted up and operating in the last 25 years:

- **Lindenberg** (Tauche), Germany, operated by DWD
- **Ny-Ålesund**, Spitsbergen (Svalbard), operated by AWI
- **Sherbrooke** (Quebec), Canada, operated by University of Sherbrooke.
- **Eureka** (Nunavut) in the Canadian Arctic, operated by University of Sherbrooke and PEARL (Polar Environment Atmospheric Research Laboratory) institute.

These four stations use an SPST system of *Dr. Schulz und Partner*. The station Sherbrooke has two systems operating. This makes six stellar photometers worldwide: five non mobile SPST systems and EXCALIBUR.

Because of technical problems, EXCALIBUR is not operated anymore for more than seven years, and Lindenberg since 2022. Therefore, there are currently only three active stations worldwide, as shown on the map of Figure 2.2.7.

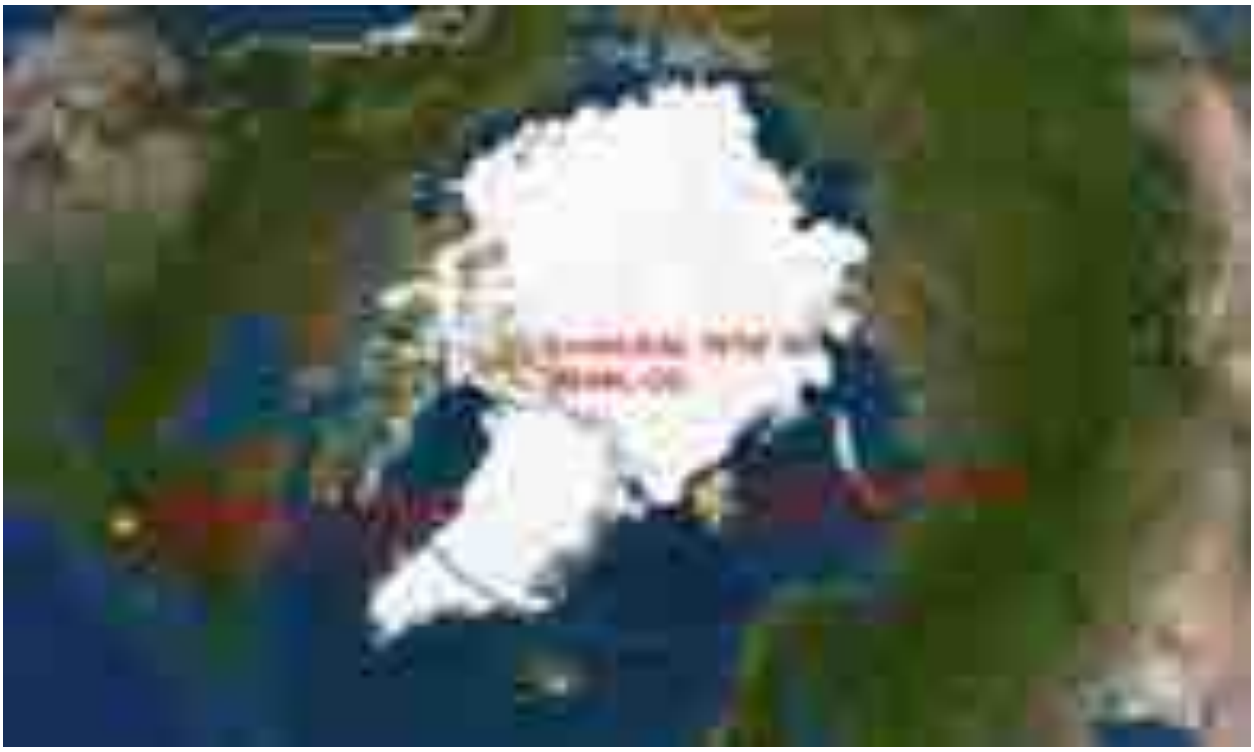


Figure 2.2.7: Localisation of the three current active star photometer stations worldwide; © presentation of Liviu Ivanescu, 2020 (in this time: University of Sherbrooke)

Although the stellar photometers discussed in this section are becoming less common (their main manufacturer, *Dr. Schulz und Partner*, ceased operations in the late 2010s) stellar photometry still has a future, thanks to alternative techniques. In Part 7, we will discuss how all-sky cameras can be used for stellar photometry at night (section 7.1), and how astronomers use wide-field telescopes to retrieve AOD (section 7.2).

2.3 AOD retrieval with the moon: lunar photometry

The Moon is a celestial body of remarkable scientific interest. Our celestial neighbour has no atmosphere, which greatly simplifies both its observation and its modelling. It is not self-luminous: it reflects solar radiation according to the Earth-Sun-Moon geometry at the time of observation, and its reflectance is not Lambertian but anisotropic, depending on the observation geometry. These properties make it an attractive calibration surface. Its reflectance changes very little over time, its background radiance is practically negligible, its spectral behaviour varies only weakly, and most Earth Observation Systems can observe it under a similar geometry every month, which makes it well suited to post-launch calibration. It also has drawbacks: its brightness covers only

a fraction of the dynamic range of most sensors, its libration introduces periodic changes in the visible surface, and its surface is uneven, with maria and highlands of different reflectance.
The most relevant consequence of all this is that a lunar irradiance model is needed to account for these periodic changes in illumination. Because the Moon's reflectance and, consequently, its irradiance vary over months and years, these variations can only be modelled reliably if a sufficiently precise and extensive series of measurements is available, including the longer cycles such as lunar libration and nodal line oscillation. Observation itself is also constrained: lunar measurements require the Sun to lie well below the horizon to avoid solar contamination, and the lunar phase angle further limits usable data to roughly half of each month, typically 12–14 days (Schafer et al., 2026). At high latitudes the problem is related to the seasonal alternation of continuous day and night, which leaves almost no overlap between solar and lunar observations.

2.3.1 Main principles

The principles are similar to those of solar photometry. Because the Moon's apparent angular diameter as seen from Earth is about 0.5°, similar to the Sun's, the same photometer can be used to observe both. Solar photometers can therefore be adapted for lunar photometry; only the electronics need to be sufficiently sensitive to measure a signal approximately 20,000 times weaker without excessive noise. Thus, the principles of lunar photometry are the same as those of solar photometry (see Figure 2.3.1 and Figure 2.1.1, respectively). The main challenge is estimating the lunar extraterrestrial irradiance, which serves as the calibration parameter for lunar photometry. This is difficult because the Moon is not a primary source of radiation; it reflects sunlight instead.

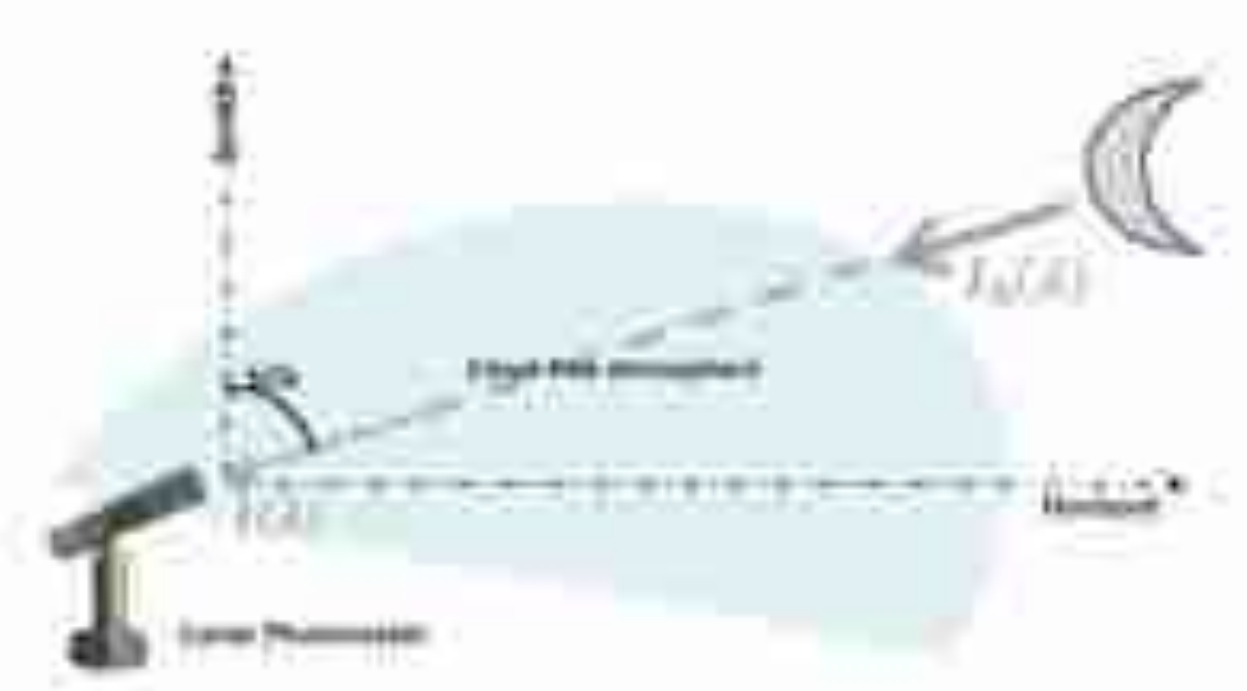


Figure 2.3.1: Principles of lunar photometry. For a lunar beam at the wavelength (λ) when the star is at a given solar zenith angle (SZA)

The lunar reflectance poses a serious calibration problem: The Moon's reflected signal varies strongly with phase angle, and the Robotic Lunar Observatory (ROLO) model, the standard reference for lunar irradiance, was developed for radiometric monitoring rather than for absolute calibration. Kieffer and Stone (2005) established the widely used ROLO formulation, but its limitations became apparent once it was applied to aerosol retrieval.

Román et al. (2020) took the next step. They used RIMO, an open implementation of ROLO, and compared the resulting AOD with the expected values for 98 pristine, stable nights at Izaña. The discrepancies were attributed to the irradiance model and expressed as a RIMO correction factor (RCF) that depends on lunar phase angle. The RCF ranged from 1.01 to 1.14, indicating that RIMO underestimated the extraterrestrial lunar irradiance (Román et al., 2020). In parallel, Uchiyama et al. (2019) modified a Prede POM-02 sky radiometer for lunar measurements and found a similar underestimation of the ROLO reflectance. They modelled the correction as a quadratic function of the absolute phase angle, which reproduced the reflectance within about 1% in most channels. Both studies showed that phase-dependent corrections could make lunar aerosol retrievals usable, but each relied on its own calibration and reference data.

The satellite community had a parallel motivation. Lunar observations are a valuable stable reference for on-orbit calibration of Earth observation sensors, and ROLO was designed for that purpose. Its stated uncertainty of 5–10% was too large for absolute calibration (Stone and Kieffer, 2004; Stone et al., 2020). This created a strong incentive to develop a more accurate, SI-traceable model. The Lunar Irradiance Model of ESA (LIME) is one response to that need. It was built from about 590 nightly observations acquired between 2018 and 2022 with a traceable CIMEL radiometer, and it targets an expanded uncertainty below 2%. Its results indicate irradiances 3–5% higher than ROLO in the visible and near-infrared (Toledano et al., 2024). Since the aerosol community relies on the same lunar irradiance models, improvements driven by satellite calibration requirements have also benefited nocturnal aerosol retrieval.

AERONET began distributing lunar AOD data in the mid-2010s, but for several years the product was labelled provisional and was not quality assured. Schafer et al. (2026) describe the updated dataset, which applies an empirical ROLO correction derived from paired solar and lunar Langley calibrations at Mauna Loa and Izaña. The dataset covers 492 sites with records dating back to 2014. Comparisons between day and night AOD across 3 h transition periods showed mean differences typically within ±0.01 at 440 nm, and statistically negligible differences at all common wavelengths under low and stable aerosol conditions. These results support the use of the lunar AOD product as a quality-assured dataset.

2.3.2 First developments

Berkoff et al. (2011) provided a proof of concept using a small-aperture automated photometer, showing that aerosol optical depth could be retrieved at night from lunar measurements. This work was extended by Barreto et al. (2013), who introduced the Lunar-Langley Method, an absolute calibration approach that adapts Langley plots to the Moon's changing illumination. Barreto et al. (2016) then described the CIMEL CE318-T "triple" photometer, a major instrumental advance that measures the Sun, the Moon and the sky with a single instrument. Its Sun-Moon gain factor method transfers established solar calibrations to the lunar mode. Prede also developed sky radiometers capable of lunar observations, such as the POM-02 modified by Uchiyama et al. (2019) for nocturnal aerosol optical depth retrieval.

Subsequent studies identified systematic errors in these retrievals. Barreto et al. (2017) compared lunar and extrapolated solar aerosol optical depth on 59 stable, low-aerosol days and found that the discrepancies depended on the Moon's phase. They attributed these errors to limitations of the ROLO model. A multi-instrument intercomparison campaign by Barreto et al. (2019) confirmed moon-phase-dependent errors for several CIMEL photometers and a LunarPFR, but not for a stellar photometer, which does not depend on a lunar irradiance model. Román et al. (2020) addressed this problem by deriving a phase-angle-dependent correction factor for RIMO, an open-source implementation of ROLO, using 98 pristine nights at Izaña Observatory. Lunar aerosol optical depth computed with this correction agreed well with independent star photometer measurements.

These developments led to the empirical correction applied in the current AERONET lunar aerosol optical depth product. Its bias correction is derived from paired solar and lunar Langley calibrations, which are used to compute a lookup table of ROLO correction factors as a function of lunar phase angle (Schafer et al., 2026). With this correction, day and night aerosol optical depth at 440 nm agree within ± 0.01 at sites with more than a decade of data, supporting the use of lunar photometry for continuous nocturnal aerosol monitoring.

2.3.3 Current state of the art

State of the art Lunar AERONET

AERONET has been acquiring direct-beam lunar measurements at six wavelengths, from 440 to 1640 nm, since the introduction of the latest-generation CIMEL CE318-T photometers into the network (Schafer et al., 2026). The current lunar AOD dataset includes observations from 492 sites, with records dating back to 2014.



Figure 2.3.2: Global distribution of active AERONET stations. © AERONET Website: https://aeronet.gsfc.nasa.gov/new_web/draw_map_display_aod_v3.html

The main change in the current operational AERONET lunar product is its treatment of the lunar irradiance. Earlier lunar AOD calculations relied directly on the ROLO model, which often produced unphysical results, including large negative AOD values during low-aerosol periods. The current dataset applies an updated empirical correction to ROLO, derived from a large set of paired solar and lunar Langley calibrations acquired at Mauna Loa and Izaña. The correction is tabulated as a function of lunar phase angle, using a LOESS-based lookup table with 0.8° resolution for each wavelength (Schafer et al., 2026). This approach is conceptually related to the phase-dependent corrections proposed by Román et al. (2020) and Uchiyama et al. (2019), but it is derived from the AERONET calibration network rather than from a single instrument or site.

Quality control has also been adapted to the lunar measurement. The lunar sequence does not include the cross-scan aureole measurement used during solar operation to detect thin cirrus through the curvature test. The effect of omitting this test has been assessed by comparing solar AOD with and without it: the monthly differences are small, with 97 % of individual monthly means differing by less than 0.01 in AOD (Schafer et al., 2026). Lunar retrievals also apply a minimum signal threshold, which imposes an upper limit on measurable AOD. For lunar observations this limit is about 2–3 times lower than for solar observations, so short-wavelength channels lose more high-AOD data. Some sites exclude more than 8 % of Level 2 lunar measurements at 440 nm (Schafer et al., 2026).

Validation of AERONET lunar product is based mainly on day–night comparisons within 3 h transition windows at sites where aerosol conditions are low and stable. Mean differences are typically within ±0.01 at 440 nm, and differences at all common wavelengths are statistically

negligible under those conditions. Schafer et al. (2026) describe the resulting dataset as Level 2, AERONET's highest quality level.

State of the art Lunar SKYNET

The paper by Uchiyama et al. (2019), means the public birth of Prede's sun-sky-moon photometry. The sun-sky photometer POM-02 described in section 3.3, with wavelengths ranging from 315 to 2200 nm, was modified for lunar photometry by adapting its optical attenuation and detector settings to the much weaker lunar signal. A new 4-quadrant sun sensor for the active tracking of the moon was designed. A highly innovative calibration approach was also developed to transfer the well-characterized solar calibration to lunar observations, accounting for the variable lunar irradiance and the Sun–Moon–Earth geometry.

After 2019, the POM-01 model, with wavelengths ranging from 315/340 to 1020 nm, was also adapted for lunar observations. Today, a small network of Prede POM sun-sky-moon photometers is active within European SKYNET radiometers network (ESR), as shown on Figure 2.3.3, although it is not accessible at current date due to a recent cyberattack.The automatic procedure for retrieving aerosol optical depth and precipitable water vapour from nocturnal measurements is currently being restored, and will be further developed thanks to new studies and advances achieved in recent years.



Figure 2.3.3: Orange: Operative sites (Rome Sapienza, Rome Tor Vergata, Izaña, Zingst, Svalbard); Violet: Campaigns (Davos); Red: future installation (Valencia, already available at the time of reporting)

3. From instruments to networks: Developments of techniques and methods

In this part we relate the genesis of the three main AOD networks and their instrument: AERONET and the CIMEL CE 318 (section 3.1), GAW-PFR and the PFR instrument (section 3.2) and SKYNET and the Prede POM and POM-02 instruments (section 3.3).

3.1. From CIMEL CE318 development to AERONET network

3.1.1. The Birth of CIMEL Photometer (CE 318)

A Short Story for a Big Purpose: From Jean-Pierre Buis and CIMEL to the birth of AERONET!

The story of the CIMEL CE318 photometer does not begin with a NASA procurement programme or with the creation of AERONET. It begins with people: In the late 1980s, Didier Tanré (white shirt on the picture of Figure 3.3.1), from the Laboratoire d'Optique Atmosphérique (LOA) in Lille, was working closely with Brent Holben (picture of the right of Figure 3.1.2) at NASA Goddard Space Flight Center (GSFC). At the same time, Didier knew Jean-Pierre Buis, Scientific Director at CIMEL Électronique. The three men shared a common scientific problem: aerosol observations needed to move from occasional, manually operated measurements towards reliable, automatic and standardized observations that could eventually be deployed around the world. And, according to the story told by Didier Tanré and confirmed by Brent Holben, the decisive moment was rather less formal than one might imagine. During a meeting in France (around a good French meal) Didier Tanré and Brent Holben discussed the need for a new generation of automatic sun photometers. Didier knew that Jean-Pierre Buis at CIMEL had the engineering expertise required to build such an instrument. The idea was essentially: *Why don't we build an automatic, robotic sun photometer?* And, Jean-Pierre Buis (left picture of Figure 3.1.2) agreed to take up the challenge. That informal commitment became the starting point for what would eventually become the **CIMEL CE318**, and, more broadly, for the instrumental foundation of AERONET… The first prototypes (Figure 3.1.1) were ready in less than three months according to the legend!



Figure 3.1.1: First prototype of the CIMEL CE318 photometer.

A fourth man should not be forgotten, Marius Canini (left picture of Figure 3.1.2), very well known for his Romanian humour and for his high skills to deal simultaneously with electronics card, firmware design and M. Buis on the phone.

From an instrument to a measurement system

The objective was quite ambitious for the time. The instrument had to operate autonomously in the field, point accurately at the Sun and the sky, measure several wavelengths, survive outdoor conditions and provide measurements suitable for quantitative aerosol research. But the concept went beyond measuring direct solar radiation. The combination of direct-Sun measurements and angular sky-radiance measurements made it possible to retrieve not only aerosol optical thickness, but also information on aerosol particle size and other microphysical properties. CIMEL's expertise in precision opto-mechanical instrumentation, combined with LOA's atmospheric-radiation expertise and NASA's requirements for large-scale observations, led to the development of the first generations of the CIMEL automatic Sun–Sky photometer. The early CE318 therefore embodied a rather unusual combination: French engineering + atmospheric optics + NASA Earth-observation science!

The first operational instruments were developed around **1991–1992**, and the CE318 subsequently became the standard instrument of the emerging AERONET: AOD and aerosol properties measurements network using CIMEL CE-318 photometer) network.

A seminal early paper is the work by Holben, Eck, Slutsker, Tanré, Buis et al. (1994), *"Multi-band automatic sun and sky scanning radiometer system for measurement of aerosols."* Jean-Pierre Buis is explicitly among the authors, illustrating how closely the CIMEL engineering development was connected to the scientific definition of the instrument.

3.1.2. The birth of AERONET

The instrument was only one part of the story. Brent Holben and his colleagues at NASA recognized that a global aerosol observing system required something more than a collection of instruments. Measurements had to be standardized, calibrated and processed in a consistent way. This led to the creation of the **Aerosol Robotic Network (AERONET)**. AERONET officially dates its beginning to **15 May 1993**. The network was established by NASA and LOA-PHOTONS (CNRS) and subsequently expanded through a large federation of international partners. The original objective was to establish a long-term, standardized global database of aerosol observations that could serve several purposes:

- characterization of aerosol optical and microphysical properties;
- validation of satellite aerosol products;
- support for atmospheric and climate research;
- near-real-time aerosol monitoring;
- integration with other atmospheric datasets.

The CE318 was particularly well suited to this task because it could operate automatically and acquire measurements according to a standardized protocol.

The network philosophy was therefore built around much more than the instrument itself:

standardized instruments → standardized calibration → standardized measurements → standardized processing → standardized data distribution.

This standardization became one of the fundamental strengths of AERONET.

The first years of AERONET

The early 1990s were a period of rapid development. The NASA team was simultaneously preparing the scientific basis for the next generation of Earth-observing satellites, while aerosol observations were becoming increasingly important for understanding atmospheric radiative effects and for validating satellite retrievals. Brent Holben's 2024 (Holben, 2024) presentation, *“AERONET: Thirty Years of Observations and Research”*, recalls this period with characteristic humour, describing the years around **1988–1992** as the “fertile fields of GSFC” and the emergence of the AERONET community as a mixture of scientific expertise, field campaigns, instruments and, occasionally, rather improvised circumstances. The first years brought together a remarkable group of scientists and engineers. Among them were Didier Tanré, Brent Holben, Jean-Pierre Buis, Tom Eck, Alexander Smirnov, Oleg Dubovik and many others. By 1998, AERONET had already reached approximately 100 instruments, according to Holben's historical presentation. The publication of **Holben et al. (1998)** was a major milestone. The paper formalized the AERONET concept as a federated instrument network and data archive for aerosol characterization. Importantly, the network imposed common standards for:

- calibration;
- measurement protocols;
- data processing;
- data distribution;

- near-real-time acquisition.

These elements are explicitly identified by Holben as the core of the AERONET standardization philosophy.



Figure 3.1.2: (From left to right) First picture: Marius Canini and Jean-Pierre Buis, around 2000;

Second Picture: Brent Holben, Oleg Dubovik and Michael King, around 2000.

From CE318 measurements to aerosol microphysics

The CE318 measurements became even more scientifically powerful with the development of sophisticated inversion algorithms. The work of Oleg Dubovik and Michael King (on the right on Figure 3.1.2) **Dubovik and King (2000)** provided a flexible inversion framework for retrieving aerosol optical properties from combined Sun and sky radiance measurements. This was a crucial step: the CE318 was no longer simply an instrument producing aerosol optical depth. Its measurements could be transformed into information on:

- aerosol particle size distribution;
- refractive index;
- single-scattering properties;
- aerosol optical properties.

The combination of CIMEL hardware, AERONET standardization and aerosol inversion algorithms therefore created a complete observing system.

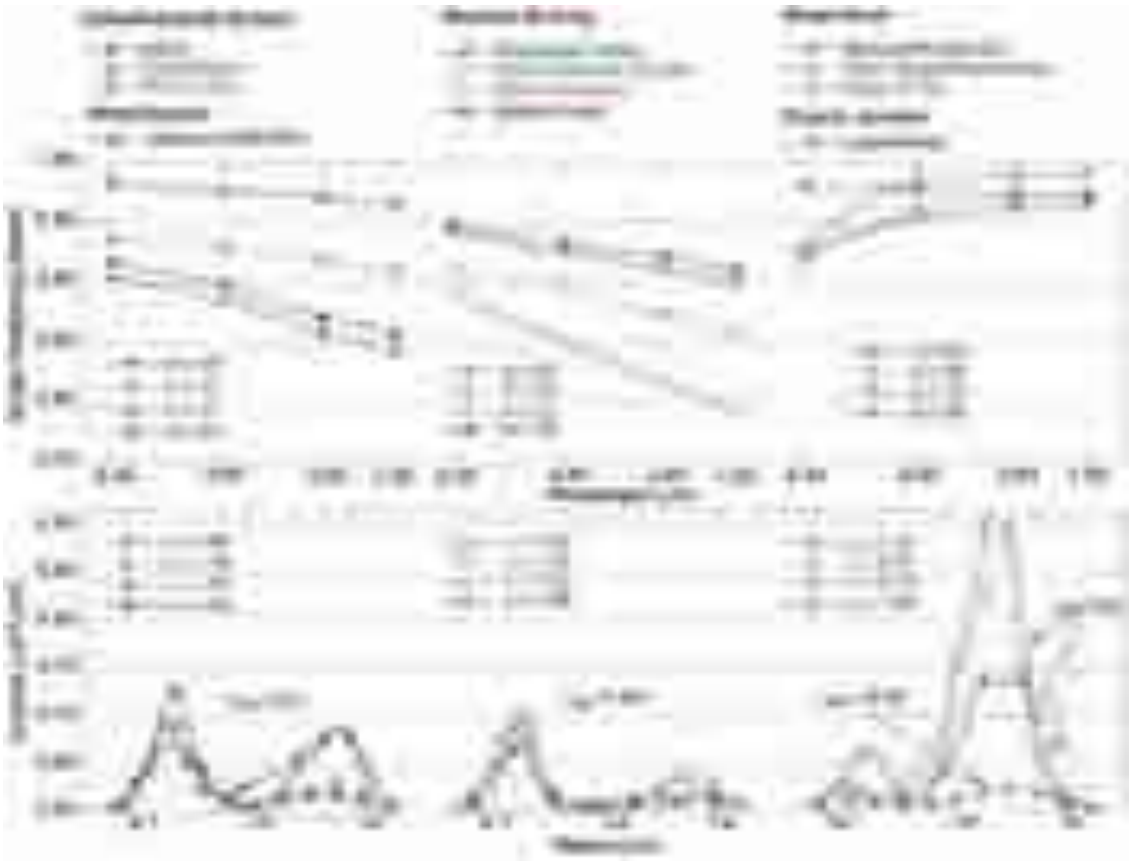


Figure 3.1.3: Main figure of the paper: Dubovik et al. 2002.

From a French dinner to a global network

There is a certain irony in the history. What would eventually become a global network with thousands of publications, hundreds of measurement sites and decades of continuous observations began with a relatively simple idea discussed by a small group of scientists and engineers?

A French scientist — Didier Tanré — knew a NASA scientist — Brent Holben. Didier knew an engineer and scientific director at CIMEL — Jean-Pierre Buis. They needed an automatic robotic photometer. They discussed it over a good meal in France…Jean-Pierre Buis and CIMEL built it… And the instrument that emerged from this collaboration became the **CIMEL CE318**, the principal measurement platform on which AERONET was built.

Thirty years later, Holben's presentation (Holbe, 2024) records AERONET as having measurements from approximately **500 sites in more than 90 countries and territories**, with more than **7,000 scientific citations**!

In that sense, the history of AERONET is also, in part, the history of the CE318…Or, perhaps more accurately: **AERONET and the CE318 grew together.**

3.2 From PFR to GAW-PFR network

The World Meteorological Organization (WMO) instigated the Global Atmosphere Watch (GAW) program in 1989 as a successor to the Background Air Pollution Monitoring Network (BAPMoN). In 1993 (WMO, 1993) it was recommended that AOD measurements, conducted previously under BAPMoN, should be discontinued until new instruments, methods and protocols could be established to collect AOD data of known and assured quality. Based on a recommendation by GAW experts, the World Optical Depth Research Calibration Center (WORCC) was established in 1996 at the PMOD/WRC in Switzerland. WORCC has since been advised by the GAW Scientific Advisory Group for Aerosols.

The World Optical Depth Research Calibration Center (WORCC) was established in 1996 at the Physikalisch Meteorologisches Observatorium Davos World Radiation Center (PMOD-WRC). The GAW-PFR network (Wehrli, 2005) was initiated within PMOD-WRC for global and long-term atmospheric aerosol monitoring and accurate detection of trends. Aerosol data series measured at 12 core sites away from local and regional pollution sources that are representative of atmospheric background conditions in different climates and environments of the planet, in addition to another 20 associated stations, are included in this global network (Kazadzis et al., 2018a). For this reason, GAW-PFR uses the PFR, an instrument measuring direct normal irradiance every minute in four narrow channels centred at 368, 412, 500 and 862 nm. PFR is hermetically sealed and temperature-stabilised, designing it to be an accurate and reliable instrument regarding its absolute response stability over time, which ensure the long-term stability of AOD measurements required for trend detection (Wehrli, 2005; Wehrli, 2008, Cuevas et al., 2019).

The GAW-PFR was specifically designed by WORCC for this goal following the technical specifications defined by the World Meteorological Organization (WMO, 2003, 2016). In 2006, the Commission for Instruments and Methods of Observation (CIMO) of the WMO (WMO, 2007) recommended that the WORCC at the PMOD-WRC should be designated as the primary WMO Reference Centre for AOD measurements (WMO, 2005).



Figure 3.2.1: Overview of the GAW-PFR network. Missing as associated stations (blue points) on the map: Valladolid (Spain) and OHP (France) since the ACTRIS cooperation.

3.3 From Prede-POM to SKYNET network

Despite the wide belief of the separate histories of AERONET and SKYNET, the two networks share a common root. The following account is based on a personal communication from Prof. Teruyuki Nakajima.

In the early 1980s, the first prototype of a skyradiometer, called the “Aureolemeter”, was developed at Tohoku University. A fully automated version was subsequently constructed in the mid-1980s by the Prede company (Nakajima et al., 1986), whose name is already mentioned in that paper. The origin of the acronym “**POM**” is rather anecdotal. According to Prof. Nakajima, it derives from a pronunciation misunderstanding by Prede’s president, Mr. Kazu Sasamoto, who referred to the instrument as the “**Prede *Oreole* Meter**”, whereas the correct English expression should have been “Prede Aureole Meter”. Between 1987 and 1990, through a collaboration among T. Nakajima, Y. Kaufman and D. Tanré at NASA Goddard Space Flight Center, the idea of establishing a network based on skyradiometer observations was developed. After Prof. Nakajima returned to Japan, the SKYNET network was further developed in collaboration with Prof. T. Takamura, supported by significant funding from the JAXA GLI satellite mission project (Takamura et al., 2004) and from the UNEP/ABC project led by V. Ramanathan in East Asia (Nakajima et al., 2007). The first generation of aerosol retrieval products was developed using the prototype of the *Skyrad* package (Nakajima et al., 1983, 1986, 1996). In 1993, Prof. Nakajima invited Dr. Oleg Dubovik to the University of Tokyo. A few years later, Dubovik joined NASA Goddard Space Flight Center, where his inversion code was introduced as the “second-generation” software for AERONET data analysis. For a short period, the *Skyrad* inversion was also available on the AERONET website, before the two development paths eventually diverged.



Figure 3.3.1: A picture of Kyoto Aerosol Workshop in 1999. First row from left to right: Teruyuki Nakajima, Jim Hansen, Daniel Rosenfeld, Yoram Kaufman, Takashi Nakajima, Didier Tanré (white shirt), at 3rd of the 2nd raw, Oleg Dubovik at 3rd of the 4th raw, Brent Holben center of the 4th raw.

The first International SKYNET Committee meeting and the **SKYNET kick-off** meeting were held during the APRS Symposium in Kanazawa, Japan, from **July 31 to August 2, 2006**. Another important step took place in 2003, when the first meeting of European users of the *Skyrad.pack* software and Prede-POM skyradiometers was held at the University of Granada, hosted by Prof. Francisco José Olmo Reyes and Prof. Lucas Alados Arboledas. The meeting brought together the first core group of what would later become the European SKYNET network: Monica Campanelli (ISAC-CNR, Italy), Víctor Estellés (University of Valencia, Spain), and Tim Smyth (Plymouth Marine Laboratory, UK).



Figure 3.3.2: A picture of attendants to the first meeting of European users of Skyrad at Granada (2003). Young Monica Campanelli, Victor Estellés and Tim Smyth surround Bruno Olivieri, with black beard.

During this meeting, experiences with the instruments and the software were exchanged, laying the foundations for a collaboration among the European users. This collaboration gradually evolved into a coordinated European network and, in 2010, the European Skynet Radiometers Network was formally established, after a postdoctoral stay of V. Estellés at PML (UK) hosted by T. Smyth. Nowadays, Skynet consists of more than 100 sites worldwide located, most of them distributed in NE Asia, and it is organized in seven regional sub-networks, whose representatives are part of the International SKYNET committee that is the decision-making body of the network. Each sub-network contributes for operating and maintaining the associated instrumentation. Some sub-networks have Regional SKYNET Data Center (RSDC) to accumulate data measured in the sub-network. Each SKYNET participant belongs to one of the seven sub-networks. The raw data are transferred from each RSDC to the International SKYNET Data Center (ISDC). The ISDC produces standard products on aerosol optical properties using the standard algorithms approved by the International committee and provides products via web. Each RSDC produces new research products, using also algorithms regionally developed. The European SKYNET radiometers network (ESR) is one of the RSDC.

More information on the SKYNET structure, data policy and data download is available at https://www.skynet-isdc.org/index.php.



Figure 3.3.3: The international SKYNET network distribution in 2026.



Figure 3.3.4: The ESR regional subnetwork in 2026.

4. Development of historical stations in Europe

History is also geography. European photometry is no exception. We continue our journey through time by focusing on places of particular significance to European photometry: stations that began their measurements very early; sites notable for their scientific interest or isolation, such as mountain summits and polar regions; and institutions that have developed instruments, organised networks, calibrated instruments across the continent, or coordinated measurement campaigns.

There are many other fascinating stories to tell. No report—even one 150 pages long—can cover everyone. So, dear colleagues, if your institution is not mentioned, or dear reader, if your country is not represented, please do not take it amiss. This does not mean that your institution or country has not contributed to European photometry. Get in touch, and together we can continue this wonderful family album beyond HARMONIA.

4.1. In Germany instrumental development and stations

4.1.1 At Observatory Lindenberg since 1977

First steps in an extinct country

The story of photometry at observatory Lindenberg (52.21 N, 14.12 E, 121 m) began in a country that has today disappeared, under a different institutional affiliation from the one we know today and the name of a different observatory: the "A*erologisches Observatorium des Meteorologischen Dienstes der Deutschen Demokratischen Republik (DDR)*" ("Aerological Observatory of the Meteorological Service of the German Democratic Republik (GDR)"): At the Observatory Lindenberg (founded in 1905 by Richard Aßmann, one of the fathers of balloon carried meteorological measurements and aerology), in Tauche in the North-East German Region of Brandenburg, aerosol optical depth (AOD) has been investigated using photometric techniques since 1977. **Continuous and unbroken daytime AOD measurements have been conducted since 11 February 1986** (Figure 4.1.5, Beker et al., 2021) using solar spectrophotometers and sunphotometers. Nighttime AOD retrievals began in 1992 using stellar photometry, and continuous lunar-photometric observations have been performed at Lindenberg since 2015.
The first developments started in 1977 with the BAS (*Boden-Atmosphäre Spektralfotometer*: Earth - Atmosphere Spectrophotometer) spectrophotometers within the (East) German– Russian (USSR) INTERKOSMOS programme (Leiterer and Weller, 1985 & 1988). The spectrophotometer shown in Figure 4.1.1 is one of the oldest instruments of its kind worldwide. It was operated manually and covered the spectral range from 380 to 1120 nm in 40 steps, each with a bandwidth of 10–15 nm. The instrument was used for measuring nadir radiance during airborne observations, hemispherical irradiance, and airborne albedo.

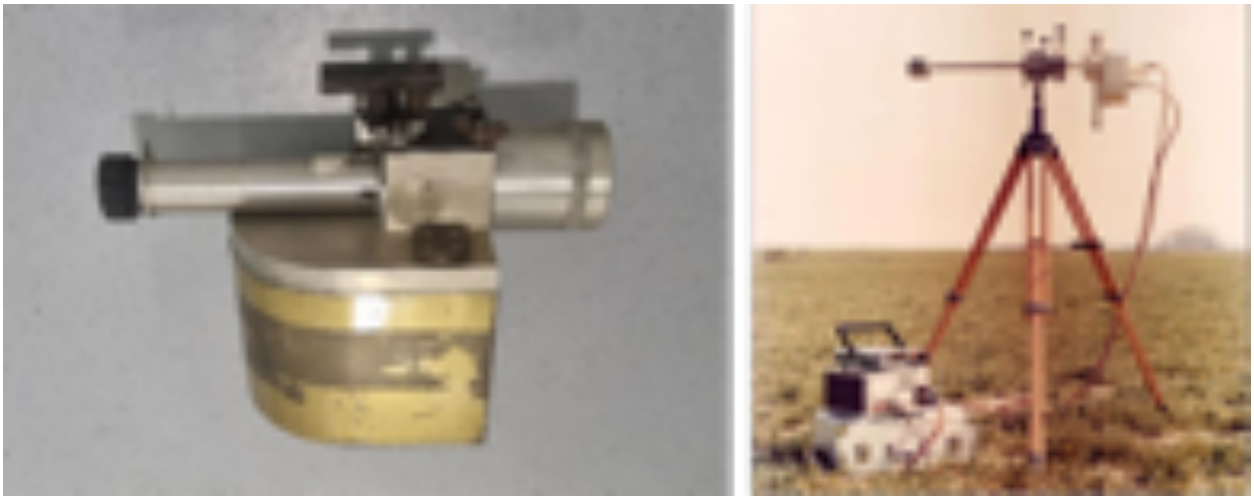


Figure 4.1.1: Left: BAS spectrophotometer developed at Observatory Lindenberg in INTERKOSMOS program. Right: ABAS instrument operating measurement on a tripod

Spectral optical-depth measurements were performed using transmission measurements and Beer–Lambert–Bouguer retrievals based on direct-sun photometric observations. These measurements enabled AOD retrievals at several wavelengths. Real-time data processing of AOD began in 1983. In 1986, continuous daily ground-based AOD monitoring began at the Lindenberg Observatory using the ABAS instrument (Figures 4.1.1 and 4.1.6), an automatic version of BAS. The Lindenberg continuous AOD record is the world's longest daily AOD time series obtained using photometric techniques. The BAS/ABAS instruments were subsequently improved and developed into an automated version called ROBAS (*Robotic Boden-Atmosphäre-Spektralfotometer*, or Robotical Earth–Atmosphere Spectrophotometer). This instrument can perform measurements and automatically track the sun without manual intervention. ROBAS is also equipped with a dome that protects it from inclement weather and frost (see Figure 4.1.2). Continuous AOD monitoring with ROBAS at Lindenberg began in 1987.



Figure 4.1.2: Dome of the ROBAS spectrophotometer on the radiation platform of Meteorological Observatory Lindenberg (DWD).

In 1989, the local story of Lindenberg was swept up in world history: the Berlin Wall fell on 9 November. On 3 October 1990, Germany was reunified. The German Democratic Republic (DDR) ceased to exist and was incorporated into the Federal Republic of Germany (*Bundesrepublik Deutschland*, BRD). The *Meteorologischer Dienst der DDR* was absorbed into the West German *Deutscher Wetterdienst* (DWD), bringing major structural changes. Lindenberg was renamed the *Meteorologisches Observatorium Lindenberg* (MOL) and became part of the DWD. Half of its staff had to leave the observatory. Among them was Karl-Heinz Schulz (Figure 4.1.9), a leading expert in photometry and one of the developers of the BAS, ABAS, and ROBAS photometers. He left the observatory and founded his own photometer-manufacturing company, *Dr. Schulz und. Partner Gmbh* (section 4.1.2)

The nineties: Integration into the DWD and the beginning of stellar photometry

From this point on, photometers from Lindenberg were no longer manufactured at the observatory but by *Dr. Schulz und Partner GmbH*. This marked the beginning of the SP* series (*Schulz und Partner*), including solar photometers: the SPH/SP2H instruments, developed by Karl-Heinz Schulz at the observatory in 1987 and later manufactured by *Schulz und Partner*, followed by the SP1A, introduced in 1994 and produced for

many years, into the 2010s. Partner GmbH (section 4.1.4)... But also stellar photometers (Figure 4.1.3), which ushered in a new era of photometric measurements: nighttime AOD measurements!



Figure 4.1.3: Starphotometer domes and radiation station in Lindenberg at the beginning of starphotometry in 1992 (a) and today (b); André Knöfel (DWD) operating theSPST7 starphotometer of Lindenberg (c).

Stellar photometry began in Lindenberg at the beginning of the 1990s, using SPST (*Schulz und Partner Sternphotometer*). The first developments are presented in Leiterer et al. (1995). In 2013, the old starphotometer was replaced by the current one: the SPST7 and a new dome was built (Figure 4.1.3 (b and c)).

2000 - 2020 Joining the three networks and lunar photometry

Returning to solar photometry, in the 2000s the new PFR reference instruments from PMOD/WRC (Davos, Switzerland) took over routine measurements at MOL-RAO. In 2013, the Lindenberg Observatory acquired a CIMEL CE318 and joined AERONET (sections 2.1.3 and 3.1). Two Prede POM-02 instruments also joined SKYNET and its European subnet, ESR (sections 2.1.3 and 3.3). Since 2013, MOL-RAO has been the only station worldwide to belong to all three reference networks—GAW-PFR, AERONET, and SKYNET—using PFR, CIMEL CE318T, and POM-02 instruments, respectively (see Figure 4.1.4).



Figure 4.1.4: The three main instruments of the current Lindenberg AOD measurement suite: CIMEL, Prede and PFR. With specifications of exact instrument denomination, Network to which each instrument belongs and since when the instrument is active (in brackets since when the current used dataset is disponible).

These three instruments (PFR, CIMEL, and Prede) provide a robust operational basis for daytime AOD measurements using solar photometry, while also enabling intercomparisons for validation (deliverables D1.2 and D1.3: Doppler et al., 2024, 2026). With continuous AOD measurements since 1986 Lindenberg has one of the world's longest continuous measurement records.

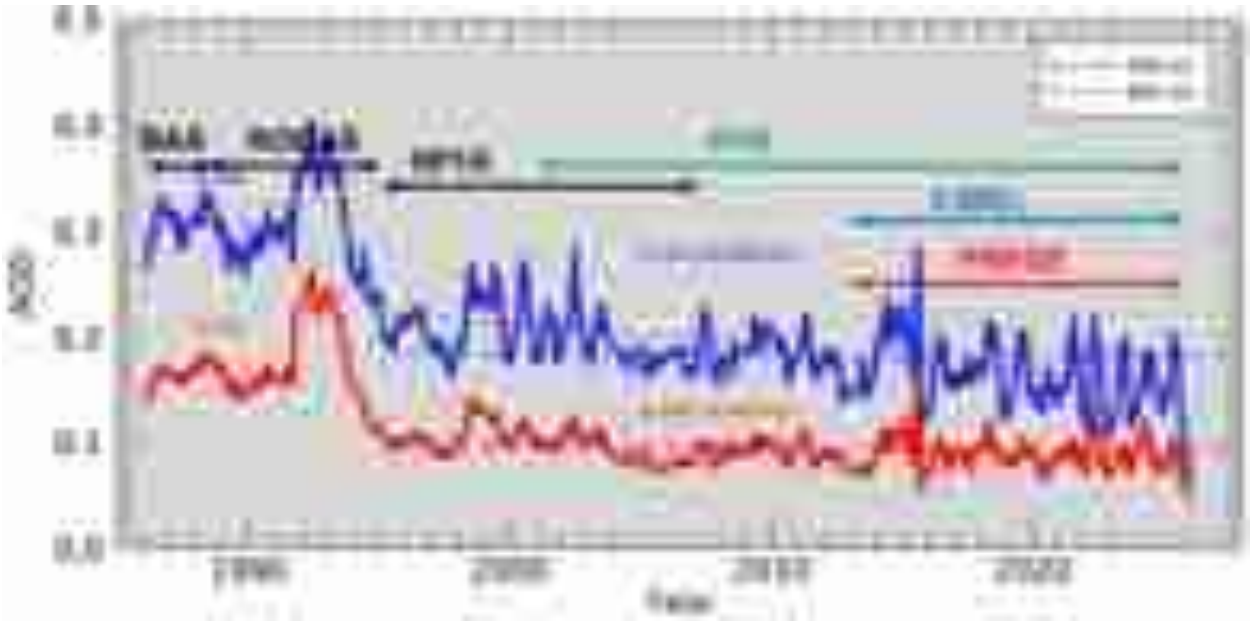


Figure 4.1.5: 1986 - Today: Long-term AOD daily measurement record (500 and 862 nm) at Meteorological Observatory Lindenberg; durations of activity of each photometric system are indicated with arrows.

Figure 4.1.5 shows the long-term records at 500 nm (blue) and 862 nm (red). The pronounced maximum in 1992 was caused by the eruption of Mount Pinatubo in the Philippines. Since the 2000s, the atmosphere has been considerably cleaner than in the 1980s: AOD at 500 nm is now approximately 0.15–0.2, compared with around 0.3 previously. This improvement is attributable to more environmentally friendly developments in cities, industry and transport.
In June 2015, spectral AOD measurements began, following the acquisition of PSR (Precision Spectroradiometer, see Figure 4.1.7a, see also Deliverable D1.2, Doppler et al., 2024) instruments from PMOD/WRC.
In October 2015, a new era began with the acquisition of a CIMEL CE318-T triple photometer, which measures the Sun, sky, and Moon, and the start of lunar photometry measurements at Lindenberg. This complemented the stellar measurements, enabling nighttime AOD retrievals. For several years, until other stellar-observation stations—Eureka, Ny-Ålesund, and Sherbrooke (section 2.2.3)—also acquired CIMEL lunar photometers, Lindenberg was the only station worldwide to make operational lunar, solar, and stellar measurements in parallel.

The SCILLA campaign (August - September 2020)

In this context, DWD Lindenberg organised the SCILLA campaign (Summer Campaign for Intercomparison of Lunar Measurements of Lindenberg's Aerosol) in August–September 2020 (See deliverable D1.3: Doppler et al., 2023). Seventeen institutions from ten countries took part, either by providing instruments or by actively participating in the workshop. The campaign brought together three CIMEL lunar–solar photometers, complementing the two already at Lindenberg. A lunar–solar Prede photometer from Japan's National Institute of Polar Research (NIPR)—then

still a prototype—also took part, as did the prototype lunar PFR from PMOD/WRC and ISP-CNR (Bologna), based at CNR's *Dirigibile Italia* station in Ny-Ålesund. A University of Sherbrooke STSP stellar photometer joined Lindenberg's SPST07 star photometer. Together with Lindenberg's solar PFR and Prede POM-02, the instruments involved were:

- Two SPST stellar photometers
- Five CIMEL CE318-T (lunar & solar photometers)
- Two PFR photometers (one lunar & solar and one solar)
- Two Prede photometers (one lunar & solar and one solar)

The campaign took place during the COVID-19 pandemic. Almost no staff from participating institutions or instrument principal investigators could attend in person. All guest instruments have been shipped. DWD technical staff installed and operated all the instruments, and the scientific workshop was held online.



Figure 4.1.6: Summer campaign SCILLA at Lindenberg: Left solar and lunar photometers of CIMEl, Prede and PFR on the rooftop of the radiation lab; Right: On the additional platform of Lindenberg, a starphotometer of type SPST of University Sherbrooke.

After 2020: New innovations and partnerships - HARMONIA

The SCILLA campaign strengthened cooperation between DWD Lindenberg and GOA-UVa (University of Valladolid: Section 4.2.2). CIMEL instruments have been calibrated at GOA-UVa since 2017, and Lindenberg is part of its CÆLIS network. The collaboration was further expanded when Lindenberg hosted an OMEA red–green–blue (RGB) all-sky camera.

Initially, the camera was intended to complement the SCILLA instrument suite and support cloud detection (Roman et al., 2024; Longarela et al., 2026; Herrero del Barrio et al., 2026). Further applications include radiation retrievals (González-Fernández et al., 2024) and nighttime AOD

retrievals using multi-stellar photometry (section 7.1 and Roman et al., 2025). The camera completes the current AOD measurement suite at DWD Lindenberg, shown in Figure 4.1.7b.



Figure 4.1.7: Lindenberg Photometry instrument suite today

In the 2020s, DWD Lindenberg was actively involved in the COST Action HARMONIA (2022–2026). A highlight was organising and hosting the “Sky Over Berlin” school on 8–10 April 2024 at Freie Universität Berlin (FUB) and the DWD Observatory Lindenberg (MOL-RAO).



Figure 4.1.8: Group picture of the HARMONIA training school “Sky over Berlin” (FU Berlin & DWD Lindenberg, 8-10 April 2024), in front of the stellar photometer dome.

4.1.2 in Buckow with Carl-Heinz Schulz

As explained in the preceding section 4.1.1, *Dr. Schulz und Partner GmbH* was founded in the early 1990s, following German reunification, by Karl-Heinz Schulz (Figure 4.1.9), a photometry expert and co-developer of the photometers designed at the Lindenberg Observatory in the 1980s, during the GDR era. He established the company in his home village of Buckow, near Beeskow, about 10 km from DWD Lindenberg.



Figure 4.1.9: Karl-Heinz Schulz, father of the SPST stellar photometers and SP1A solar photometers, here with sunphotometers on a sun tracker.

*Dr. Schulz und Partne*r initially manufactured the last instruments designed at the Lindenberg Observatory in the late 1980s. Since 1987, these instruments had been operating at the Zingst station on the Baltic coast (section 4.1.4). They were renamed SPH and SP2H (Figure 4.1.10) and were also operated at DWD Hohenpeißenberg (section 4.1.3), where continuous AOD monitoring began in 1993.



Figure 4.1.10: Right: SP2H sunphotometer developed by *Dr. Schulz und Partner GmbH*. Left: SP2H making measurements on a tripod.

A highly productive period followed, marked by the development of SPST stellar photometers (sections 2.2 and 4.1.1). These instruments were first deployed at Lindenberg (Figure 4.1.3), and later at Sherbrooke (Canada), Eureka (the Canadian Arctic), and Ny-Ålesund (Svalbard) (Figure 2.2.7).

In parallel, *Dr. Schulz und Partner* developed SP1A solar photometers (Figure 4.1.11), which entered service in 1995. They were used at Lindenberg (1995–2014), Hohenpeißenberg (2000–2006), and at stations along the "*Zu-Zi Trasse*" (section 4.1.4): Zingst (1999–2010), Zugspitze (2002–2007), and Potsdam throughout the station's operational lifetime (1994–2003). SP1A instruments were also deployed internationally, notably by ISP-CNR in Bologna and by the Alfred Wegener Institute (AWI), Germany's polar research institute, in polar regions such as Ny-Ålesund (Svalbard).



Figure 4.1.11: Right: SP1A sunphotometer developed by *Dr. Schulz und Partner GmbH*. Left: SP1A making measurements on a sun tracker together with a sunphotometer PFR.

Dr. Schulz und Partner GmbH ceased operations in the late 2010s / early 2020s, when Karl-Heinz Schulz retired. He remained involved in the early development of lunar photometry—not as a manufacturer, but as an experienced observer and trusted adviser who generously shared his expertise. This is reflected in his participation in the first meeting of the “Lunar AOD” community, held in Valladolid in June 2015 (Figure 4.1.6).

4.1.3 At DWD Hohenpeißenberg since 1993

Another historical site for AOD measurements is the Meteorological Observatory Hohenpeißenberg (47.80 N, 11.02 E, 980 m), operated by the *Deutscher Wetterdienst* (DWD) in the German pre-Alps. This historic site has been conducting meteorological measurements since 1781. Today, it serves as a supersite for meteorological observations and measurements of atmospheric chemical composition. It is a GAW (Global Atmosphere Watch) centre for ozone and aerosols and contributes to ACTRIS. Remote sensing of AOD using photometric techniques at Hohenpeißenberg began in 1993 with the manual SP2H instrument produced by *Dr Schulz und Partner* (Figure 4.1.10). A SP1A sun photometer—an automatic instrument also developed by *Dr. Schulz und Partner*— (Figure 4.1.11) was added to enable automated operation. Parallel measurements with the SP2H continued until January 2001. From then until the end of 2006, measurements were carried out with the SP1A, with interruptions due to calibration procedures and tracker problems. Since 1999, the DWD Observatory Hohenpeißenberg has been equipped with a PFR (Precision Filter Radiometer), a four-channel instrument developed by PMOD/WRC (Davos, Switzerland), and has been part of the GAW-PFR network. Calibration was carried out at PMOD/WRC in Davos, which also processed the data within the GAW-PFR network framework (Wehrli, 2002). The data are submitted to the European database EBAS.



Figure 4.1.12: PFR (left) and CIMEL (right) making parallel AOD measurements at Meteorological Observatory Hohenpeißenberg (DWD).

From 1999 to 2000, all three instruments—the SP2H, PFR, and SP1A—were operated in parallel. Between 2001 and 2005, the SP1A and PFR were operated in parallel. In 2013, a CIMEL CE318 sun photometer was added at Hohenpeißenberg, and the site joined the AERONET network as the HohenpeissenbergDWD station. Since then, CIMEL and PFR measurements have been conducted in parallel at Hohenpeißenberg (see Figures 4.1.12 and 4.1.13). Additionally, Meteorologischer Observatorium Hohenpeißenberg has been integrated into the AOD network of *Deutscher Wetterdienst* (DWD) named "*Zu-Zi Trasse*" (section 4.1.4). The measurements results until 2005 are presented and analysed in Weller and Gericke (2005). In 2017, the CIMEL instrument was upgraded for lunar measurements. Since then, a nighttime AOD dataset has also been available for Hohenpeißenberg.

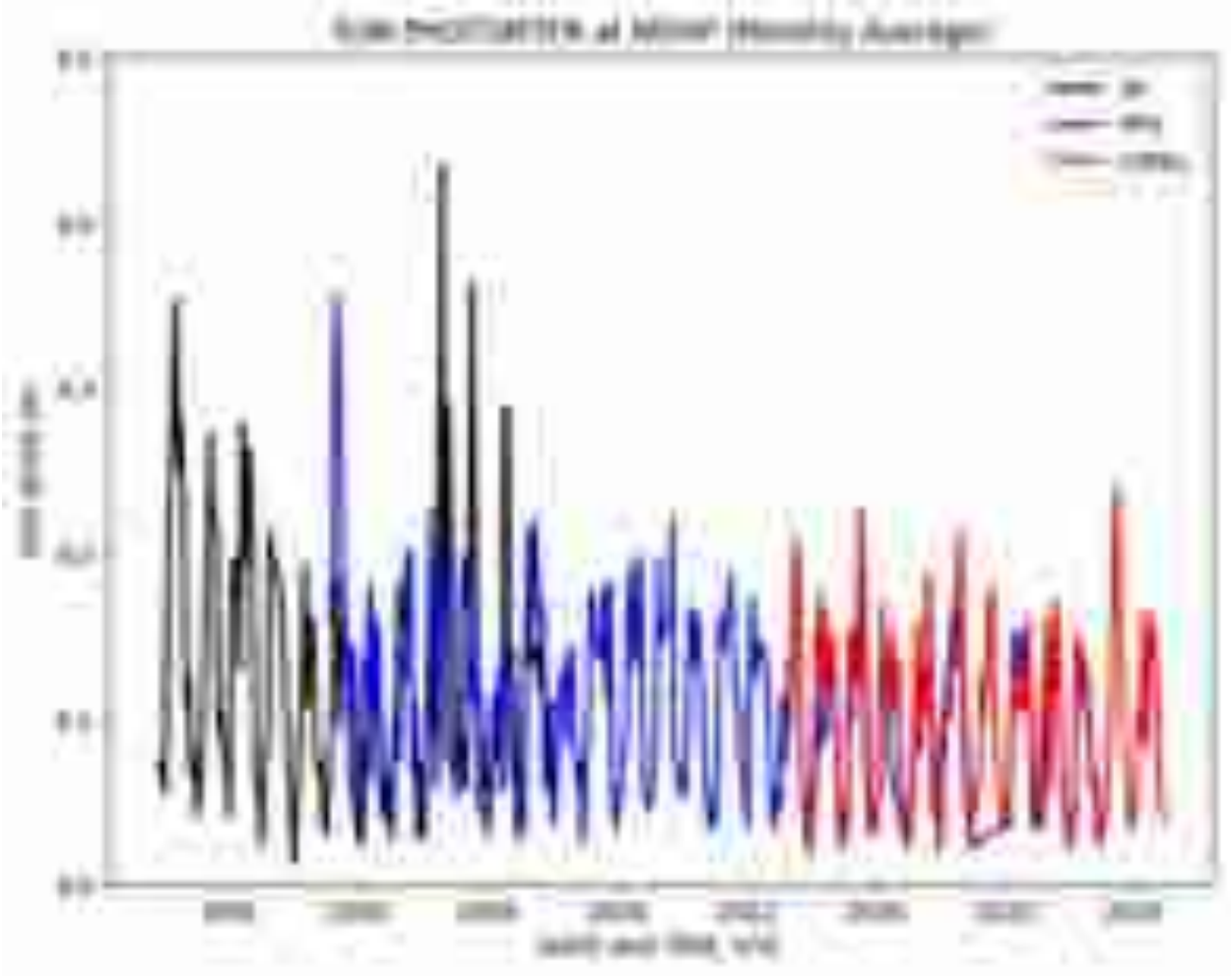


Figure 4.1.13: 1993 - Today: Long-term AOD daily measurement record (500 nm) at Meteorological Observatory Hohenpeißenberg (DWD); The active instruments are documented with colors. From Wagner et al. 2026

4.1.4 The "*Zu-Zi Trasse*" (Zugspitze - Zingst Trail)

During the East German period, which ended in 1990, the Lindenberg Observatory was responsible for aerosol photometry and equipped another station of the Meteorological Service of the GDR (*Meteorologischer Dienst der DDR*, MD) with a SPH photometer in 1987: the Zingst station on the Baltic coast. After German reunification and the integration of the MD into the DWD in 1990, Lindenberg continued to play a leading role in AOD measurements. It equipped the Hohenpeißenberg Observatory with SPH photometers and then SP1A photometers from 1993 to 2006 (section 4.1.3) and the Potsdam Observatory with SP1A photometers, which were used from 1994 until the observatory closed in 2003. Lindenberg was responsible for calibrating the instruments and supervising the measurements. In 2002, it also equipped the DWD weather station at Zugspitze, the highest mountain in Germany, with an SP1A photometer.

This marked the beginning of the "*Zu-Zi Trasse*" (Zuspitze - Zingst trail) a north–south chain of stations—Zugspitze, Hohenpeißenberg, Potsdam, and Zingst (see the map in Figure 4.1.14)—equipped with photometers for AOD measurements and instruments for measuring radiation. The concept was developed by Dr. Michael Weller of DWD Lindenberg, and its first results were presented in Weller et al. (2000) and Weller and Gericke (2005). The following sections describe the two main stations on the "Zu-Zi route": Zingst on the Baltic coast and Zugspitze in the Alps.



Figure 4.1.14: Stations of the German AOD and radiation measurement trail "*Zu-Zi - Trasse*" (Zugspitze-Zingst Trail)

4.1.4.1. DWD operated station at Zingst on the German Baltic Coast

The Zingst station was formerly operated by the East German Meteorological Service MD (*Meteorologischer Dienst der Deutschen Demokratischen Republik*), where middle-atmosphere research was conducted using rocket measurements. After German reunification, the Zingst station was incorporated into the German Environment Agency (UBA; *Umweltbundesamt*) as an air-quality monitoring station.

The station is located on the Zingst Peninsula on the Baltic Sea coast in northeastern Germany. In addition, today, the UBA and the Federal Office for Radiation Protection (BfS; *Bundesamt für Strahlenschutz*) operates a spectrometer at the station to measure ultraviolet (UV) radiation.



Figure 4.1.15: Zingst Station instruments in 2007 (a) and today (b1 and b2)

DWD Lindenberg has conducted aerosol optical depth (AOD) measurements at Zingst since 1987 (Figure 4.1.16). Measurements were initially made with an SPH instrument (Figure 4.1.10) from 1987 to 1999, followed by measurements with an SP1A instrument (Figure 4.1.11) from 1999 to 2010. PFR measurements were carried out in 2007–2008 (Figure 4.1.15a) and have continued since 2010. A new sun tracker was installed in 2010 (Figure 4.1.15b1).

DWD Lindenberg measures broadband radiation in shortwave and longwave all four radiation components. Since 2019, UV radiation has also been measured using a UV pyranometer, including the UV Index and UV-A radiation. In 2023, DWD Lindenberg added a Prede POM-02 solar + lunar photometer (Figure 4.1.15 b2), which is part of the SKYNET network.

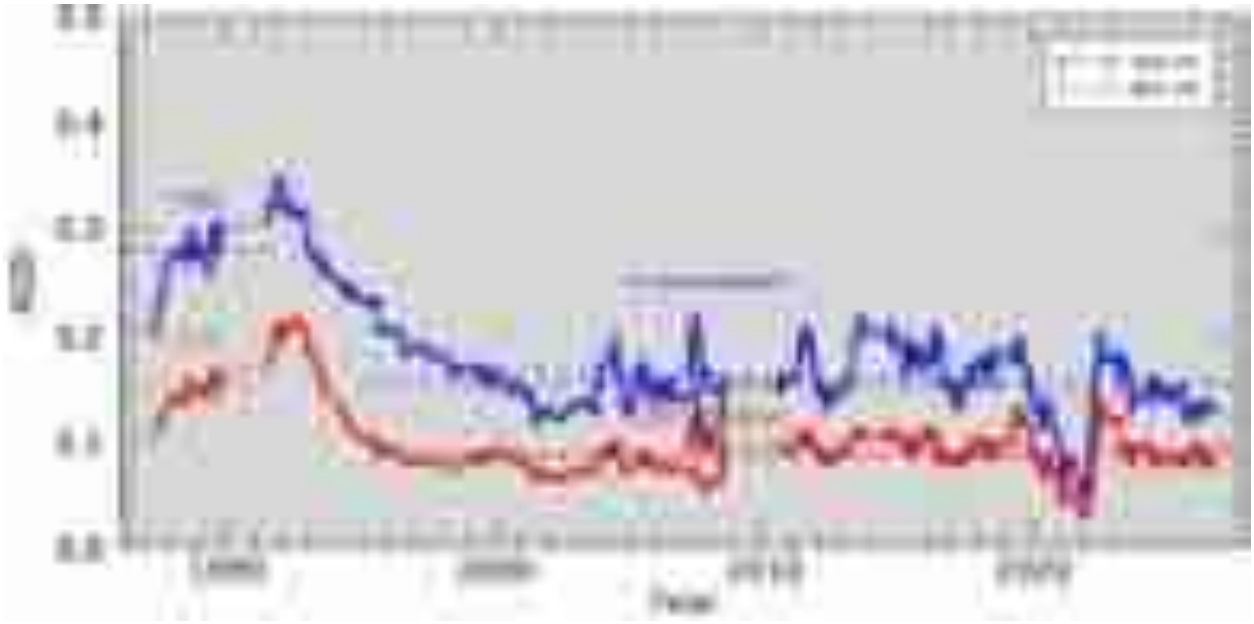


Figure 4.1.16: Zingst Station time series: 1987 - today.

4.1.4.2. DWD Station at Zugspitze (2960 m), summit of the German Alps

The Zugspitze, at 2,960 m above sea level, is Germany's highest mountain and is located in the Alps, on the Austrian border in the far South of Germany. The German Meteorological Service (DWD) has operated a historical meteorological station there since 1900.



Figure 4.1.17: Zugspitze Station, instruments in 2007 (left) and since 2014 (middle), sometimes under hard weather conditions (right).

In the early 2000s, DWD Lindenberg established a radiation and photometry station at the summit. It was equipped with a sun tracker carrying a pyrheliometer, a pyranometer, and pyrgeometers with shadow devices, as well as two PFR photometers. Global radiation is also measured at the station using a pyranometer without a shadow ring. The Zugspitze AOD data series began in 2002 with SP1A instruments (Figure 4.1.11), followed by PFR measurements from 2007 onward. Operational monitoring of direct normal irradiance (DNI) using a SCAPP instrument also began in 2007. A continuous aerosol optical depth (AOD) data series without interruptions has been available since 2014. In that year, a new sun tracker was installed, carrying the currently used radiative instruments: pyranometers and pyrgeometers with shadow devices for measuring diffuse horizontal irradiance (DHI) and atmospheric thermal-infrared radiation.

Since 2020, the Karlsruhe Institute of Technology (KIT), with sites in Karlsruhe and Garmisch-Partenkirchen, Germany, has operated a CIMEL photometer approximately 50 m away, also at the summit. The AERONET station is designated *Zugspitze_KIT*. Its measurements enable quality comparisons and provide complementary information, including AERONET inversion products such as single-scattering albedo (SSA), phase functions, and particle-size distributions. In addition, unlike PFR instruments, the CIMEL photometer can provide nighttime AOD measurements through lunar photometry.

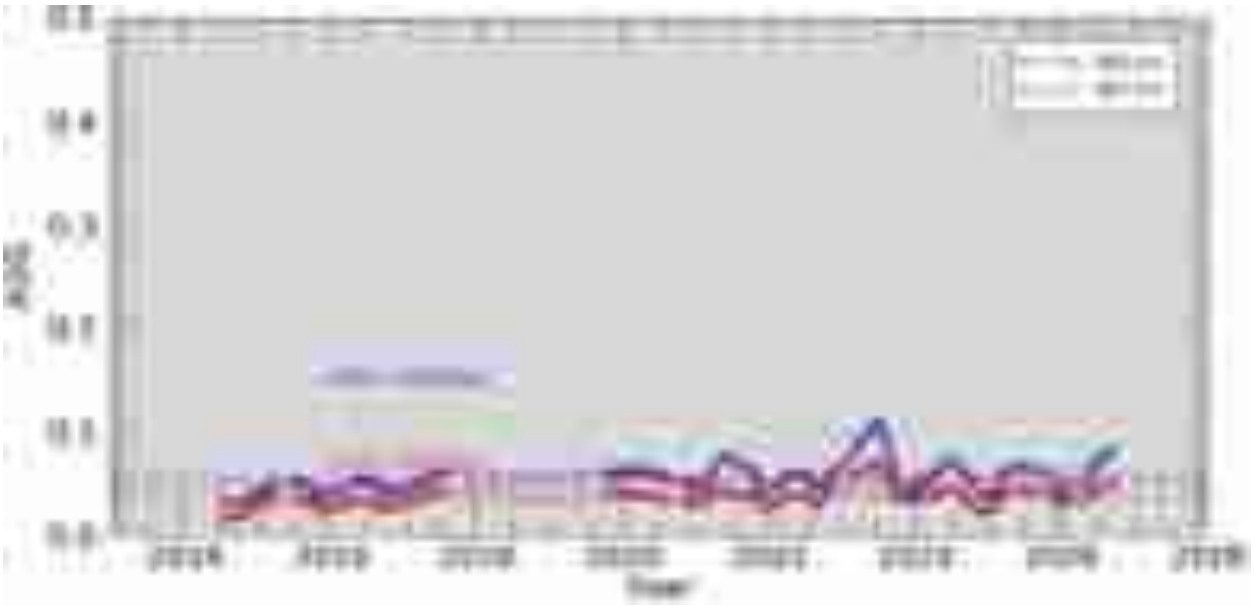


Figure 4.1.18: Zugspitze Station time series.

4.1.5 German Polar research about Aerosols: AWI Potsdam and Ny-Ålesund station

Another important German contributor to European photometry is the Alfred Wegener Institute (AWI), Germany's polar research institute, based in Bremerhaven and Potsdam. In particular, the Potsdam group operates the Raman lidar and stellar photometer at the AWIPEV station in Ny-Ålesund, Svalbard (section 5.2.2). Notable contributions include the works of Andreas Herber (Herber et al., 2002) and that of Christoph Ritter and Sandra Graßl (Graßl and Ritter, 2019; Graßl et al., 2024; Graßl, 2025; Herrero-Anta et al., 2019, among others). Most of their work is discussed in the section on AOD measurements in the polar regions (Part 5). The AWIPEV station is described in more detail in section 5.2.2.

4.2. In Spain: In Izaña and Valladolid

4.2.1 In Izaña at AEMET/IARC observatory

✝ In Memoriam

This section is dedicated to **Dr. Emilio Cuevas Agulló**, director of the Izaña Observatory (AEMET/IARC) from 1999 to 2023.

Emilio passed away far too soon on 26 February 2026, during the HARMONIA COST Action. Without his dedication and commitment, much of what is described in this deliverable—at Izaña, across Spain, and throughout the European photometry community—would not have been possible.

Thank you, Emilio. May you rest in peace.



✝ In memoriam Dr. Emilio Cuevas Agulló (1961 - 2026), former director of Izaña Observatory.

Izaña Observatory - History

The Izaña Observatory (Figure 4.2.1) is located at 2373 m a.s.l. on the island of Tenerife (Canary Islands, Spain) and is managed by the Izaña Atmospheric Research Center (IARC) of the State Meteorological Agency of Spain (AEMET). Its origins date back to the early 20th century, when the European scientific community showed growing interest in establishing a permanent observatory on the summits of Tenerife. After a provisional German observatory had operated at Las Cañadas del Teide from 1909, a commission of the Spanish National Geographic Institute selected the Izaña mountain in 1911. The observatory was inaugurated on 1 January 1916 and has operated without interruption since then (de Ory, 2016). Its location in the free troposphere, above the trade-wind temperature inversion, provides pristine skies and clean air for most of the year. During summer, however, the station is frequently affected by the Saharan Air Layer, which makes it a privileged site for studying both background aerosol and mineral dust (Cuevas et al., 2019).



Figure 4.2.1: Izaña Observatory in 1916 (on the left) and in 2026 (on the right).

Radiation measurements on Tenerife have a long history, including the solar radiation observations of Knut Ångström in 1895 and 1896 (sections 2.1.1 and 4.5.2) and the pyrheliometric measurements carried out at Izaña in the first decade of the 20th century (de Ory, 2016). AOD measurements, in contrast, began much later. In 1984, Spain and Germany signed a cooperation agreement under which Izaña joined the WMO Background Atmospheric Pollution Monitoring Network (BAPMoN), a programme that operated from 1972 to 1992 and was the most ambitious early attempt to monitor background AOD worldwide. Within this framework, Klaus Fröhlich, then director of PMOD/WRC (Davos, Switzerland), initiated the AOD measurement programme at Izaña in 1984 using a sun photometer provided by PMOD/WRC (Cuevas et al., 2019). That same year, in April 1984, Izaña hosted one of the first international AOD intercomparison campaigns, promoted and coordinated by PMOD/WRC (WMO, 1986; Cuevas et al., 2019). The low precision and stability of the early hand-held photometers of that period, however, limited their usefulness for long-term trend detection (WMO, 1994). In 1989, BAPMoN merged with the Global Ozone Observing System to form the WMO Global Atmosphere Watch (GAW) programme, of which Izaña is one of the principal global stations.

Continuous instrumental AOD monitoring at Izaña began in 1996 with a Multi-Filter Rotating Shadowband Radiometer (MFR-SR, Figure 4.2.2). This instrument measures global horizontal, diffuse horizontal and direct normal irradiances in six narrow passbands between 410 and 940 nm. The global irradiance is measured directly, whereas the diffuse and direct components are derived from a sequence of three measurements. In the central measurement, a shadow band blocks the strip of sky containing the Sun; in the other two, the band blocks strips of sky 9° to either side. These side measurements correct for the excess sky blocked during the central measurement, which is needed to determine the diffuse horizontal irradiance. The direct normal irradiance is then obtained by subtracting the diffuse from the global horizontal irradiance (Harrison et al., 1994).



Figure 4.2.2: Multifilter Rotating Shadowband Radiometer (MFR-SR) in operation at Izaña Observatory.

The 2000s: GAW-PFR and AERONET networks

In June 2001, a Precision Filter Radiometer (PFR) from PMOD/WRC began operating at Izaña as part of the GAW-PFR network (precisions about the instrument PFR and the network GAW-PFR in section 3.2), the WMO reference for AOD. Measurements within AERONET started with CIMEL radiometers in 2003, following a short campaign in summer 1997 (Barreto et al., 2014; Cuevas et al., 2019). Since then, Izaña has become one of the two sites worldwide, together with Mauna Loa, where reference instruments of both AERONET and GAW-PFR are calibrated by the Langley plot technique (Toledano et al., 2018). In July 2014, the WMO also designated Izaña as a CIMO test bed for aerosol and water vapour remote-sensing instruments (WMO, 2014). Izaña's role became even more critical after the eruption of Mauna Loa volcano in late 2022, when lava flows cut the access road and power lines to the Mauna Loa Observatory, leaving Izaña as the only facility worldwide for the calibration of AERONET reference photometers.

The simultaneous operation of both AERONET-CIMEL and GAW-PFR networks at the same site has made it possible to assess their long-term comparability. Cuevas et al. (2019) compared more than 70 000 synchronous 1 min AOD measurements from three GAW-PFR and 15 AERONET-CIMEL radiometers between 2005 and 2015. The fraction of data meeting the WMO traceability criteria exceeded 92 % at 380 nm and 95 % at 440 and 500 nm, and reached 98 % at 870 nm. The authors concluded that both datasets represent the same AOD population, although further improvement is needed in the UV. They attributed the remaining discrepancies under high dust loads mainly to the different fields of view of the two instruments, which lead to slightly lower AOD values from the PFR.

A long-term AOD series from an astronomical instrument.

Although routine aerosol photometry at Izaña became continuous only in the 1990s, the AOD record at this station can be extended back to 1976 thanks to an instrument originally built for a completely different purpose. The Mark-I spectrometer, located at the SolarLab of the *Instituto de Astrofísica de Canarias* in the Teide Observatory, about 1.5 km from the Observatory, was designed as a reference instrument for helioseismology. It measures the solar radial velocity using resonant scattering in a potassium vapour cell at 769.9 nm and has operated almost continuously since 1976. Barreto et al. (2014) recovered a 37-year AOD series (1976–2012) from its solar irradiance measurements (Figure 4.2.3). Because the instrument relies on outdoor mirrors that were periodically cleaned, realigned and replaced, it was not photometrically stable. The authors overcame this with a quasi-continuous Langley calibration and a refinement procedure that removes fictitious diurnal AOD cycles.

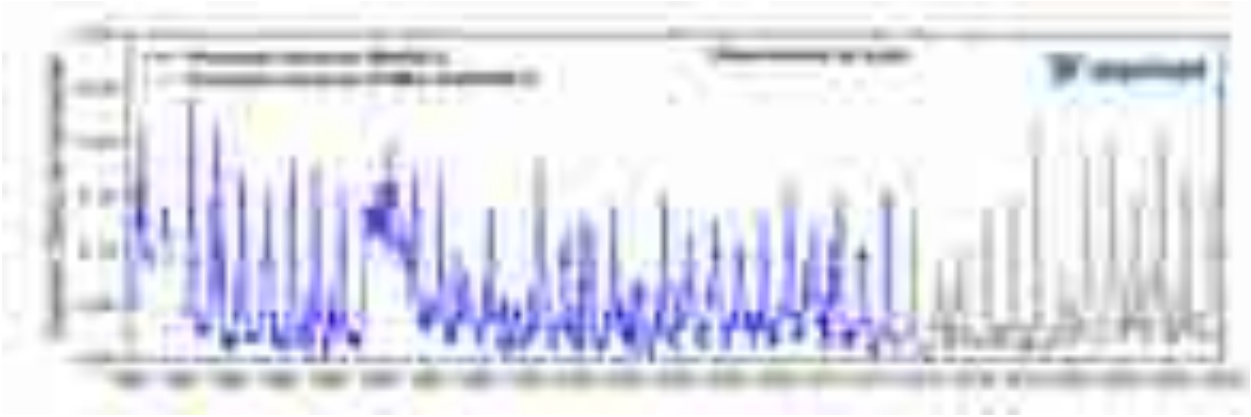


Figure 4.2.3: AOD time series at Izaña, covering MARK-I and AERONET measurements.

The recovered series agreed well with collocated AERONET and PFR measurements, with an absolute mean bias of 0.01 or less over the 10- and 12-year comparison periods. It therefore allows the Izaña AOD record to be extended from the present back to 1976. The series clearly captures the impact of the Mount Pinatubo eruption, with a maximum anomaly of 0.049 in 1992 and a highest monthly mean AOD of 0.14 in July 1992, as well as a smaller signal from El Chichón in 1982. A preliminary analysis of winter data, when Saharan dust is virtually absent, showed a nearly constant background AOD of about 0.02 and no significant trend between 1984 and 2012 (Barreto et al., 2014).

Nighttime photometry.

Izaña has also played a central role in the development of lunar photometry. A lunar photometer prototype was tested there to develop the Lunar-Langley method (Barreto et al., 2013). A lunar photometry validation campaign took place in June 2017 (Barreto et al., 2019) during which Izaña , IARC hosted the second international workshop of the lunar AOD community (Fig. 4.2.4) Data from the reference CIMEL CE318-T at Izaña were later used to derive a phase-angle-dependent correction for the RIMO lunar irradiance model (Román et al., 2020). Since 2018, the lunar radiometer used to build the ESA lunar irradiance model LIME has operated at Izaña and Teide

Peak (Toledano et al., 2024). Solar and lunar Langley calibrations at Izaña and Mauna Loa also underpin the empirical correction applied in the current AERONET lunar AOD product (Schafer et al., 2026).



Figure 4.2.4: Group picture of the second international workshop of the lunar AOD community in Izaña during the first lunar AOD validation campaign - June 2017

AEMET Izaña and HARMONIA

AEMET Izaña is very engaged in COST Action HARMONIA with participation in the Core Group, Co-Lead of Working Group 4 (manufacturer community). A highlight of this participation was the organisation of the HARMONIA school “Above the Clouds” in Izaña in May 2025.



Figure 4.2.5: Group picture of the “Above the Clouds” school of HARMONIA (26-28 May 2025).

4.2.2 At University of Valladolid: The GOA-UVa group

The University of Valladolid (UVa) has been involved in the AERONET calibrations since 2006, when the Group of Atmospheric Optics (GOA) signed an agreement with NASA for starting a calibration centre (Figure 4.2.6). This facility is part of the so-called AERONET-Europe, and works in close collaboration with the University of Lille (PHOTONS centre at LOA, see section 4.6) and the Izaña Atmospheric Research Center (AEMET/IARC). It later became part of the ACTRIS research infrastructure through several European projects (ACTRIS, ACTRIS-2, etc.) until it consolidated as a unit of the ACTRIS Center of Aerosol Remote Sensing (ACTRIS-CARS). Apart from the calibration operations, research, new algorithms and quality assurance tools have been developed by the GOA-UVa group. The CÆLIS software platform (Fuertes et al., 2018; González et al., 2020) was developed for research and network management purposes.



Figure 4.2.6: The GOA-UVa station with all CIMEL instruments being calibrated on the rooftop of University of Valladolid.

The contribution of Valladolid calibration facility is remarkable in the fields of photometer calibration (Toledano et al., 2018), lunar photometry (Barreto et al., 2018 ; Román et al., 2020; Toledano et al., 2024 and participation to all the lunar photometry workshop, organizing the first one in June 2015 at University of Valladolid: Fig 4.2.7) and instrument synergy studies by

combination of remote sensing instrumentation (e.g. CAECENET, Herrero del Barrio et al., 2025, see also section 6.2.2).
GOA-UVa also supported AOD measurements in Polar area as well as in the Arctic (section 5.2.1) and in Antarctica (section 5.3.1) and supported the AOD measurements with CIMEL instruments in Norway (section 4.5.1).



Figure 4.2.7: Group photo of the first lunar photometry workshop at University of Valladolid (June 2015). Standing behind from left to right: Benjamin Torres (UVa), David Fuertes (LOA), Julian Gröbner and Natalia Kouremeti (PMOD/WRC), Antti Arola (FMI), Norman O'Neil (Univ Sherbrooke), Victoria Cachorro and Carlos Toledano (UVa), Konstantin Baibakov (Univ. Sherbrooke), Christoph Ritter (AWI), Ángel de Frutos (UVa), Lionel Doppler (DWD), Mauro Mazzola (CNR), Ramiro González and Roberto Román (UVa), Masataka Shiobara (NIPR), Karl-Heinz Schulz (*Schulz und Partner*), Cristian Velasco (UVa), Thomas C. Stone (USGS); sitting in front rank, from left to right: Emilio Cuevas (AEMET), África Barreto (CIMEL & AEMET), Maria Ángeles and David Mateos (UVa), Kerstin Stebel (nilu), Vito Vitale (CNR), Allison McComiskey (Univ. Colorado), Robert S Stone (NOAA), Angelo Lupi (CNR), Jakub Juryšek (CAS) - Affiliations are the ones at the time of the picture.

The University of Valladolid is a major contributor to COST Action HARMONIA: it holds the Vice-Chair position (Carlos Toledano) and leads Working Group 4 (WG4), while two of its members serve on the Core Group. GOA-UVa hosted a WG4 meeting in Valladolid on 30 June 2026 (Figure 4.2.8).
GOA-UVa also contributes actively to HARMONIA's scientific output, with numerous papers by its researchers published in the Atmospheric Measurement Techniques special issue and in Atmospheric Chemistry and Physics, both published by EGU, under the theme "Sun-photometric measurements of aerosols: harmonization, comparisons, synergies, effects, and applications." of COST action HARMONIA. These include work by established researchers (Roman et al., 2025; Mateos et al., 2026) as well as by early-career researchers—master's and PhD students and postdoctoral researchers (Herrero del Barrio et al., 2026; Herrero-Anta et al., 2026; Longarela et

al., 2026). The first two early-career researchers mentioned participated actively in all HARMONIA schools and undertook several highly beneficial scientific exchanges through Short-Term Scientific Mission (STSM) grants, contributing to both their research and the wider HARMONIA community.



Figure 4.2.8: Group photo of the WG4 Meeting of HARMONIA on the rooftop of University of Valladolid (UVa) - 30 June 2026

4.3. In Switzerland: Davos (PMOD/WRC) and associated stations

4.3.1 PMOD/WRC at Davos

Davos holds one of the longest records of atmospheric column transparency. Pyrheliometric measurements of direct solar irradiance began at the Physikalisch-Meteorologisches Observatorium Davos (PMOD, founded by Carl Dorno in 1907) in 1909 and continue today, making it the longest stationary direct irradiance record worldwide. Before spectral photometry, the aerosol load could only be inferred from these broadband observations, through turbidity indices and the apparent atmospheric transmission from the pyrheliometric ratioing technique (Hoyt and Fröhlich, 1990, covering 1909–1979). In 1982 new instrumentation for continuous direct-irradiance measurement was installed, and against the 1909–1970 reference the

stratospheric aerosol cloud from the El Chichón eruption could be clearly identified and quantified by comparison with lidar data from southern Germany (Heimo and Fröhlich, 2000). Lachat and Wehrli (2012) later homogenised the different instruments and scales of the full record to the World Radiometric Reference, and found small but highly significant phases of early brightening, dimming and brightening. A follow-up study separated out Rayleigh scattering and water vapour, interpreting the residual as aerosol extinction to give a broadband AOD series for 1909–2010. Because PMOD/WRC lies upwind of Davos and local anthropogenic pollution is marginal, the AOD trend mainly reflects the larger-scale aerosol background.

The move from broadband turbidity to multi-wavelength sun photometry came in the 1990s. PMOD/WRC developed the Precision Filter Radiometer (PFR), and long-term PFR AOD measurements started in 1995 at Davos and from 1999 at other locations worldwide. The GAW-PFR network is calibrated through frequent comparison with a reference triad of three PFRs operating at Davos.



Figure 4.3.1: PFR group at PMOD-WRC

4.3.2 Station Jungfraujoch (3580 m asl)

Jungfraujoch (3580 m a.s.l., see Figure 4.3.2) is the main high-alpine station associated with Davos and a core GAW-PFR site. Nyeki et al. (2012) re-calibrated, augmented and for the first time homogenised the AOD climatologies of Jungfraujoch, Davos and Hohenpeissenberg for 1995–2010. Trends at 500 nm were weak (Jungfraujoch +0.002, Davos .0.004 and Hohenpeissenberg −0.004 per decade) and for Jungfraujoch the stratospheric contribution from

Pinatubo and later eruptions made a 1995–2005 fit (−0.003 per decade) more appropriate (Nyeki et al., 2005; 2015). More recent PFR data at Davos for 2007–2019 show trends of about −0.017 and −0.007 per decade at 500 and 862 nm, with very small differences from the co-located AERONET CIMEL (Karanikolas et al., 2022). 2004 to 2025 Davos AOD trends at 500nm show a decrease of ~0.07 per decade. Across the high-altitude GAW-PFR stations, including Jungfraujoch, mean AOD at 500 nm ranges from 0.01 to 0.1, with very small positive changes per year during the last 25 years. Both Davos and Jungfraujoch show small but significant decreasing trends during the period 2008 to 2016 and small increasing trends for the other periods. Time series and statistics for both can be found in Figure 4.3.3.



Figure 4.3.1: PFR photometers at the station Jungfraujoch (left), the Sphinx Observatory, Jungfraujoch (right)

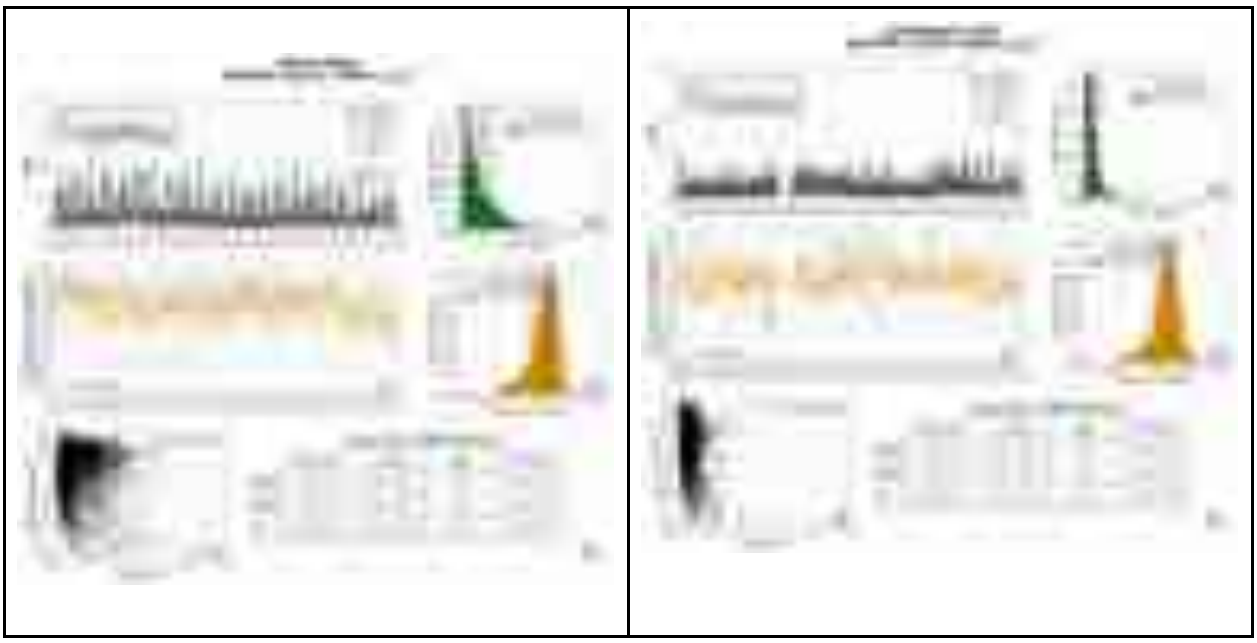


Figure 4.3.3: Davos and Jungfraujoch time series for four wavelengths (upper-left), relative frequency of AOD at 500nm (upper-right), Ångström exponent series and histogram (middle) and AOD vs Ångström exponent and relevant statistics (bottom).

4.3.3 The world in Davos, HARMONIA and PMOD/WRC

The Davos observatory PMOD/WRC is internationally renowned in the photometry community. It is officially recognized by the World Meteorological Organization (WMO) for managing the GAW-PFR network (Global Atmosphere Watch–Precision Filter Radiometer) and operating its calibration centre, WORCC (World Optical Depth Research and Calibration Centre).
In addition to this PMOD/WRC is also known for organising for the WMO the Filter Radiometer Comparison (FRC) campaigns. These are scheduled every five years and are simultaneously carried out with WMO campaigns IPC (International Pyrheliometer Comparison) and IPgC (International Pyrgeometer Comparison). During these campaigns, national meteorological centres and manufacturers of radiometric equipment install their instruments to calibrate them against the reference. Afterwards, these centres organise regional calibration campaigns to ensure traceability within their region. FRC is the campaign for photometry and AOD retrievals with filter radiometers or spectroradiometers involved. FRC are organised by PMOD/WRC and the WORCC. Last FRCs were FRC-IV (fourth FRC, in 2015, Kazadzis et al., 2018a), FRC-V (fifth FRC in 2021, Kazadzis et al. 2023) and FRC-VI (sixth FRC, 2025, Figure 4.3.4) are presented in HARMONIA. Deliverables D1.1 (Doppler et al. 2023) and D1.3 (Doppler et al., 2024) report about FRC-V and FRC-VI respectively.



Figure 4.3.4 Instruments participating to FRC-VI Campaign at PMOD/WRC in Davos (Sep-Oct, 2025)

PMOD/WRC plays a leading role in COST Action HARMONIA, in the literal sense of the word: It holds the positions of Action Chair (Stelios Kazadzis) and Grant Holder Scientific

Representative (Eliane Tobler), and has three members on the Core Group as well as two Working Group co-leaders (WG1 and WG2).

PMOD/WRC hosted the COST Action's first Management Committee meeting in Davos in May 2025 (Figure 4.3.5) and, during FRC-VI, the first meeting of Working Group 4 (Figure 4.3.6).



Figure 4.3.5 Group picture of first HARMONIA meeting at PMOD/WRC in Davos (9-10 May 2023)



Figure 4.3.6 Group picture of HARMONIA WG4 meeting at PMOD/WRC in Davos (8 October 2025)

4.4. In Italy: From the peninsula to the poles

4.4.1 The Genesis of Atmospheric Photometry in Bologna (1970s–1980s)

The origins of atmospheric sun photometry in Italy are rooted in Bologna during the late 1970s and early 1980s, primarily driven by researchers at the Institute for the Study of Microphysics and Radiation of the Lower and Upper Atmosphere (FISBAT-CNR) (Tomasi et al.,1983). Initial motivation to develop sun-photometric capabilities and establish an observational network stemmed from the need to monitor—and, where possible, provide timely warnings for—intense incursions of Saharan dust across the Italian peninsula (Prodi and Tomasi, 1983). Equally important were broader climate-related questions and the role played by aerosols in marine environments (Tomasi and Prodi, 1982). Finally, there was a growing awareness of aerosol impacts on human health and air quality. This concern was particularly acute in the Po Valley, a natural basin where high levels of industrial output caused clear, tangible environmental impacts, most notably severely degraded visibility manifesting as persistent fog.

Under the pioneering leadership of Claudio Tomasi (Figure 5.1.1 who unfortunately passed away during HARMONIA in 2024 and whom we pay tribute to ✝), the group initially focused on

evaluating atmospheric extinction, water vapor absorption, and aerosol–radiation interactions over the Po Valley—a region characterized by dense industrial pollution, persistent winter temperature inversions, and complex aerosol microphysics (Tomasi, 1982). With a broad spectrum of scientific objectives, instrument development quickly became a top priority. At the time, the only commercially available instrument was essentially the Volz photometer; in 1974, an enhanced version of the original 1959 model was released, featuring an expanded set of operating wavelengths and a broader spectral range. However, commercial instruments were expensive and difficult to maintain, as repairs could only be performed in the United States. Given the imperative to establish a local network, an in-house solution was required. Leveraging the Institute's technical resources, two primary systems were designed:

- The UVISIR System: Covered the standard spectral range up to 1 μm while offering robust coverage in the ultraviolet (UV) region, enabling measurements of atmospheric ozone (O_3) and nitrogen dioxide (NO_2). Two versions were developed: a highly portable unit that could be mounted on a compact tripod, and a fixed-site version designed for long-term monitoring stations (Prodi and Tomasi, 1983).
- The IR-RAD System: Extended spectral coverage beyond the standard 1 μm limit of conventional silicon photodetectors, reaching nearly 4 μm into the shortwave infrared region. Because traditional photodiodes could not operate at these longer wavelengths, the system was built around a thermopile detector. This design introduced significant technical challenges, particularly regarding the precise thermal stabilization required for accurate radiometric measurements. Standard quartz optics were replaced with specialized sapphire components, with the main optical entrance protected by a small sapphire window. Because its operational physics differed fundamentally from conventional solar photometers, it was designated IR-RAD to emphasize its radiometric rather than photometric nature.



Figure 4.4.1: Vito Vitale (CNR/SP, Bologna) by the installation of a sunphotometer ASP-15WL with its tracker at Monte Cimone - End of the 90s.

4.4.2 National and International Collaborations (1990s–2010s)

Initial observational campaigns were conducted across Northern and Central Italy, as well as at strategic sites in Southern Europe, to investigate regional radiative forcing, planetary boundary layer dynamics, and desert dust transport.

While early efforts to maintain a continuous Saharan dust monitoring network faced funding constraints, research rapidly pivoted toward aerosol impacts on regional climate and air quality within the Po Valley. Particular emphasis was placed on measuring precipitable water vapor and refining methodologies to retrieve trace atmospheric constituents (O_3 and NO_2) across extended wavelength ranges. These photometric activities directly supported three major initiatives:

- Complementing ground-based lidar profiling measurements, which were gaining significant momentum across Italy;
- Supporting dedicated field studies on fog formation and dynamics;
- Providing ground-truth calibration and input parameters for satellite retrievals and atmospheric transfer models.

Activities at mid-latitudes reached their peak with the group's participation in the second Aerosol Characterization Experiment (ACE-2). Coordinated by the International Global Atmospheric Chemistry (IGAC) program, the ACE projects aimed to quantify the physical, chemical, radiative, and cloud-nucleating properties of atmospheric aerosols to reduce uncertainties in global climate models (Bates et al., 1998; Raes et al., 2000). ACE-2 specifically investigated anthropogenic and natural aerosol plumes traveling thousands of kilometers from North-Central Europe to the North Atlantic during summer. By conducting coordinated observations from southern Portugal to the Canary Islands, researchers tracked particle evolution and cloud-interaction processes driven by wet deposition and aging (Raes et al., 2000). The Canary Islands provided an ideal location for *in situ* cloud–aerosol studies: at Mount Teide, the boundary layer cloud deck typically rests at 1,800–2,000 meters altitude, leaving pristine, free-tropospheric air above. Meanwhile, stations in southern Portugal characterized the outflow before its Atlantic transit. Utilizing high-performance instrumentation, the CNR group supported multi-altitude measurements across sites in Sagres, Monchique, and Mount Foia (the highest peak in the Algarve region at nearly 1,000 meters). The scientific findings of this campaign were documented in a series of landmark papers (Durkee et al., 2000; Tomasi et al., 2000; Vitale et al., 2000a, 2000b).

During the late 1990s and early 2000s, the Italian National Research Council (CNR) underwent a major structural reorganization. To consolidate research efforts and achieve critical mass in specialized fields, approximately 300 smaller institutes were restructured into roughly 100 larger, focused entities. In atmospheric science, this led to two key institutional transitions: in 1997 FISBAT in Bologna merged with the IMGA Institute in Modena to form the Institute for Atmospheric and Oceanic Sciences (ISAO-CNR). In 2002 ISAO merged with several other atmospheric research groups across Italy to form the Institute of Atmospheric Sciences and Climate (ISAC-CNR). Throughout these institutional changes, the Bologna photometry team maintained continuous observational programs and instrument development. Under ISAC-CNR, the team led several international aerosol monitoring campaigns and spearheaded the establishment of Polar photometric networks.

4.4.3 Early Antarctic Fieldwork for CNR Bologna and current State at the Institute of Polar Sciences (ISP-CNR)

Concerning Antarctica, in 1985, Italy launched the National Antarctic Research Programme (PNRA), creating a vital opportunity to apply ground-based photometric techniques to high-latitude environments critical to global climate dynamics. This contribution is reported in part 5, devoted to the polar regions in section 5.3 (Antarctica), section 5.3.2 (Italian contribution)

Concerning the current time, in 2019, the long legacy of Polar research in Italy culminated in the establishment of the Institute of Polar Sciences of CNR (ISP-CNR), bringing together specialized Polar atmospheric, cryospheric, and oceanic research groups. Today, the original Bologna photometer group operates directly within ISP-CNR.



Figure 4.4.2: The CIMEL CE318 at Monte Cimone during summer 2025.

The ISP-CNR group continues to develop and maintain ground-based aerosol optical observations, with particular emphasis on extending measurement capabilities and improving the continuity of long-term datasets. In 2026, a Prede lunar photometer was deployed at Ny-Ålesund, Svalbard (see Figure 5.2.6) in the Arctic, to provide aerosol optical depth measurements during the Polar night, complementing conventional daytime observations and contributing to the development of year-round aerosol monitoring in the Arctic. In parallel, the group operates CIMEL sun photometers at the Monte Cimone and San Pietro Capofiume atmospheric observatories in Italy (Figure 4.4.2). These measurements provide valuable information on aerosol optical properties under contrasting atmospheric conditions, from the high-altitude background environment of Monte Cimone to the Po Valley environment at San Pietro Capofiume, which is strongly influenced by regional emissions and atmospheric pollution. Together, these activities strengthen the group's expertise in photometric observations, instrumental performance assessment and the investigation of aerosol variability across different atmospheric environments, while supporting the broader scientific objectives of Polar-AOD.

4.4.4 And also in Rome (ISAC-CNR and partners)

Photometry in Italy is also the Prede and SKYNET developments from the ISAC-CNR in collaboration with UVEG of Valencia (principally Monica Campanelli for CNR and Victor Estellés for UVEG). These developments have been presented in section 3.3. ISAC-CNR manage the Prede network of Italy (as part of SKYNET/ESR) and the instrument of Ny-Ålesund (Figure 5.2.6)

In addition, ISAC-CNR in cooperation with italian software company Serco and the university Sapienza Università di Roma (Rome) and CNR Institute on Atmospheric Pollution (IIA-CNR) of

Montelibretti in the region of Latium) operates the Boundary-layer Air Quality-analysis Using Network of Instruments (BAQUNIN) supersite that brings together ground-based active and passive remote-sensing instruments to support satellite validation and planetary boundary-layer (PBL) studies. It comprises three sites: urban (Sapienza University, Rome), semi-rural (ISAC-CNR, Tor Vergata), and rural (IIA-CNR, Montelibretti). Each hosts at least one Pandora spectrometer; the Sapienza site also houses a wide range of other atmospheric remote-sensing instruments. Permanent ESR/SKYNET and AERONET sites have operated at Sapienza University since 2010 and 2016, respectively.



Figure 4.4.3: Instrument suite of the BAQUNIN site of Sapienza Università di Roma (Rome). © Picture: ISAC-CNR.

In the field of remote-sensing education, particularly photometry, Monica Campanelli of ISAC-CNR in Rome regularly organises the SORBETTO schools (Solar Radiation-Based Established Techniques for Atmospheric Observations), with support from Sapienza University of Rome and Serco. Four schools have been held: a summer school in July 2018, an online summer school in September 2021, a winter school in February 2023—with additional support from COST Action HARMONIA—and a summer school in September 2026.

ISAC-CNR is actively involved in COST Action HARMONIA, with representation on the Core Group, joint leadership of Working Group 2 with the University of Valencia, and the hosting of numerous short-term scientific missions (STSMs). The 2023 and 2026 SORBETTO schools have been important educational events for HARMONIA's early-career community. SORBETTO-III, held in February 2023, was an official HARMONIA school—the Action's first school and HARMONIA first event, just four months after it began in October 2022. Figure 4.4.4 shows the official group photo of SORBETTO-III.



Figure 4.4.4: Group picture of SORBETTO - III at the site of ESA/ESRIN in Rome

4.5. In the nordic Europe

The Nordic countries—Norway, Sweden, and Finland—have a long history of contributions to photometry, dating back to the Ångström family 100 years ago (section 2.1.2). Today, these countries remain highly active, with numerous photometry stations (see map of the currently active stations in Figure 4.5.1), strong participation in international networks and workshops, and significant contributions to the research community. The history and activities of each country are presented below.

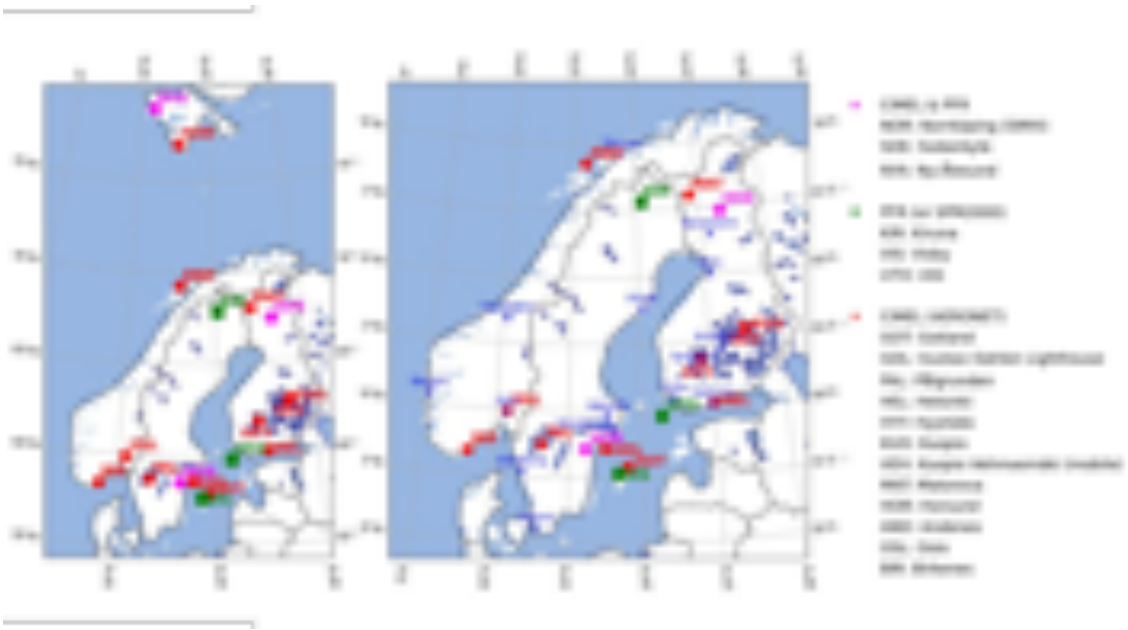


Figure 4.5.1: Map of the North-European photometer stations with indication of the instruments' type used.

4.5.1 Photometry in Norway in the past and today:

In May 2002, Physical Meteorological Observatory in Davos / World Radiation Center (PMOD/WRC), in collaboration with NILU (Norway meteorological service), started AOD observations in Ny-Ålesund as part of the global AOD network on behalf of the WMO GAW program. A Precision Filter Radiometer (PFR) is used to measure the direct solar radiation in four narrow spectral bands centred at 862 nm, 501 nm, 411 nm, and 368 nm (see Figure 4.5.2). The instrument is located on the roof of the Sverdrup station, Ny-Ålesund, close to the EMEP station on the Zeppelin Mountain (78.9°N, 11.9°E, 474 m a.s.l.).

In Ny-Ålesund, during summer months it is possible to measure day and "night" if the weather conditions are satisfactory. The sun is below 5° of elevation from 10th October to 4th March, limiting the period with sufficient sunlight to the spring and early autumn season. Lunar photometers can close the gap in obtaining a year-around aerosol climatology. As a collaborative initiative between NILU, PMOD/WRC and ISAC-CNR, seasonal deployments of a lunar photometer, which is owned by PMOD/WRC, were already made in the winters between 2014 and 2017. For further information see Mazzola at al., 2024. In the framework of the SIOS infrastructure project, multiple-season deployment started in autumn 2018.

Nowadays Ny-Ålesund is a 'super-station' with various types of photometers. Measurements taken at Ny-Ålesund by the AWI and the University of Valladolid using a CIMEL CE318-T, by the AWI with an SP1A, and the above mentioned PFR (see Figure 4.5.2), and Pulimeno (2026) for more information. An interesting example showing observations with multiple photometers is the publication by Herrero-Anta et al. (2026) on high AOD over Svalbard in summer 2019.



Fig 4.5.2: Left: GAW-PFR located at the Sverdrup station, Ny-Ålesund, Svalbard. Right: CIMEL at AWIPEV station in Ny-Ålesund, Svalbard.

Scandinavian photometer observations of aerosol properties were part of the POLAR-AOD network and discussed in the frame of the bi-Polar observations (see Toledano et al., 2006; Mazzola et al., 2012, Tomasi et al., 2015, Pulimenoa et al., 2026). The early development of the sun photometer network in Scandinavia and Svalbard is documented by Toledano et al. (2012), see Figure 4.5.3.



Fig 4.5.3: Location of sun photometer sites in the European Arctic sector and Scandinavia: (a) Until 2003: (b) From 2004 on. Colour symbols denote networks: AERONET sites (red), GAW-PFR (green), Polar-AOD (blue) - Figure and capture are from Fig. 1 of Toledano et al. (2012).

Long term records of photometer observations in Northern Norway exists from the (Arctic Lidar Observatory for Middle Atmosphere Research (ALOMAR) station (Andøya island, Norway, 69°16′N, 16°00′E) (Rodriguez, 2006, Toledano et al., 2006, Rodriguez, 2007, Chen et al., 2016). Sun-photometer observations at the ALOMAR observatory began in 2002, initially as summer

measurement campaigns. Since spring 2006, a CIMEL CE-318 solar photometer has been operated at the site on a permanent basis as part of RIMA/AERONET (see Fig 4.5.4).



Fig 4.5.4: View of the sunphotometer at the ALOMAR station.

In the southern part of Norway, the Birkenes atmospheric research station (58,23N, 8.15E, 230 m asl.) has operated since 1971 as a joint supersite for EMEP and GAW and situated. In 2009 the site was expanded with a measurement container for aerosol and climate gas measurements, including a sun-photometer. AOD measurements started in spring 2009, utilizing an automatic sun and sky radiometer (CIMEL type CE-318, see Figure 4.5.5). Calibration is performed about once per year, at the Atmospheric Optics Group at the University of Valladolid (GOA-UVa), Spain. Due to the large gaps in data acquisition, a second CIMEL instrument was purchased. It was taken into operation in fall 2018. This model CE318-T performs not only sun and sky, but also lunar light measurements, which leads to better data coverage, in particular during the winter months. Since August 2021, Vaisala CL61 Lidar Ceilometer is co-aligned with the sun-photometer.



Fig 4.5.5: Left: View of the photometer on top of the container; right: Location of the container on top of a ridge (view from the North), near the old air Birkenes pollution monitoring site.

A relatively new AERONET site can be found in southern Norway (Figure 4.5.6). The location operated by the Norwegian weather service is located on the roof of the Norwegian Meteorological Institute in Oslo (59.94200° N, 10.72100°E, 50 m). The site is expected to be mainly influenced by urban and sea salt particles. Observations started in summer 2023. It is co-aligned with CHM15k ceilometer, as seen in Figure 4.5.6.



Figure 4.5.6: The CIMEL sunphotometer is installed next to a CHM15k ceilometer on the roof of the Norwegian Meteorological Institute in Oslo.

AOD data from Svalbard, Birkenes and the Norwegian Antarctic site: Troll/Trollhaugen, are used for reporting to the Norwegian Environment Agency (e.g. Platt et al., 2025). Below, as an example, the updated Figure 4.5.7, with additional data for 2025. In Ny-Ålesund, the seasonal trends compensate each other; in southern Norway, we observe a downward trend, and the very low Antarctic values seem constant over the time period.

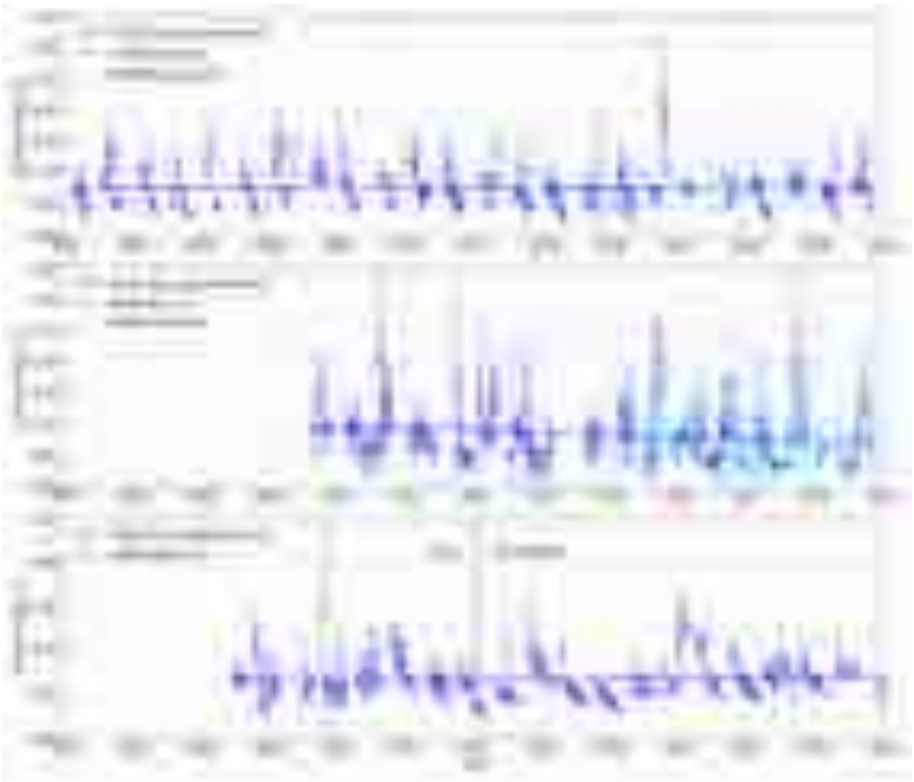


Figure 4.5.7: Time series of AOD at 500 nm wavelength in the atmospheric column above Ny-Ålesund (2002 to 2024, upper panel), Birkenes (2009 to 2024 middle panel), and Toll/Trollhaugen (2007/2014 to 2024, lower panel, sun photometer only). Monthly mean values and standard deviations are given. Sun- and moon photometer observations are shown in dark blue and cyan, respectively.

4.5.2 Photometry in Sweden in the past and today:

4.5.2.1. Background

Before narrow band sun photometers were available, the atmospheric turbidity could be estimated from pyrheliometer measurements. The total direct irradiance was measured and were combined with measurements behind one or more Schott glass filters to derive the irradiance in broad spectral bands. Since the invention of the Ångström compensation pyrheliometer, this kind of instrument was frequently used during a large part of the 20th century in Sweden. Now almost a hundred years ago, Anders Ångström, using the compensation pyrheliometer invented by his father, proposed how the wavelength dependence of aerosol optical depth, $\tau_{a,\lambda,}$ could be approximately described by the relation $\tau_{a,\lambda}=\beta\lambda^{-\alpha}$, where β is the Ångström turbidity coefficient (= τ_a at 1000nm), λ is the wavelength in μm and α is the Ångström wavelength exponent. A representative average value of α was also estimated to 1.3 by Ångström (1929 and 1961).

Unfortunately, the pyrheliometer measurements at the oldest Swedish stations were made over rather short periods and the earliest measurement results from e.g. Uppsala, Stockholm and

Abisko have not been digitized (or might not even be available on paper). The first longer time series available, of relatively frequent manual measurements with an Ångström pyrheliometer equipped with a RG2 filter, was measured with Å-171, at the Swedish Meteorological and Hydrological Institute (SMHI) in Norrköping. These measurements were carried out over the 21-year period 1977-1997. The pyrheliometer measurements were evaluated for β, assuming α =1.3, according to the tables developed for the International Geophysical Year (IGY) in 1957-1958. Combining measurements of total direct (normal) irradiance with measurements taken with a RG2 filter, the integrated direct irradiance for wavelengths <630 nm was calculated. The reason to use these values for determination of β is to avoid influence of the unknown amount of precipitable water vapor in the atmosphere. A problem which is hard to avoid in manual measurements by skilled personnel, is that they could only be performed during working days and when other work tasks allowed the Å-171 measurements to be made. Another major reason for taking the Å-171 measurements was to calibrate field instruments for the radiation network of SMHI. This also contributed to concentrate the measurements to certain periods of the year, especially spring and autumn.

The first continuous pyrheliometer measurements started in 1983 in Sweden. Then a network of twelve automatic solar radiation stations was taken in operation. All of the stations were equipped with sun trackers and Eppley NIP thermopile pyrheliometers. Using an algorithm developed by Gueymard (1998), which also assumes α =1.3, the Ångström turbidity coefficient has been calculated for all the direct irradiance measurements in the Swedish network since 1983. In the first automatic measurements the highest temporal resolution was 6-minute mean values. This is not as good as today when 1-minute means are collected, but 6-minute data are still useful for a functional cloud screening. To make the time series of beta homogenous over time the 1-minute data, introduced in 2007, are resampled to 6-minute means for the calculations of β so that the same cloud screening is applied to the whole time series.

The results show that, generally, the turbidity decreases from South to North over Sweden (Persson, 1999). Also, the effect of the major volcanic eruptions of El Chichon and Mount Pinatubo are clearly seen with strongly increased β values for a couple of years. Importantly, for non-volcanic years there is also a decreasing trend in β since the 1980-ies. The measurement results are similar at the other two long-term stations Kiruna and Visby.

4.5.2.2. Sunphotometer measurements at SMHI

To improve the coarse estimates of atmospheric turbidity and aerosol optical depth from pyrheliometer measurements the first attempts using a sunphotometer was started in the late 1980-ies at SMHI in Norrköping. However, there were numerous problems with the first instrument and the measurement setup, and it never succeeded in making the measurements operational. A better instrument was purchased in the early 1990-ies. This was a 3-channel SPM2000 (serial No. 16), an instrument that had partly been developed at PMOD/WRC and was manufactured by the Swiss company CSEM (Centre Suisse d'Electronique et de Microtechnique). After a lot of initial sun tracker problems, operational retrievals of spectral AOD at the three wavelengths 368, 500 and 778 nm could at last be started in May 1995 in Norrköping. During the first decade of measurements there are some gaps in the data when the single SPM2000 was sent to Davos for

calibration, which could result in several months of lost data. This is not a unique problem to the measurements in Norrköping.

Using multiple SPM2000s, equipped with different narrowband filters, AOD could be retrieved at many more wavelengths than just three (Schmid and Wehrli 1995; Ingold et al 2001). At SMHI an attempt was made to use a portable Licor Inc. LI-1800 spectroradiometer equipped with a collimator for spectral direct irradiance measurements and to derive AOD at many wavelengths between 300-1100 from this. However, it turned out that the LI-1800 measurements were not accurate enough to derive meaningful AOD values, especially for $\lambda<500$ nm and $\lambda>950$ nm (Carlund et al. 2003).

Since 1988, SMHI also performs total ozone measurements in Norrköping using a Brewer spectrophotometer (see Figure 4.5.8). Until 1995 measurements were taken with a Mark II Brewer and thereafter a Mark III Brewer has been used. If properly calibrated, AOD in the UV can be retrieved from the direct sun measurements of the Brewers. This was tested for a shorter period and compared with AOD values from the SPM2000 in Norrköping, as well as in Arosa/Davos and Uccle (Cheymol et al. 2006). Due to the limited resources at SMHI the Brewer AOD retrievals could not be continued in Norrköping.

In 2006-2007 the Swedish solar radiation network was upgraded. The number of stations with sun trackers and pyrheliometers was strongly reduced from twelve to three, but instead measurements with PFR sunphotometers, developed and manufactured by PMOD/WRC (Wehrli, 2000), were introduced at the three sites Kiruna, Norrköping and Visby. One of the Swedish instruments, PFR-N-35, is regarded as reference instrument and regularly calibrated against the WORCC triad in Davos and the rest of the Swedish PFRs are calibrated at the main station in Norrköping against the reference instrument using the ratio-Langley method.



Figure 4.5.8: The solar radiation station at SMHI in Norrköping. The SPM2000 is mounted to the left on the left suntracker and two PFRs are mounted to the right on the right tracker.

In Figure 4.5.9, a summary of the results from different AOD retrievals in Norrköping is plotted. Annual averages of AOD at six wavelengths are shown. The earliest datapoints are based on the manual and more sporadic measurements with Å-171 (blue line with plus signs). The major reason for the relatively low correlation between β from the Å-171 and the automatic pyrheliometer measurements (black line with dots), respectively, is the averaging of fewer and unevenly distributed datapoints over the year from the Å-171.



Figure 4.5.9. Annual mean aerosol optical depth in Norrköping. AOD at 1000 nm has been estimated from pyrheliometer measurements. AOD at the other wavelengths were retrieved from measurements of SPM2000 (S) and PFR (P) sunphotometers, respectively.

There is also a relatively large difference between the SPM2000 (indicated by “S” in the legend) and the PFR (indicated by “P” in the legend) at their coincident wavelengths 368 nm and 500 nm. Under true clear sun conditions, the AOD from these two instrument types agree very well. The SPM2000 is simply calibrated against the reference PFR in Norrköping. However, there are small differences in both measurement routines and cloud screening, which are thought to result in different selection of data points used for calculation of daily, monthly and in the end yearly averages of AOD.

The spectral AOD values from the sunphotometers are definitely more accurate than the estimates based on broadband direct irradiance measurements. On the other hand, the SPM2000 and PFR data represents shorter time series. To conclude, it is encouraging to see that results from all three measurement systems indicate small but clearly declining trends in AOD from the start of the measurements until today.

Recently, work on the next upgrade of the Swedish solar radiation network has started. Most likely, the SPM2000-measurments in Norrköping will soon be terminated. But the aim is to continue the PFR measurements at the three current stations also in the next generation of the network.

4.5.2.3. AERONET measurements in Sweden

For applications to satellite remote sensing of coastal waters and lakes three sites within AERONET has been established in Sweden. These stations are mainly operated during the summer half of the year. Principal investigators of these stations are researchers at Stockholm university as well as at the Joint Research Centre of the European Commission.

The first AERONET site was started in July 1999 on Gotland and the last month with data was May 2004 (see Figure 4.5.10). The same instrument, CIMEL #194, has also been located at SMHI in Norrköping temporarily in 2001 and 2004-2006.

From the two other marine and coastal sites there are now fairly long measurement series during summer months. The station on top of the Gurstav Dahlen lighthouse in the Baltic Sea on the Swedish east coast started in 2005 and has been operating several months each year since then. The station Pålgrunden is located on the shore of lake Vänern and has been running a number of months each year since 2008. From 2018 and 2019, also lunar AOD was introduced at Gustav Dahlen lighthouse and Pålgrunden, respectively. An example of studies using the Swedish AERONET stations was reported by Mélin et al.(2013).

So far, there have been two more very short-term AERONET stations in Sweden. From Abisko, Lapland, there were some months of measurements in 2007. And finally, at the station Onsala on the Swedish west coast, AERONET measurements were made for some months in 2024 and 2025.



Figure 4.5.10: The CIMEL sunphotometer at the AERONET station Gotland.

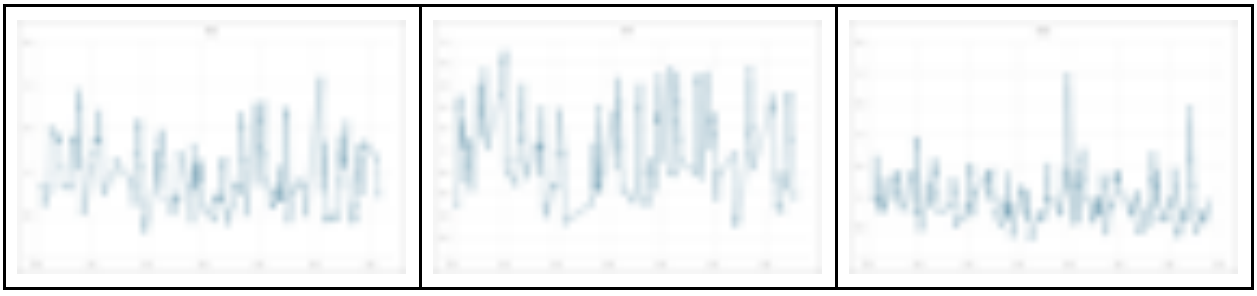
4.5.3 Photometry in Finland in the past and today:

Photometer network started in Finland by Finnish Meteorological Institute (FMI) in early 2000s with PFR instruments in observatories of Jokioinen (60.82 N, 23.50 E, 105 m asl) and Sodankylä (67.37 N, 26.63 E, 190 m asl) in 2004. At both locations, the PFR was attached to a 2AP sun tracker that had operative solar radiation sensors ready with lower tracking requirements than those of the PFRs. Furthermore, the measurements in Sodankylä and Jokioinen were located at 12-m and 24-m height towers without a guy-wire system, which caused some swaying for the

towers, although their horizons were excellent. Therefore, the results from the first years suffered from poor pointing accuracy, especially in Jokioinen. The PFR measurements in Jokioinen PFR were stopped in 2015 and moved to Utö (59.78 N, 21.37 E, 11 m asl), Finnish archipelago, in 2017. In Utö, the PFR is installed on top of a measurement container, attached as the only instrument to Kipp&Zonen SOLYS Gear Drive sun tracker (see Figure 4.5.13). From the start, the PFR pointing at Utö shows excellent tracking accuracy. In Sodankylä, the tracker has been installed on top of a DIY-stand (see Figure 4.5.13). The sun sensor could not be activated due to a mechanical problem with the tracker. Since the operational measurements cannot be interrupted and the existing problem cannot be corrected on site, the tracking problem visible in the results still persists. The plans to solve the problem are ongoing. The ambient temperatures in early spring have been lower than the recommended temperature for the instrument. Therefore, we have tested external heating cables around the PFR tube.

The measurements with CIMEL sun photometers started in 2008 in Hyytiälä (61.85 N, 24.30 E, 210 m asl.), Kuopio (62.89 N, 27.63 E, 105 m asl.), and Helsinki (60.20 N, 24.96 E, 53 m asl.), and 2013 in Sodankylä. The CIMEL instruments in Sodankylä and Kuopio were changed to triple mode versions in 2017 and 2018, respectively. Lately, FMI introduced CIMEL instruments in Matorova (68.00 N, 24.24 E, 340 m asl), Pallas in 2020 and Vehmasmäki (62.74 N, 27.54 E, 192 m asl), near Kuopio, in 2025 (see Figure 4.5.12). Unlike the other FMI sites, Vehmasmäki AERONET station is a home base for a mobile CIMEL photometer, which participates in measurement campaigns together with PollyXT lidar. In addition to standard AERONET stations, there was a CIMEL photometer at Helsinki Lighthouse ocean color station located at the Gulf of Finland, operating between 2006 and 2019. To improve the device's tolerance to icy and cold weather, FMI introduced external heating to robot units at highest latitudes, e.g. in Sodankylä. The original wet sensors have also been replaced with another implementation to avoid the igloo effect.

Being spread over a wide area throughout the country, the Finnish AOD measurement network serves as a good research platform for the dispersion of the aerosol plumes, e.g. the smoke from Russian wildfires. The existing datasets suffer from gaps due to instrument problems. Perhaps in the future, the number of the measurement stations will be decreased slightly.



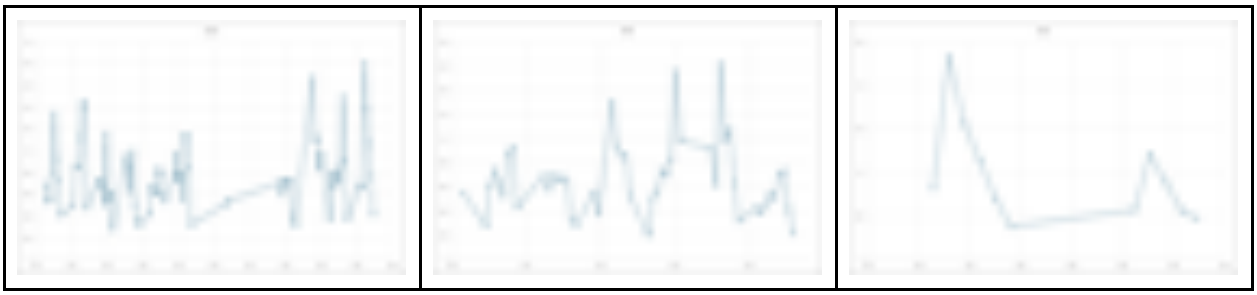


Figure 4.5.11. Monthly means of AOD at 500 nm measured with the CIMEL sun photometer at Helsinki, Hyytiälä, Kuopio, Sodankylä, Matorova, and Vehmasmäki. The data is based on AERONET Level 2.0 except for Matorova and Vehmasmäki, which are Level 1.5.



Figure 4.5.12. FMI CIMEL photometers starting from top left: Helsinki, Hyytiälä, Sodankylä, Kuopio, Matorova, and Vehmasmäki.



Figure 4.5.13 PFR sun photometers in Sodankylä and Utö.

FMI actively contributes to COST Action HARMONIA by sharing datasets for research, participating in meetings, and hosting the Action's final meeting at its headquarters in Helsinki (Figure 4.5.14).



Figure 4.5.14 Group picture of the HARMONIA Endmeeting in Helsinki (4-5 September 2026)

4.6. Photometry in France today and in the past:

Activities in photometry at the Laboratoire d'Optique Atmosphérique (LOA, CNRS-University of Lille) connect radiation physics, instrument development, retrieval methods and satellite observations. Building on early work combining solar extinction, sky radiance and polarisation, LOA developed a complete chain from instrument design and calibration to data production and scientific analysis. PHOTONS with the support from CNES, EU, ACTRIS, ESA and EUMETSAT have sustained this activity and extended it to night-time measurements, mobile platforms and synergies with lidar, spectroscopy and in situ observations.

4.6.1. Historical foundations and satellite observations

LOA's photometric observations, including rooftop measurements, date back to the 1980s. Field campaigns were already supporting satellite validation: at M'Bour, Senegal, direct-sun and diffuse-radiation measurements in April-May 1986 characterised desert-dust radiative properties (Tanré et al., 1988), establishing collaborations in Africa before PHOTONS was organised.

Photopolarimetry is another major legacy of this period. LOA research exploited light polarisation to provide additional constraints on particle properties. Balloon-borne experiments were already investigating stratospheric aerosols in the 1980s (Herman et al., 1986). This expertise later supported the exploitation of satellite polarimetric observations, particularly from POLDER and PARASOL (Herman et al., 1997; Tanré et al., 2011). This heritage is especially relevant to the international expansion of multi-angle polarimetric operational satellite observations such as 3MI. Ground-based measurements provide both a validation reference and an experimental basis for assessing the information content of polarisation and evaluating retrieval methods.



Figure 4.6.1: Milestones in photometry at LOA: (a) early ground-based instruments; (b) the first CE318 photometer deployed in Africa; (c) the LOA rooftop photometer platform; (d) the OHP sun-calibration platform; (e) the HEXTASE simulation platform at LOA; (f) instrument development, from CIMEL photometers to Advanced PLASMA; (g) the ACTRIS research infrastructure and LOA staff involved in PHOTONS; (h) the first operational shipborne CE318 photometer installation aboard R/V Marion Dufresne; and (i) the low-cost, handheld Calitoo sun photometer.

4.6.2. Retrieval methods and polarimetry

LOA's retrieval developments connect spectral extinction and angular sky radiances with aerosol optical and microphysical properties. Work on single-scattering albedo and inversions using total and polarised radiances (Devaux et al., 1998; Vermeulen et al., 2000) was extended by Z. Li at LOA, implementing Devaux's earlier approaches and codes (Li et al., 2006). Alongside the foundational AERONET inversion of Dubovik and King (2000), Fedarenka et al. (2016) demonstrated the added value of polarimetry for microphysical retrievals, supporting its integration into PHOTONS CIMEL photometers. The GRASP code was developed at LOA by O. Dubovik and colleagues (Dubovik et al., 2014). Its GRASP-AOD version retrieves size-distribution parameters and fine- and coarse-mode optical contributions from spectral AOD alone, it assumes a bimodal log-normal particle size distribution and a fixed optical refractive index constraint based on the monthly site climatology (Torres et al., 2017). In addition, GRASP has been used to retrieve the volume fractions of aerosol components by assuming known complex refractive indexes for pure species (Li et al., 2019). The code is also used in collaboration with the NASA GSFC AERONET team and LOA scientists to explore cutting-edge topics in aerosol retrievals, such as the characterization of super-coarse particles (e.g., desert dust with modal radii exceeding 10 μm) and the extension of retrieved optical properties to broader wavelength ranges (380 to 1640 nm, compared to the standard 440–1020 nm). After his time at LOA, Z. Li developed China's SONET network, extending work on multi-wavelength polarimetry, calibration and retrievals to diverse environments and satellite-validation applications (Li et al., 2018). Early 2020 photometer studies demonstrated that column observations can constrain stratospheric aerosol microphysics, including sulfate growth and persistence after Hunga Tonga in 2022 (Boichu et al., 2023) and particle properties following Raikoke in 2019 (Ruyneau de Saint-George et al., 2026). Size-mode analysis, comparisons across stations identify the stratospheric contribution. This approach is extended to biomass-burning aerosols injected by megafires developing in our changing climate.

4.6.3. AERONET and the PHOTONS National Observation Service

French-US cooperation in the early 1990s, involving CIMEL and support from CNRS, CNES and NASA, contributed to the creation of the automatic CE318 photometer and the founding of AERONET network, combining instrument automation with common calibration, processing and dissemination procedures (Holben et al., 1998). PHOTONS, the historical French component, developed through French and African stations and wider international partnerships. African observations, supported by local teams and institutions and contributions from LISA Laboratory, remain central to studies of Saharan dust, combustion aerosols and Atlantic transport. French sites and partnerships span urban, rural, coastal and island environments, including Lille, Dunkerque, Palaiseau, Clermont-Ferrand, Arcachon, Toulouse, Carpentras, Observatoire de Haute Provence, Observatoire du Pic du Midi and Mediterranean and overseas locations. The 2026 map presents active stations under LOA's responsibilities. Recognition by CNRS-INSU in

1998 established a long-term observation service covering station operation, monitoring, maintenance, instrument rotation, calibration, training and user support. AERONET network provides spectral AOD and Ångström exponents worldwide with more than 600 active sites nowadays; suitable sun-sky observations also support retrievals of size distribution, refractive index, single-scattering albedo and particle-shape indicators. Standardised processing and AERONET V3 quality control underpin data consistency (Giles et al., 2019). Records extending back to the 1990s support studies of variability, extremes and long-term change, illustrated here by Banizoumbou, Beijing and Lille. LOA's PHOTONScope processing and visualisation complements central AERONET tools through technical monitoring and real-time AOD processing for internal service and research needs. AOD uncertainty is comparable to AERONET V3, subject to differences in ancillary gas and pressure inputs. Real-time processing remains operational and also serves mobile systems. In contrast, its optical and microphysical retrievals existed only in research mode, based on Devaux, Vermeulen and Li's work (Devaux et al., 1998; Vermeulen et al., 2000; Li et al., 2006).



Figure 4.6.2: 2026 network managed at LOA, including ACTRIS NF/CF functions and the 6 ships, in total ~105 stations.

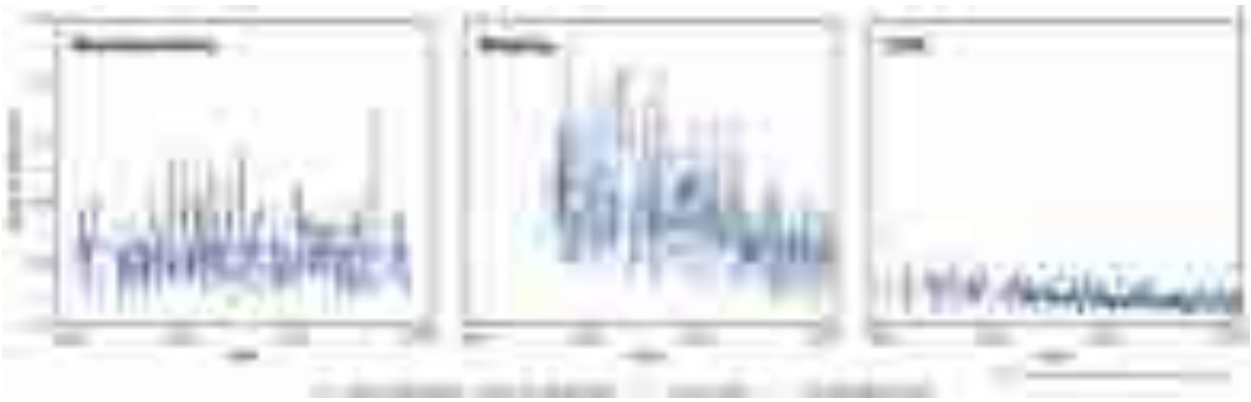


Figure 4.6.3: AOD time series at Banizoumbou (Niger), Beijing (China) and Lille (France).

4.6.4. Calibration, metrology and traceability

PHOTONS has progressively developed calibration capacity for French stations and international partners. In 2001, following the 11 September attacks in the United States, a decision was made to undertake all French calibration activities within the PHOTONS mission in France. These activities were organised at Lille and Carpentras, in collaboration with Météo-France, and later at the Observatoire de Haute-Provence. The calibration chain also draws on observations at sites suitable for calibrating reference instruments and in cooperation with international partners, including NASA, the University of Valladolid's (Group GOA-UVa) and AEMET at Izaña Atmospheric Observatory. Calibration activities are conducted in close cooperation with NASA, using a shared tool developed by NASA. This cooperation supports consistent procedures across AERONET. LOA also has an equivalent tool developed in-house for its R&D needs. The European Space Agency supports LOA's photometric activities, particularly calibration, metrology and measurement traceability, to meet metrology requirements for the validation of satellite observations.

The solar calibration chain combines the determination of extraterrestrial calibration constants using the Langley method with their transfer to field instruments through intercomparison. Pre- and post-deployment calibrations, maintenance and documentation of instrument history are essential for monitoring drift and ensuring traceable records. Sky-radiance and polarisation measurements require dedicated laboratory characterisation and instrumental references.

LOA has also developed calibration-transfer methods. Li et al. (2008) described the transfer of direct-sun calibration to sky radiances based on characterisation of the instrument's solid angle. This indirect calibration method, known as Direct-Sun-to-sky transfer, links the sun and sky channels through prior characterisation and appropriate calibration. Not yet operationally used, it offers a promising complementary approach to monitoring radiometric consistency and simplifying network management.

Developments also address polarisation. Li et al. (2010) proposed a calibration of the degree of linear polarisation using sunlight. The quality of this characterisation determines how effectively polarimetric information can be used in retrievals. Li et al. (2016) subsequently presented a method for transferring solar calibration to the lunar calibration coefficient. This complements CE318T developments enabling night-time AOD measurements (Barreto et al., 2016). Lunar

photometry extends temporal coverage, depending on lunar phase and visibility and provides further opportunities for comparison with night-time lidar observations.

4.6.5. ACTRIS and photometer-lidar networks

ACTRIS-1 (2011-2015) and ACTRIS-2 (2015-2019) strengthened European calibration and quality-assurance services. French-Spanish cooperation, coordinated with NASA, was central to AERONET-Europe. Micro-lidars installed at Lille and Dakar in 2006 established routine synergies between column photometry and vertical profiling. At Dakar-M'Bour, nearly a decade of combined measurements supported aerosol climatology and radiative-effect studies (Mortier et al., 2016); GARRLiC provided a methodological milestone in joint photometer–lidar inversion (Lopatin et al., 2013).

National tropospheric lidar activities joined the PHOTONS perimeter in 2019. Within ACTRIS-RI, the Center of Aerosol Remote Sensing (CARS) coordinates aerosol remote-sensing expertise and quality assurance. Lille and OHP combine National Facility observation functions and French activities of the CARS Central Facility, both shown on the map. Partnerships also link photometry with Météo-France's operational micro-lidar network, deployed from 2016 with an instrument co-located with LOA, and the UK Met Office lidar–photometer network for volcanic-ash monitoring.

4.6.6. Mobile photometry and synergies at sea

Mobile observations resolve spatial gradients and cover gaps between fixed stations. PLASMA, whose specifications began in 2003, measures spectral extinction above aircraft altitude and supports comparison with lidar profiles (Karol et al., 2013). MAMS combines photometry, lidar and in situ measurements on a ground-based mobile platform for pollution, transport and satellite-validation studies. MAMS is capable of on-road aerosol measurements, demonstrating its versatility for aerosol characterization during campaigns (Popovici et al., 2018, 2022; Warneke et al., 2023; Sanchez Barrero et al., 2024).The recently established HEXTASE simulation platform supports further mobile photometry development.

Shipborne adaptations developed with CIMEL maintain solar and lunar tracking despite vessel motion. Within AERONET-SPARROW, LOA manages photometric observations on six ships in 2026: R.V. Marion Dufresne, R.V. Gaia Blu, R.V. Sarmiento de Gamboa, R.V. Mário Ruivo, Persévérance and MS Richard With, all represented on the map in Figure 4.6.4. MAP-IO has supported recurrent observations aboard Marion Dufresne since 2021. Torres et al. (2025) documented the adapted CE318T, three years of automated AERONET-compatible observations (July 2021-June 2024) and sun-sky aerosol retrievals at sea.

TRANSAMA campaign combined a CE318T photometer and micro-lidar during the April-May 2023 Réunion-Barbados crossing (Sanchez-Barrero et al., 2026a). Complementary educational activities use the handheld Calitoo photometer co-developed by TENUM, LOA and CNES through the Calisph'Air educational program. CALINET database provides online access to these measurements and geolocated plots. Access CALINET data

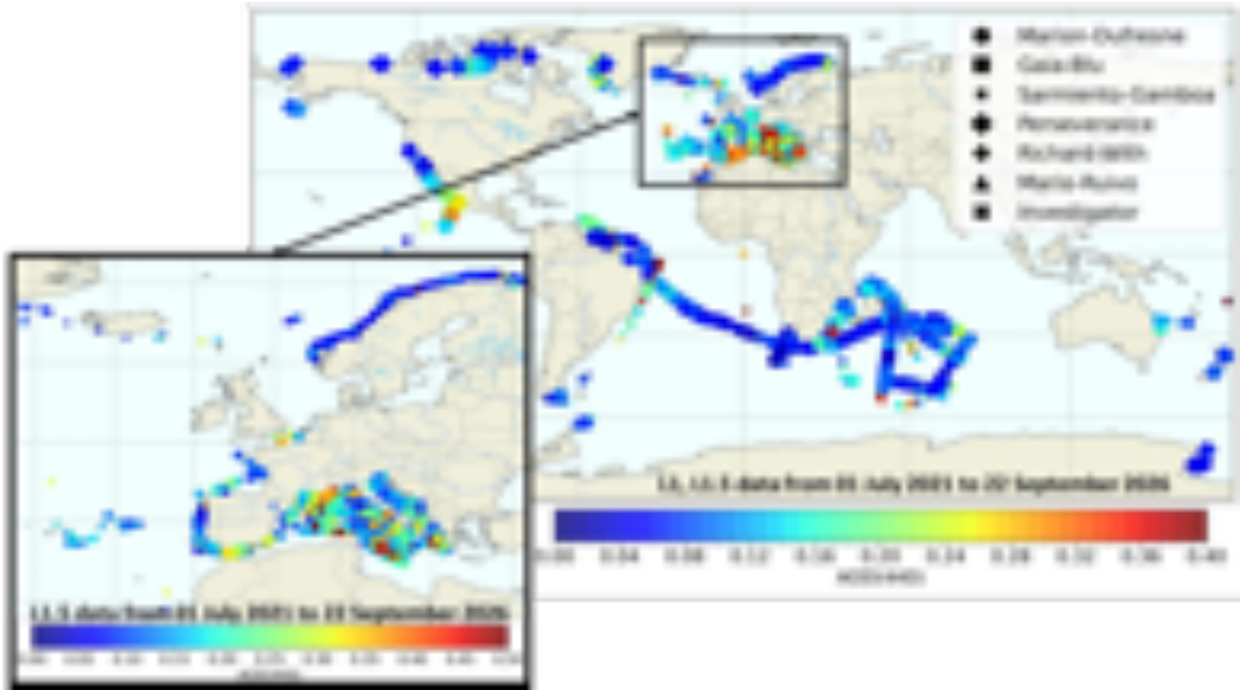


Figure 4.6.4 : AERONET-SPARROW vessels, main operating regions and observation coverage (source figure : Sanchez-Barrero et al., 2026b)



Figure 4.6.5: Various mobile vectors involving PLASMA mobile photometers.

4.6.7. AGORA-Lab and LOA-CIMEL cooperation

Decades of LOA-CIMEL cooperation have translated station and campaign requirements into automated, reliable instruments with polarimetric, lunar and mobile capabilities. Established in 2020, AGORA-Lab provides a joint framework for instrument development. Tests at observation

platforms and during campaigns connect research and instrumental expertise with operational feedback, improving instruments and measurement and calibration procedures.

4.6.8. Next steps

The continuation of these activities depends first on preserving long-term records and their metrological quality. Measurement continuity, calibration traceability and documentation of instrument changes determine their value for investigating atmospheric change.

Future directions include expanded mobile and oceanic measurements and products combining photometry with lidar and in situ. Ground-based polarimetry remains essential for evaluating retrieval methods and supporting satellite observations. Fixed stations provide enduring references, while mobile platforms help assess the spatial representativeness of satellite comparisons.

These developments are accompanied by initiatives to establish a complete, sovereign and resilient European system for processing photometric data. Designed to meet operational needs, these initiatives will combine service continuity and control over processing with a strong capacity for instrumental and software innovation. It would support new products and strengthen services to the scientific community within a framework of international cooperation and interoperability with existing networks.

4.7. Photometry in Austria, Pandora and Pandonia network

4.7.1 The Innsbruck Atmospheric Observatory (IAO-MUI)

In Austria, one of the main sites for solar radiation measurements is located in Innsbruck, where the working group Solar Radiation and Air Quality of the Medical University of Innsbruck (MUI) operates its instruments on the roof of a university building close to the city centre, at the bottom of the Inn Valley (47.26 N, 11.39 E, 620 m a.s.l.). These long-term measurements are today also part of the more recently established Innsbruck Atmospheric Observatory at MUI (IAO-MUI); Karl et al., 2020). While the IAO focuses mainly on in-situ observations of urban air quality and climate, the MUI measurements contribute the radiation and column remote-sensing component.

Spectral and broadband UV irradiance has been measured routinely since 1995. Since then, the following instruments have been added to the measurement programme:

- since 2000: all-sky camera (ASI, Schreder; Kreuter et al., 2009)
- since 2006: Precision Filter Radiometer (PFR) sun photometer, calibrated at PMOD/WRC in Davos, but not officially part of the GAW-PFR network
- since 2016: Pandora spectrometer systems (e.g. Pandora 106 and 110), operated by LuftBlick within the Pandonia Global Network (PGN)
- since 2022: CIMEL CE318 photometer, AERONET station Innsbruck_MUI
- since 2023: BTS-UV (300–440 nm) and BTS-IR (1400–1700 nm) diode-array spectroradiometers

The PFR provides a continuous AOD record since 2007 (Fig. 4.7.1), whose climatology and trends at this Alpine valley site have been analysed by Wuttke et al. (2012) and, for the extended

period 2007–2023, by Wagner et al. (2024). Since 2022, the co-located CIMEL provides an independent, parallel AOD record within AERONET.



Fig. 4.7.1: AOD from PFR measurements in Innsbruck since 2007: range of single measurements, daily medians, monthly geometric means and monthly climatology (mean ± standard error).

Other Austrian sites measuring AOD within AERONET are located in Vienna, at the University of Vienna and at the University of Natural Resources and Life Sciences (BOKU), and on the Gerlitzen, a mountain site in Carinthia (South of Austria).

Within ACTRIS, MUI together with LuftBlick, operates a calibration unit of the Centre for Reactive Trace Gases Remote Sensing (CREGARS), and the IAO is also a National Facility (NF) for in-situ trace-gas measurements.



Fig. 4.7.2: Atmospheric radiation measurements at the Innsbruck Atmospheric Observatory. Left: BTS-UV and BTS-IR spectroradiometers and CIMEL photometer; right: two Pandora systems.

4.7.2. Pandora and the Pandonia Global Network (PGN)

Pandora is a spectrometer system based on a diode-array spectrometer, designed for direct-sun and sky spectral measurements in the ultraviolet and visible. Its primary purpose is the retrieval of atmospheric trace gases: total columns of O_3, NO_2, SO_2, HCHO and H_2O from direct-sun

spectra, and tropospheric columns and near-surface concentrations from sky scans. A prototype of the instrument was developed within a NASA project in 2007 (Herman et al., 2009).

Since 2019, the instruments have been operated as the Pandonia Global Network (PGN) by LuftBlick in Innsbruck, as a collaboration between ESA and NASA with support from further agencies such as EUMETSAT and NIER (Korea). The network provides standardised instrument calibration, common operation and central processing, delivering quality-controlled data products in near-real time. Today the PGN comprises more than 220 instruments worldwide and serves as a major reference for the validation of satellite trace-gas products.

Although Pandora is primarily a trace-gas instrument, its absolutely calibrated direct-sun spectra in principle also allow the retrieval of spectral AOD across the UV–VIS range. However, as the radiometric stability of the instrument is limited, AOD is not (yet) an operational PGN product. Pandora also measures in direct-moon mode, providing nighttime NO_2 and NO_3 columns.

5. The specificity of Polar regions

One region of the globe deserves particular attention: the polar regions, both Arctic and Antarctic. Aerosols play a distinctive role in the climate of these regions (Schmale et al., 2021, 2022; Graßl, 2025; Pulimeno, 2026). Low solar elevation angles, the high albedo of snow-covered land and sea ice, and low clouds can trap solar radiation in the lower troposphere, where aerosols are present. This can enhance aerosol absorption and, in turn, disrupt the radiative balance (Graßl et al., 2024; Graßl, 2025). It is therefore important to characterise aerosols accurately, particularly by measuring AOD in polar regions.
Our aerosol remote-sensing, AOD-measurement, and photometry community has taken up this challenge. The polar regions experience several months of darkness each year—during the austral winter (May–August) and the boreal winter (November–February). This has encouraged the development of instruments capable of measuring aerosols during the night: first stellar photometers in the 1990s (section 2.2), followed by lunar photometers in the 2010s (section 2.3).
In this part, we first outline the history of photometry in the polar regions (section 5.1) and then review the current state of the art (5.2), focusing first on the Arctic (5.2.1) and then on the Antarctic (5.2.2), with an emphasis on the contributions of the institutes active in polar photometry.

5.1 Historical approach of AOD retrieval in Polar regions

5.1.1 Polar-AOD: Long-term observations and advances in Polar aerosol research

The Polar-AOD programme represents a long-standing international effort to improve the characterization of atmospheric aerosols in the Arctic and Antarctic through coordinated measurements of aerosol optical depth (AOD) and related optical properties. Developed with a substantial contribution from the Italian National Research Council (CNR), the programme brings

together observations from different Polar research stations and international monitoring networks, providing a common framework for investigating the spatial distribution, seasonal variability and long-term evolution of atmospheric aerosols in high-latitude environments (Polar-AOD, 2026).

The characterization of aerosols is particularly challenging in Polar regions, where generally low aerosol concentrations, extreme meteorological conditions, large solar zenith angles and prolonged periods of darkness limit the applicability of conventional measurement techniques. Furthermore, the remoteness of Polar stations and the uneven geographical distribution of observations make the development of consistent, long-term datasets particularly important.

5.1.2 Development of the programme and scientific achievements

The Polar Aerosol Optical Depth (Polar-AOD) programme originated in October 1999, during a meeting in Bologna between researchers from the Italian National Research Council (CNR) and the US National Oceanic and Atmospheric Administration (NOAA), who were already conducting aerosol optical measurements at selected Arctic and Antarctic sites, including Terra Nova Bay, South Pole and Barrow. Under the initial leadership of Claudio Tomasi (ISAC-CNR), the initiative aimed to establish an international network of sun photometers for the long-term monitoring of aerosol optical depth (AOD) in Polar regions, promoting data sharing, harmonized measurement procedures and collaborative scientific analyses. A first instrumental intercomparison was conducted at Mario Zucchelli Station during the 2002–2003 austral summer, while a workshop held in Bologna in 2003 formally established Polar-AOD as an international programme, expanding participation to several European and North American research institutions. The programme subsequently gained international recognition as a legacy project of the International Polar Year 2007–2008 (IPY Project No. 171), with the objective of characterizing the spatial distribution, seasonal variability and long-term trends of aerosol optical properties and their effects on the Polar radiation budget. During the IPY, Polar-AOD involved approximately 40 research groups from 22 countries, collecting observations at 15 Arctic and 16 Antarctic sites, with ISAC-CNR playing a leading role in coordinating intercalibration activities, data management and scientific analyses. Over the following decades, the programme progressively expanded its observational capabilities, incorporating airborne measurements and lunar photometry to address the challenges of aerosol monitoring during the Polar night. Since 2023, ISP-CNR has renewed the programme's coordination and visibility through the development of the Polar-AOD web platform, aimed at preserving historical observations and facilitating access to aerosol optical measurements collected across both Polar regions (Polar-AOD, 2026).

The scientific foundations of Polar-AOD were established through the systematic collection and analysis of historical aerosol observations from Arctic and Antarctic stations. An important early contribution was provided by Tomasi et al. (2007), who compiled several decades of aerosol optical measurements to investigate the characteristics and long-term evolution of Polar aerosols. Their analysis highlighted a general decrease in background aerosol optical depth in the Arctic over the preceding decades, while no statistically significant long-term trend was identified for Antarctica. The study also demonstrated the value of combining historical observations from

different instruments and locations to investigate large-scale changes in Polar atmospheric composition.

An important contribution to Arctic aerosol research was made during the PAM-ARCMIP airborne campaign in April 2009, conducted aboard the AWI Polar-5 research aircraft. The campaign employed an eight-channel sun photometer jointly developed by NOAA and ISAC-CNR to investigate the horizontal and vertical distribution of aerosol optical depth across the Arctic. As reported by Stone et al. (2010), the measurements revealed widespread Arctic haze, with AOD at 500 nm ranging from approximately 0.12 to more than 0.35, significantly higher than typical background conditions. Aerosol extinction was generally greatest within and immediately above the near-surface temperature inversion, highlighting the influence of long-range transport of anthropogenic pollution from Eurasia. The study demonstrated the value of airborne sun photometry for providing a three-dimensional characterization of Arctic aerosols and complementing observations from ground-based monitoring stations.

Building on these results, the programme progressively addressed the need for improved comparability among the different photometric instruments operating at high latitudes. The Polar-AOD intercomparison campaigns, described by Mazzola et al. (2012), represented an important methodological milestone. These activities evaluated the performance of different Sun photometers under challenging Polar observing conditions, with particular attention to calibration procedures, instrument characteristics and the uncertainties associated with measurements at large solar zenith angles. The results helped identify instrumental limitations and improve the consistency of AOD retrievals, providing a stronger basis for the integration of observations from different stations and monitoring networks.

Subsequent studies substantially expanded the geographical and temporal coverage of the Polar-AOD dataset. Tomasi et al. (2012) updated the analysis of Polar aerosol optical properties using observations collected during the International Polar Year, examining long-term variations in aerosol optical depth and Ångström exponent at several Arctic and Antarctic stations. The results highlighted the importance of distinguishing background aerosol conditions from episodic perturbations associated with volcanic eruptions, Arctic haze and biomass-burning emissions. In particular, the analysis found no substantial long-term change in summer background AOD at Ny-Ålesund and Barrow over the periods considered, illustrating the sensitivity of trend estimates to the selection of aerosol conditions and observation periods.

A further major contribution was the comprehensive review by Tomasi et al. (2015), which combined multi-year photometric observations from 12 Arctic and 9 Antarctic sites with information on aerosol microphysical properties, atmospheric transport and radiative effects. This study established an extensive reference framework for Polar aerosol remote sensing, highlighting differences between Arctic and Antarctic aerosol regimes and providing a basis for subsequent analyses of long-term variability. Complementary methodological investigations also addressed the specific challenges of high-latitude observations, including the characterization of Rayleigh-scattering optical depth and the calculation of optical air mass under Polar atmospheric conditions (Tomasi et al., 2010, 2015). These contributions improved the physical consistency of

aerosol retrievals and helped reduce systematic uncertainties associated with the extreme observing geometry typical of Polar regions.

A major limitation of conventional Sun photometry in Polar regions is the absence of sunlight during the Polar night. Addressing this observational gap has become an important component of Polar-AOD activities. Herber et al. (2002) presented the first measurements with stellar photometer (developments of Leiterer et al. 1995) in Ny-Ålesund and Mazzola et al. (2024) demonstrated the success of monitoring aerosol optical depth during the Arctic winter using modified photometers capable of exploiting moonlight as an alternative radiation source (developments of Berkoff et al., 2011 and Barreto et al., 2013). Measurements performed at two Arctic sites showed that lunar photometry can provide reliable AOD observations even under the very low aerosol loading conditions typical of the Polar atmosphere, with uncertainties comparable to those obtained using conventional solar measurements. This methodological development represents a significant step towards more continuous aerosol monitoring throughout the year and reduces the seasonal bias traditionally affecting Polar AOD climatologies.

The most comprehensive recent synthesis of the programme's scientific results was presented by Pulimeno et al. (2026), who analysed aerosol optical properties from 15 Arctic and 11 Antarctic sites, extending the historical dataset through December 2024. The study combined ground-based solar photometry with lunar and stellar observations, allowing a more complete characterization of seasonal aerosol variability, including periods previously affected by substantial observational gaps. The analysis confirmed important differences between Arctic and Antarctic aerosol regimes. In the Arctic, aerosol optical depth generally reaches its highest values during winter and early spring, reflecting the influence of Arctic haze and the long-range transport of anthropogenic pollution from mid-latitude source regions. Long-term observations indicate an overall decline in AOD at several Arctic sites, consistent with reductions in anthropogenic emissions, particularly in Europe. At the same time, biomass-burning emissions are emerging as an increasingly relevant source of aerosol variability, with episodic transport events capable of producing substantial enhancements in atmospheric aerosol loading. In Antarctica, aerosol optical depth is generally lower over the high-altitude interior plateau than at coastal stations, reflecting differences in aerosol sources, transport pathways and atmospheric conditions. The analysis also revealed seasonal changes in aerosol particle-size characteristics, with a relatively stronger contribution from fine-mode particles during summer and autumn and from coarse-mode particles during winter and spring. Positive AOD trends were identified at some Antarctic stations, although their interpretation requires caution because of observational uncertainties, instrumental changes and the limited temporal coverage of some datasets.

Beyond these regional findings, Polar-AOD has contributed to the development of a more coherent observational framework for comparing aerosol conditions between the two Polar regions. The integration of observations from different stations and measurement techniques supports the investigation of aerosol transport processes, the evaluation of atmospheric models and satellite retrievals, and the assessment of aerosol-related climate effects.

5.1.2.1 International cooperation, data integration and future perspectives

An important characteristic of Polar-AOD is its international collaborative structure, involving research institutions and observational programmes operating across both Polar regions. The programme has promoted the exchange of measurements, methodological expertise and scientific results, while encouraging harmonized data processing and improved documentation of observational uncertainties.

5.1.2.2 International Polar-AOD meetings and workshops

Over the years, the Polar-AOD programme has organized several international meetings, workshops and instrument intercomparison campaigns to strengthen scientific cooperation and improve the quality and consistency of aerosol optical measurements in Polar regions. Following the initial meeting in Bologna, major activities included the sun photometer intercomparison campaigns at Ny-Ålesund (2006) and Izaña, Tenerife (2008), which contributed to the harmonization of measurement procedures and data processing (Mazzola et al., 2012). With the growing interest in extending AOD observations throughout the Polar night, subsequent activities increasingly focused on lunar photometry, including the first Lunar Workshop in Valladolid (2015, Fig. 4.2.7), a further intercomparison campaign at Izaña (2017), and the Polar-AOD Lunar Retreat hosted by Robert Stone in North Canaan, Connecticut (2019), see Fig 5.12.



Figure 5.1.1: Claudio Tomasi (1939 - 2024) at the first Polar-AOD workshop in Bologna, Italy, in 2003.

These initiatives promoted the evaluation of lunar irradiance models, calibration strategies and instrumental performance under nighttime conditions (Barreto et al., 2019). In 2020, a dedicated Lunar-AOD intercomparison campaign was conducted at Ny-Ålesund, involving CNR, NOAA, AWI and other international partners. Together, these activities have played an important role in consolidating the Polar-AOD scientific community, fostering methodological developments and supporting coordinated long-term aerosol observations across the Arctic and Antarctic (Polar-AOD, 2026).



Figure 5.1.2: The group of scientists participating to the Polar-AOD 2019 Retreat in North Canaan (USA).

Overall, Polar-AOD demonstrates the importance of sustained international cooperation and long-term observations for understanding atmospheric changes in the Polar regions. Through its scientific publications, methodological developments and integration of multi-station datasets, the programme has provided a significant contribution to Polar aerosol climatology and established a valuable foundation for future investigations of aerosol–climate interactions in the Arctic and Antarctic.

5.2 AOD in Polar regions today

Continuous measurements of AOD in the Polar region is a necessary task for environmental monitoring for a number of reasons. First, due to the typically high surface albedo and low solar elevations, aerosols and clouds which tend in other regions to cool the planet will have a warming effect in the Polar regions. Second, the low convection over the cold Polar regions reduces upgliding of air parcels, compared to low- or mid latitudes, hence cloud properties and life-time will depend more critically on aerosol than elsewhere. In fact, the high cloud cover over large parts of the Arctic and the Southern Ocean is a surprise, given the frequently clean conditions (Fiddes et al. 2022). Overall, the complex interactions between the shallow and stable Polar boundary layer and knowledge deficits on clouds and aerosol in this part of the world result in a large uncertainty in current global climate models (Griesche et al. 2024, Fu et al. 2026). Finally, the deposition of absorbing aerosol like BC on snow can potentially decrease the albedo and lead to an increased melt rate. While this effect may overall be small (+0.17Wm2), further observations are highly needed to constrain this value (Zhang et al. 2024).
A recent overview of Polar AOD measurements has been presented by Pulimeno et al. 2026. In table 1 of this paper, 17 Arctic sites, north of the Polar Circle, are summarized, which are or very recently have been active in monitoring the AOD. They are distributed all over the Arctic (Canada: 4 sites, Alaska: 3 sites, Greenland: 3 sites, Svalbard: 3 sites, Scandinavia: 3 sites, Russia: 1 site). However, in the sector between 30° E and 180° E only Cape Baranona (79.1° N, 101.3° E) contributes to measurements in the Eastern part of the Arctic.

5.2.1 Today in the Arctic

A typical annual cycle for Arctic AOD is given in the Figure 5.2.1 below. It is taken from Pulimeno et al. 2026 and describes the multi-annual mean of AOD (at 500nm, left) and the Ångström exponent (right, measured between 440nm and 870nm) for the site Thule in NW Greenland. The figure shows: i) typically low AOD_500 values below 0.1 ii) a slight annual cycle with more AOD and larger particles in late winter and early spring. These increased values of AOD at a lower Ångström exponent are due to the Arctic Haze phenomenon (Shaw 1995, Quinn et al. 2007).
The smaller particles in summer are due to local aerosol production from the Arctic Ocean. These particles are younger than the Arctic Haze in winter, when cold temperatures and stable vertical temperature gradients reduce wet deposition. For this reason the particles can slowly grow into the accumulation mode in winter (Shaw 1995, Stohl 2006).
This typical annual cycle of Arctic AOD agrees to aerosol in-situ measurements in the atmospheric boundary layer, which also report fewer but larger particles in late winter and spring, while the summer months are dominated by very small aerosol that hardly scatter visible light (Tunved et al. 2013, Freud et al. 2017).

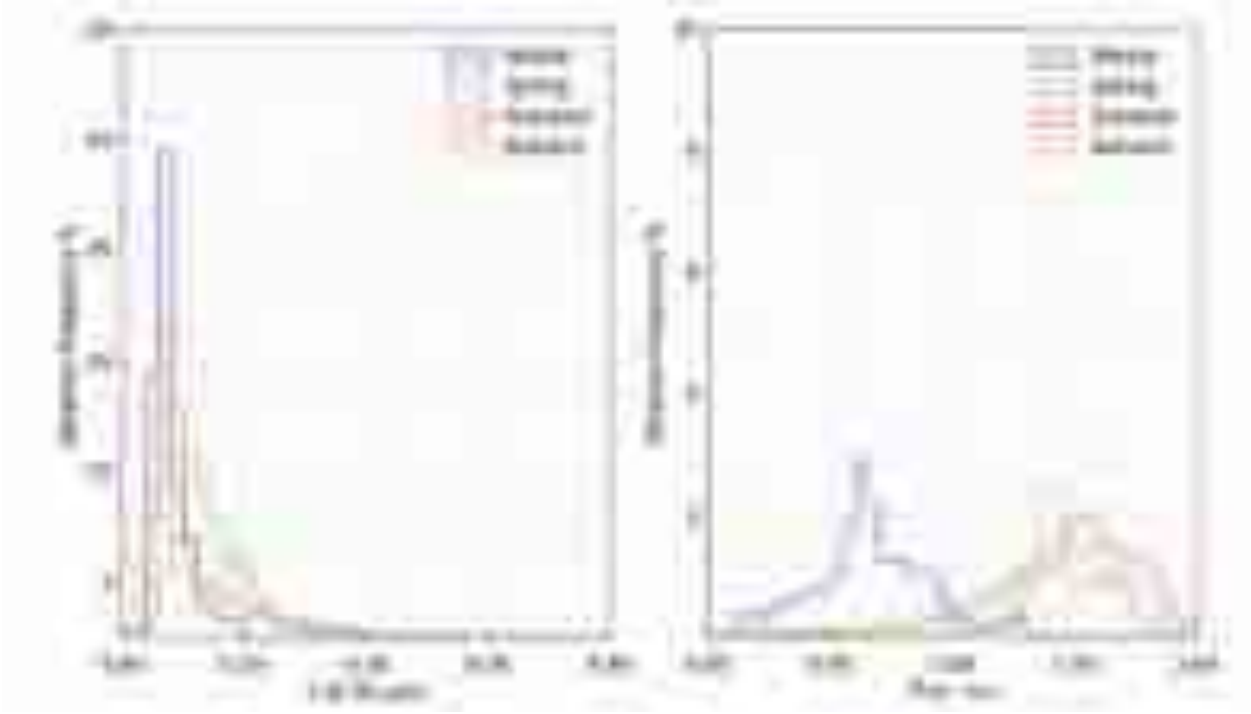


Figure 5.2.1: AOD (right) and Angstroem exponent (left) for Thule, Greenland. Data from 2007 to 2023 has been considered, Figure taken from Pulimeno et al., 2026.

There are aerosol distributions, which deviate from Fig 5.2.1. This can either be due to a sheltered location, which is protected from high wind speeds that favor long range advection from aerosol source regions. Another possibility is that Arctic sites in summer are affected by biomass burning aerosol from the northern continents or from local dust. An example for this pattern is shown in Figure 5.2.2 for the site Kangerlussuaq in West Greenland. Here it can be seen that in summer few events of high AOD occur. However, the different seasons show a similar pattern for the Ångström exponent as the difference between winter / spring to summer / autumn is not very pronounced.

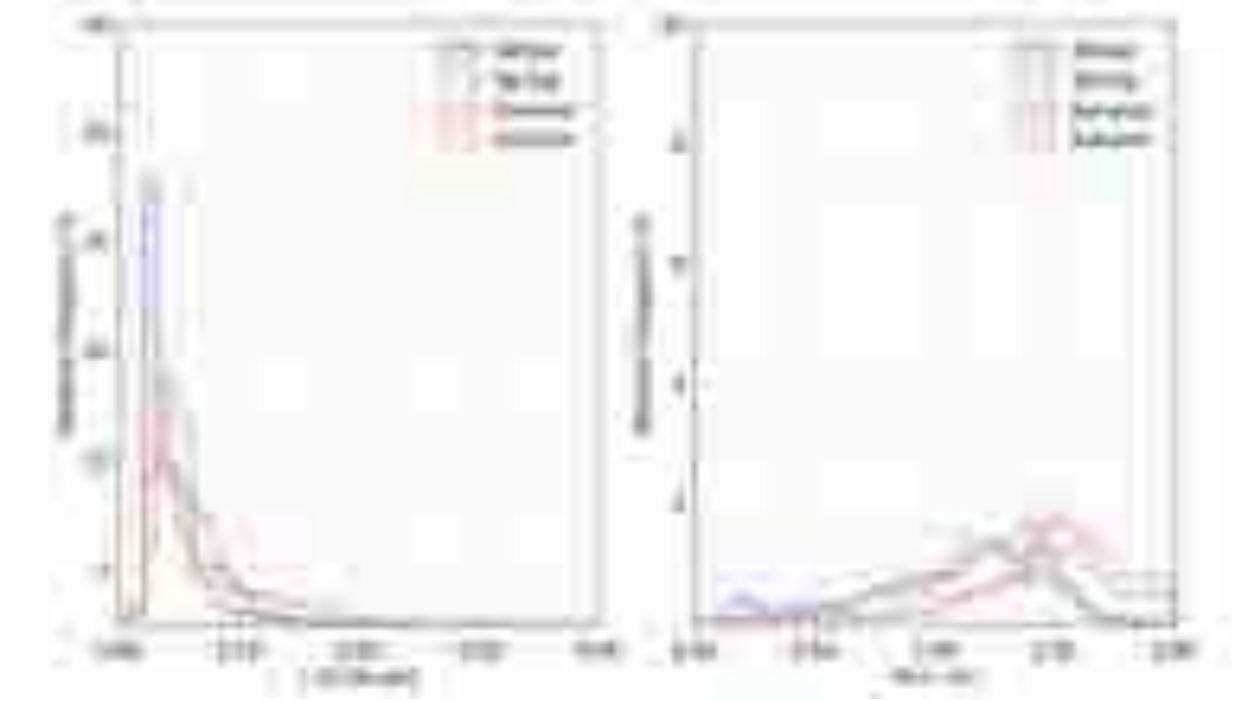


Fig 5.2.2: AOD (left) and Angstroem exponent (right) for Kangarlussuaq, W Greenland.

A trend analysis of how the AOD changes over time has been performed by Pulimeno et al. 2026 for the Norwegian site Andenes and by Graßl et al. 2024 for Ny-Ålesund (Spitsbergen Svalbard). While for Andenes a small decrease of AOD of 2.4% per year in the period from 2004 to 2024 has been found, a trend for Ny-Ålesund is not clear, see Fig 5.2.2. The most striking feature is the extreme high AOD of Aug 2019. This is caused by several events, mostly biomass burning that entered the European Arctic both in tropo- and stratosphere (Herrero-Anta et al. 2026). Apart from this month, it can be seen that winter is the most interesting season: In the early years (2004 to 2008) the mean AOD in Jan and Feb decreases clearly. Between 2010 and 2018 the AOD was quite constant for all seasons. However, starting in 2020 there is a clear trend for rising AOD in Nov and Dec. The reason for this increasing trend is not completely clear yet.

Graßl et al. 2024 briefly discussed the possibility that winter time AOD in the Arctic may be affected by Polar Stratospheric Clouds (PSCs). In Ny-Ålesund, parallel observations of PSCs in photometer and lidar do exist. For a limited set of observations it seems that the PSC over Spitsbergen typically consist of particles which are larger than the tropospheric aerosol, hence potentially reducing the Ångström exponent. However, Graßl et al. 2024 concluded that the annual cycle of AOD in Ny-Ålesund is probably not significantly disturbed by PSCs. A similar picture may be true for other Arctic sites as well: The low Angstroem exponent of Thule in winter (Fig 5.2.1) may be an indication that PSCs may have contributed. However, the winter AOD is nevertheless very low.

As climate variability (sea currents, mean air flow, albedo changes) affect both sources and sinks of aerosol in the Polar regions, no definite prediction on future aerosol distributions can be made without further monitoring.

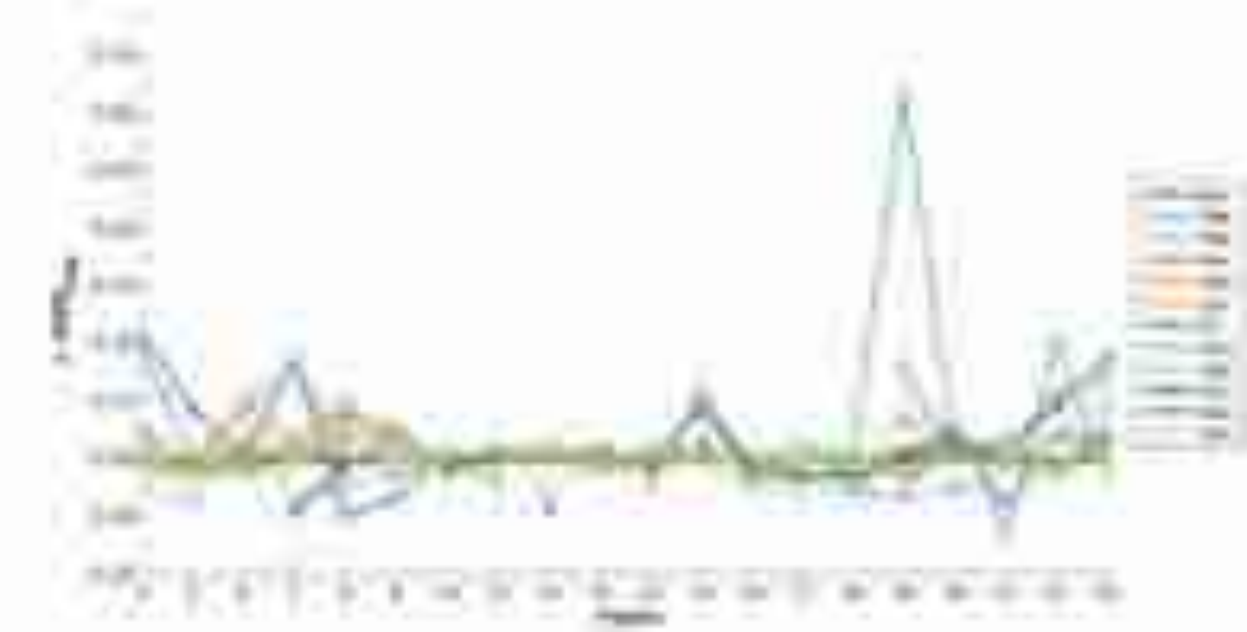


Fig 5.2.3: Trends in AOD for Ny-Ålesund, Spitsbergen, taken from Graßl et al. 2024.

5.2.2 Spanish contribution

The GOA-UVa group of University of Valladolid has participated in various campaigns and experiments in the Arctic since 2002 (e.g. Toledano et al., 2006; Herrero-Anta et al., 2026). Two long photometric datasets are maintained: ALOMAR (Arctic Lidar Observatory for Middle Atmosphere Research) station (Andenes, Andøya Island, Norway, 69N, 16E) since 2006, in collaboration with the Andøya Space Center; and Ny-Ålesund, on Svalbard (79N, 12E), since 2017, in collaboration with the Alfred Wegener Institut (see AWIPEV in section: 5.2.3). Lunar photometry intercomparison campaigns and workshops were organized at Izaña, Valladolid and Ny-Ålesund, mainly focused on Polar night aerosol monitoring. Since 2024, shipborne mobile automatic observations have been carried out with the RV Sarmiento de Gamboa (see map on figure 5.2.4) on several campaigns reaching Iceland and north Atlantic waters. These observations are part of a very recent effort led by the University of Lille (group LOA) and with strong support by the European space agencies, given the high value of data over water for satellite calibration-validation purposes.

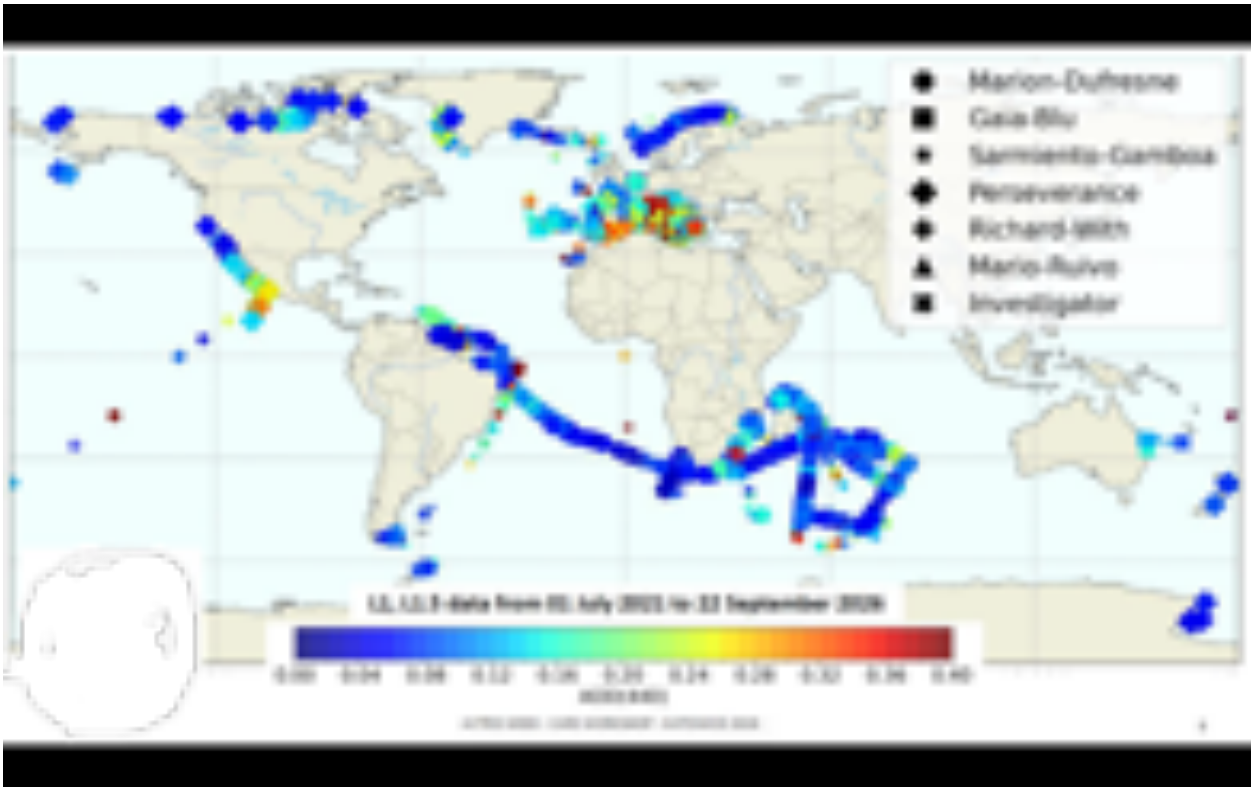


Figure 5.2.4: Shipborne traces of AOD measurements in the past 5 years (2021 - 2026)

5.2.3 The AWIPEV station

AWIPEV station in Ny-Ålesund (West coast of Spitsbergen Island on Svalbard, 78.9°N, 11.9°E) has been founded in 2003 by merging the Polar research activities of Germany (AWI: Alfred Wegener Institut) and France (IPEV: Institut polaire Paul-Émile Victor). However, the first photometer measurements on that site started already in 1991 (Herber et al. 2002). Today, AWIPEV station is an international platform that supports research in many different fields. Concerning atmospheric research, the measurements comprise e.g. a BSRN field, daily radiosounding, infrared spectroscopy and cloud remote sensing. Aerosol remote sensing is done by a Raman Lidar, a star photometer and, operated by GOA-UVa group of University of Valladolid, a CIMEL 318T (solar and lunar capabilities). Hence during Polar night, comparisons between lidar and stellar AOD measurements can be performed (Figure 5.2.5).



Figure 5.2.5: Roof platform of AWIPEV station with the open laser hutch. In the background the cupola of the star photometer.

5.2.4. Italian contribution

Italy contributes to Arctic AOD research through the ISP-CNR station *Dirigibile Italia* in Ny-Ålesund (78°55′N, 11°56′E), on the island of Spitsbergen in the Svalbard archipelago. *Dirigibile Italia* is a logistical and scientific base that supports the operation of ISAC-CNR's solar and lunar Prede POM-02 photometer (Figure 5.2.6), as well as the Lunar PFR prototype, a joint POMD/WRC and ISP-CNR project.



Figure 5.2.6: The Prede POM01M (sun and moon) installed in 2026 at Ny-Ålesund, Svalbard.

5.2.5. Norwegian and Swiss contributions

In May 2002, Physical Meteorological Observatory in Davos / World Radiation Center (PMOD/WRC), in collaboration with NILU, started AOD observations in Ny-Ålesund as part of the global AOD network on behalf of the WMO GAW program. (section 5.3.3).

5.3 In Antarctica today

For the Antarctic Pulimeno et al. 2026 analysed eleven sites: three at the Antarctic peninsula, five in Queen Maud land (East Antarctica, Atlantic sector), one in Queen Mary Land (Australian sector) and two within the continent. Only four of those have been upgraded to combined sun & moon photometers in the recent years . There is no lunar data before 2018 (Pulimeno et al. 2026), so the coverage of winter AOD measurements in Antarctica is still poor.
While at the Antarctic Peninsula AOD > 0.1 can sporadically occur, low or very low optical depths prevail at the other Antarctic sites. An example is shown in Fig 5.3.1 which shows the AOD and Ångström exponent for Dome C. It can also be seen that the Ångström exponent is slightly larger than for the Arctic. These low AOD values consisting mainly of very small particles can be explained by the remote and isolated location of Antarctica.
Nevertheless, Pulimeno et al. 2024 report an increase of AOD for some Antarctic sites. Especially at Syowa station (69°S, 39.5°E) a clear rising trend of 3.8% per year, from below 0.02 in 1997 to 0.03 in 2021.

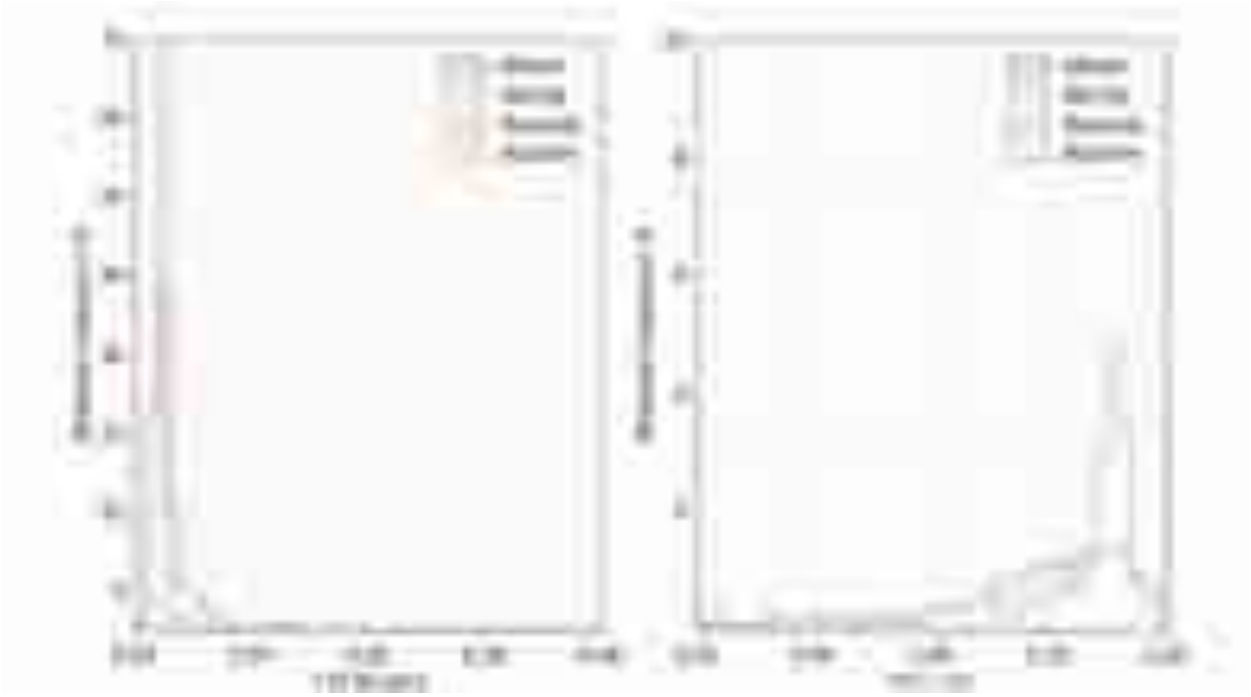


Fig 5.3.1: AOD (left) and Angstroem exponent (right) for Dome C, Antarctica. Fig taken from Pulimeno et al. 2026.

5.3.1. Spanish contribution

In Antarctica, the GOA-UVa group maintains one long-term dataset at Marambio station (64.2S, 56.6W), since 2018, in collaboration with the Argentinian Weather Service (SMN). These observations are performed during the entire year (solar in summer, lunar in winter) and are part of AERONET. These observations allowed the detection and characterization of Australian smoke over Antarctica in 2019 (González et al., 2020). During the boreal summer, sun photometer AERONET observations are also carried out at the Spanish base Juan Carlos I since 2023.

Furthermore, shipborne mobile automatic observations have been carried out with the RV Sarmiento de Gamboa on the transect between Spain and Antarctica (Shetland islands).

5.3.2. Italian contribution

The National Antarctic Research Programme (PNRA) started in 1985. Beginning in 1987, the Bologna team initiated solar photometry observations at Mario Zucchelli Station along the Ross Sea coast (Figure 5.3.2). Continuous field measurements were primarily conducted at the Campo Icaro observatory, located on the coast 3 km south of the main station. Accessible by snowmobile or on foot, Campo Icaro provided an ideal, unpolluted location for round-the-clock solar tracking during the austral summer.



Figure 5.3.2: UVSIR and IRRAD at Mario Zucchelli Station in Antarctica.

Through the 2004–2005 field season, Campo Icaro expanded from hosting the portable UVISIR, the ASP-15WL and IRRAD photometers to operating a full suite of radiation and aerosol instrumentation, followed during the years by Multi-Filter Rotating Shadowband Radiometers (MFR-SR, see Figure 5.3.3) and Prede sun photometers (deployed in collaboration with the ISAC-CNR Rome branch, see Figure 5.3.4). Research activities spanned from retrieving Aerosol Optical

Depth (AOD) and optical properties—coupled with *in situ* particle sampling—to utilizing radiometric data for characterizing cloud fraction and cloud microphysics.

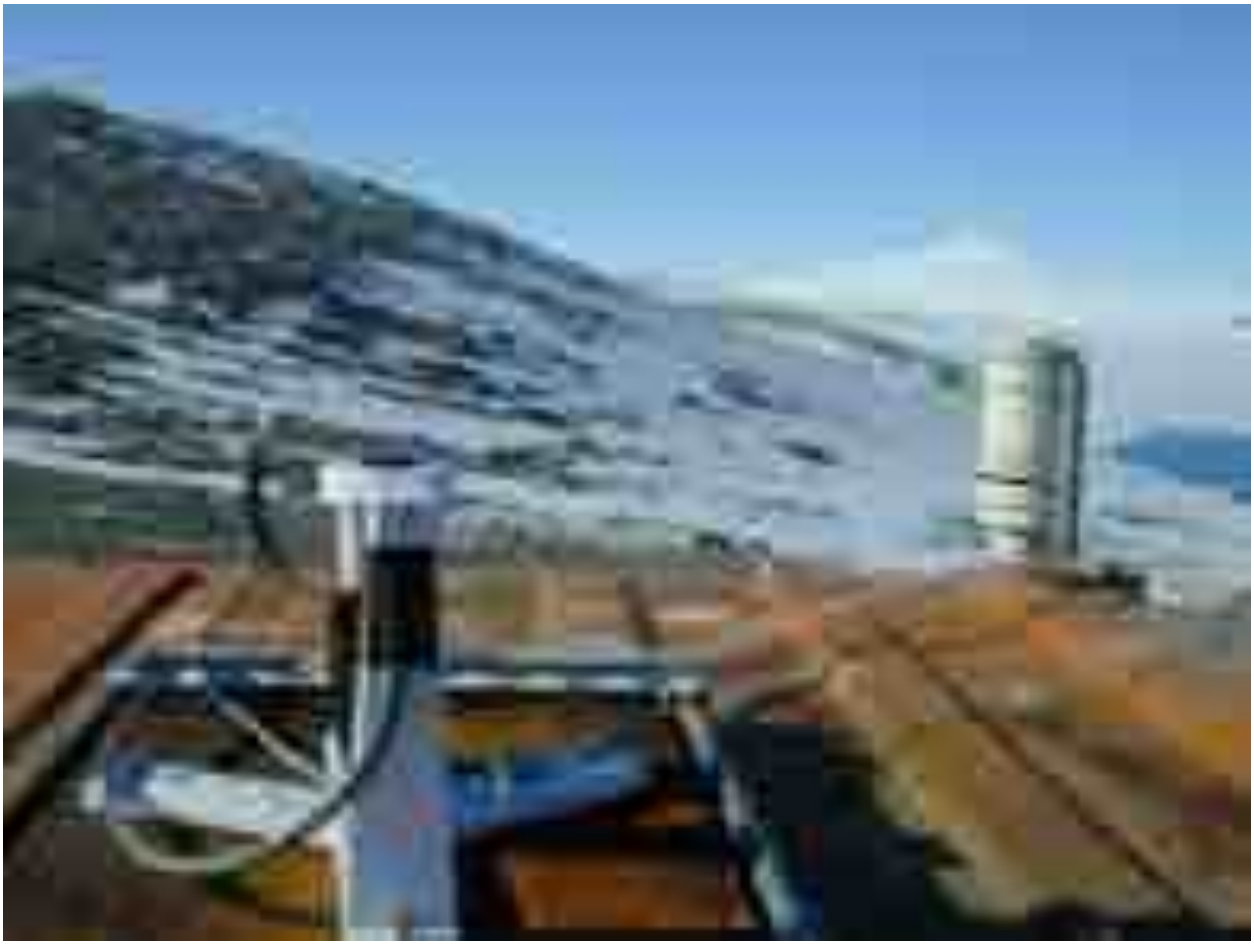


Figure 5.3.3: MFR-SR in operation at Campo Icaro, near Mario Zucchelli Station in Antarctica.

The main achievement was provided by Di Carmine et al. (2005), who analysed measurements collected with a Prede Sun-sky radiometer at Terra Nova Bay during the 2001–2002 austral summer. By combining direct solar irradiance and diffuse sky radiance measurements, the study retrieved aerosol optical depth, particle size distributions and refractive index. The results revealed extremely low aerosol loading, with AOD at 500 nm generally between 0.01 and 0.02, and highlighted the influence of katabatic winds on aerosol optical properties. This work represented an important step towards the characterization of aerosol microphysical properties in the Antarctic coastal atmosphere.



Figure 5.3.4: Prede POM01 at Campo Icaro, near Mario Zucchelli Station in Antarctica during austral summer 2001-2002.

5.3.3 Norwegian contribution

At Trollhaugen, AOD data from sun-photometer observations started in 2014, after moving the observations from Troll to the new observatory. For the first observations at Troll in 2007, see Hansen et al. (2009). AOD values at Troll/Trollhaugen in Antarctica reflect the significantly lower aerosol concentration in the Antarctic region. AOD typically ranges between 0.01 and 0.04, with occasional peaks above 0.04, particularly around 2020, when Australian bushfire smoke affected the Polar observations.

The photometer data from Troll/Trollhaugen contribute to the POLAR-AOD programme (see Tomasi et al., 2007 and http://classic.ipy.org/development/eoi/details.php?id=299). Actual insights in the Polar-AOD program and recent Advances in AOD measurements in Polar regions can be found in Pulimeno et al., (2026).

6. Harmonisation of the different systems: Recent studies on synergies

After this long journey through time and across Europe—and even to the most remote regions of the globe, the Arctic and Antarctic—we return to the present to explore recent studies, many of them conducted by early-career scientists within HARMONIA.
This section presents studies of synergies between different systems and the harmonisation of instruments—the very essence of HARMONIA. Section 6.1 begins with synergies between lunar and stellar photometers, particularly for intercomparison and validation. Section 6.2 then examines synergies between photometers, ceilometers, and other systems and methods for measuring the vertical distribution of aerosols. Finally, Section 6.3 returns to the AWIPEV station in Ny-Ålesund to explore the synergy between the Raman lidar “KARL” and a stellar photometer.

6.1 Synergies and comparisons for lunar and stellar systems

Aerosol optical depth measurements obtained through lunar photometry have been used synergistically with measurements from other instruments. For example, Román et al. (2017) combined lunar AOD measurements with measurements of sky radiance in the lunar aureole obtained using an all-sky camera (see Figure 6.1.1). Measurements from both instruments were used as input to the GRASP (Generalized Retrieval of Atmosphere and Surface Properties; Dubovik et al., 2021) algorithm to retrieve advanced aerosol properties, such as aerosol size distributions and refractive indices. In their study, a Saharan dust intrusion event over the city of Valladolid (Spain) was analyzed using this synergistic approach combining a lunar photometer and an all-sky camera. The retrieved aerosol properties, including refractive indices, the fraction of spherical particles, and size distribution parameters, were consistent with the nearest daytime AERONET retrievals (see Figure 6.1.2 and 6.1.3). The nighttime GRASP retrievals showed an increase in coarse-mode aerosol concentration throughout the night, while fine-mode properties remained relatively constant.

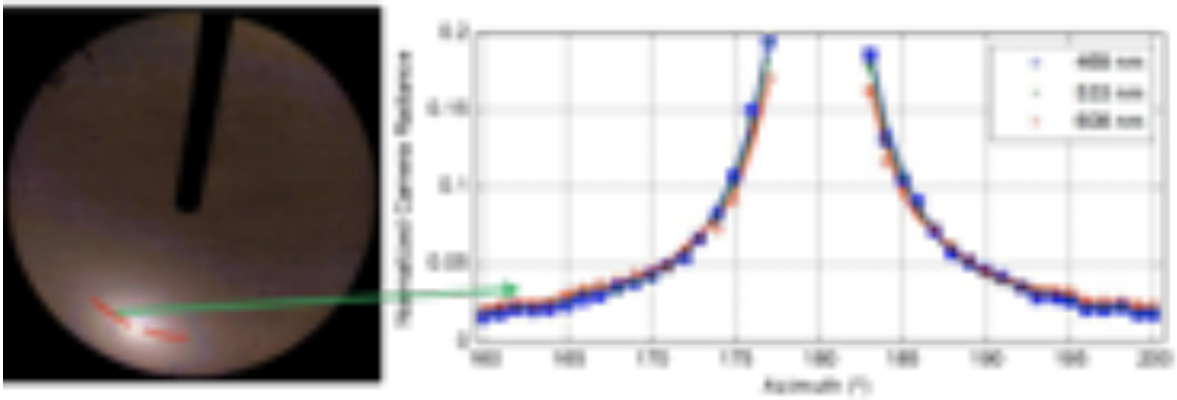


Figure 6.1.1: Normalized sky radiance at three effective wavelengths in the lunar aureole obtained from a high dynamic range all-sky image following the method of Román et al. (2017).

This synergistic approach was further developed by Benavent-Oltra et al. (2019), who combined lunar photometer AOD measurements and sky radiance measurements in the lunar aureole obtained with an all-sky camera with the lidar range-corrected signal (RCS) at three wavelengths as additional inputs to GRASP. This combination enabled the retrieval of vertically resolved aerosol properties at night. The authors evaluated the methodology during a Saharan dust intrusion event in Granada (Spain), comparing the results with those obtained using a Raman lidar and with in-situ measurements from a nearby high-altitude mountain station. The methodology yielded better agreement with in-situ aerosol volume concentration measurements than other methods, with differences of around 10% under high-AOD conditions.

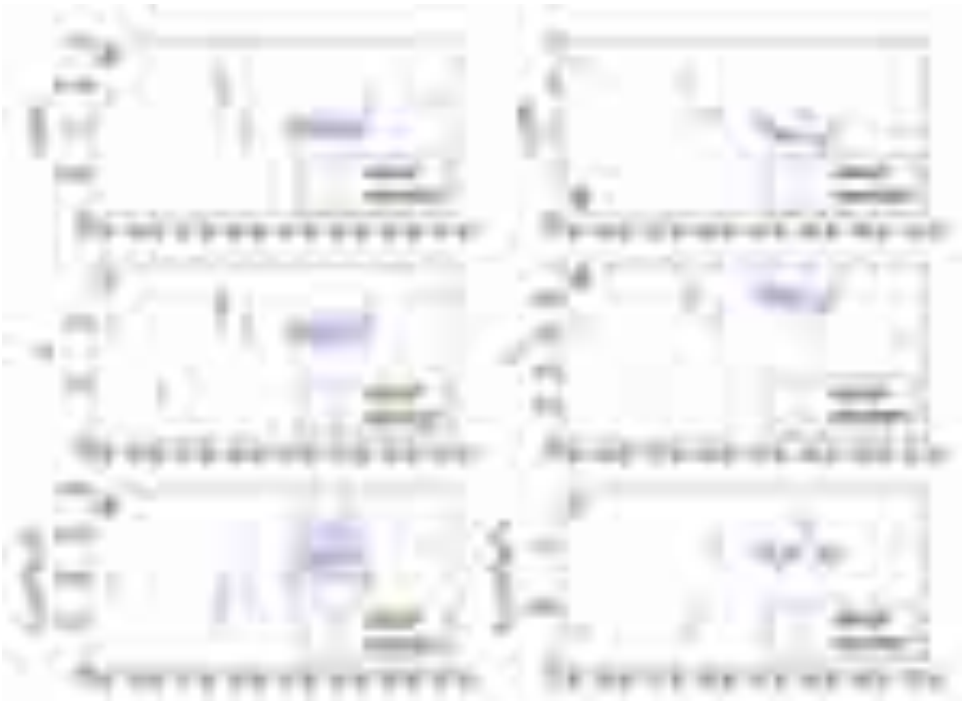


Figure 6.1.2: Parameters of the fine (panels a, c and e) and coarse (panels b, d and f) aerosol size distributions fromAERONET (black circles) and from GRASP retrieval using sky radiances in the lunar aureole with an all-sky camera and nocturnal AOD with a lunar photometer (blue crosses with error bars) at Valladolid (Spain) from 2nd to 3rd August 2015. This figure is obtained from Román et al. (2017).



Figure 6.1.3: Evolution of the real (panel a) and imaginary (panel b) refractive indices, sphere fraction (panel c) and SSA (panel d) at Valladolid from 2nd to 3rd August 2015. Diurnal values retrieved by AERONET are represented as circles, while nocturnal values retrieved by GRASP, sky radiances in the lunar aureole with an all-sky camera and nocturnal AOD with a lunar photometer, are represented by crosses with their error bars. This figure is obtained from Román et al. (2017).

Another synergistic approach evaluated by Benavent-Oltra et al. (2019) involved combining lidar measurements with lunar photometry. A similar instrumental synergy had previously been proposed by Alados-Arboledas et al. (2011), although in that case a star photometer was used instead of a lunar photometer. These authors applied the Klett–Fernald–Sasano method to retrieve backscatter and extinction profiles at 1064 nm, constraining the integrated extinction to the AOD derived from the star photometer. Using this technique, a fresh biomass-burning pollution plume in Granada (Spain) was monitored and characterized in terms of its optical and microphysical properties for the first time through a combination of Raman lidar and star and sun photometers (see Figure 6.1.4). This combination of instruments is particularly useful for the continuous, 24-hour monitoring of pollution events.

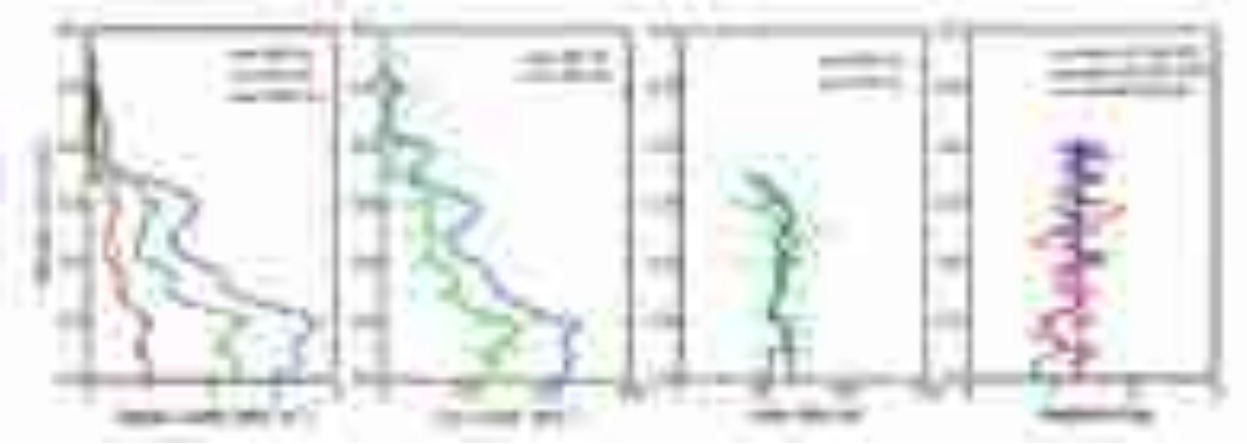


Figure 6.1.4: Mean profiles of aerosol optical properties (extinction coefficients, backscatter coefficients, lidar ratios, and backscatter-related and extinction-related Ångström exponents) for the measurement from 19:03 to 20:03 UTC on 24 September 2007 at Granada (Spain). Error bars denote one-standard deviation. This figure is obtained from Alados-Arboledas et al. (2011).

6.2 Synergies photometer - ceilometers

Photometers provide information on the total aerosol column but cannot resolve the vertical distribution of aerosols. Active remote-sensing systems, such as lidars and ceilometers, can provide this information. In this section, we explore three studies examining how ceilometers can complement photometer measurements to characterise the vertical profile of aerosols, and how photometer data can, in turn, improve ceilometer measurements.

6.2.1 The GRASP approach

Although synergies between lidar systems and star/lunar photometers were not widespread a decade ago, mainly due to the limited availability of star and lunar photometers, combining lidar measurements with sun photometers was already a well-established approach. This combination was primarily used to retrieve aerosol extinction and backscatter profiles using the aforementioned Klett–Fernald–Sasano method (Mitev et al., 1992; Ansmann et al., 2002, Pérez et al., 2006; Benavent-Oltra et al., 2021).

More sophisticated lidar–photometer synergy methods incorporated not only AOD measurements but also sky radiance measurements from the photometer. In this regard, the LIRIC algorithm (Lidar-Radiometer Inversion Code; Chaikovsky et al., 2016) is particularly noteworthy. LIRIC combines lidar measurements with column-integrated aerosol properties retrieved by AERONET from AOD and sky radiance measurements. A similar approach was adopted by GARRLiC, which is now integrated into GRASP. GARRLiC performs a joint inversion of AOD and sky radiance measurements together with lidar RCS values (Lopatin et al., 2013; Benavent-Oltra et al., 2017).

Both methodologies, explained in Figure 6.2.1, provide vertically resolved aerosol properties, including volume concentration, extinction, and backscatter coefficients. These methods were initially developed for use with multiwavelength lidar systems. However, such systems are generally less common due to their high cost and often lack continuous, uninterrupted measurements because of operational constraints.

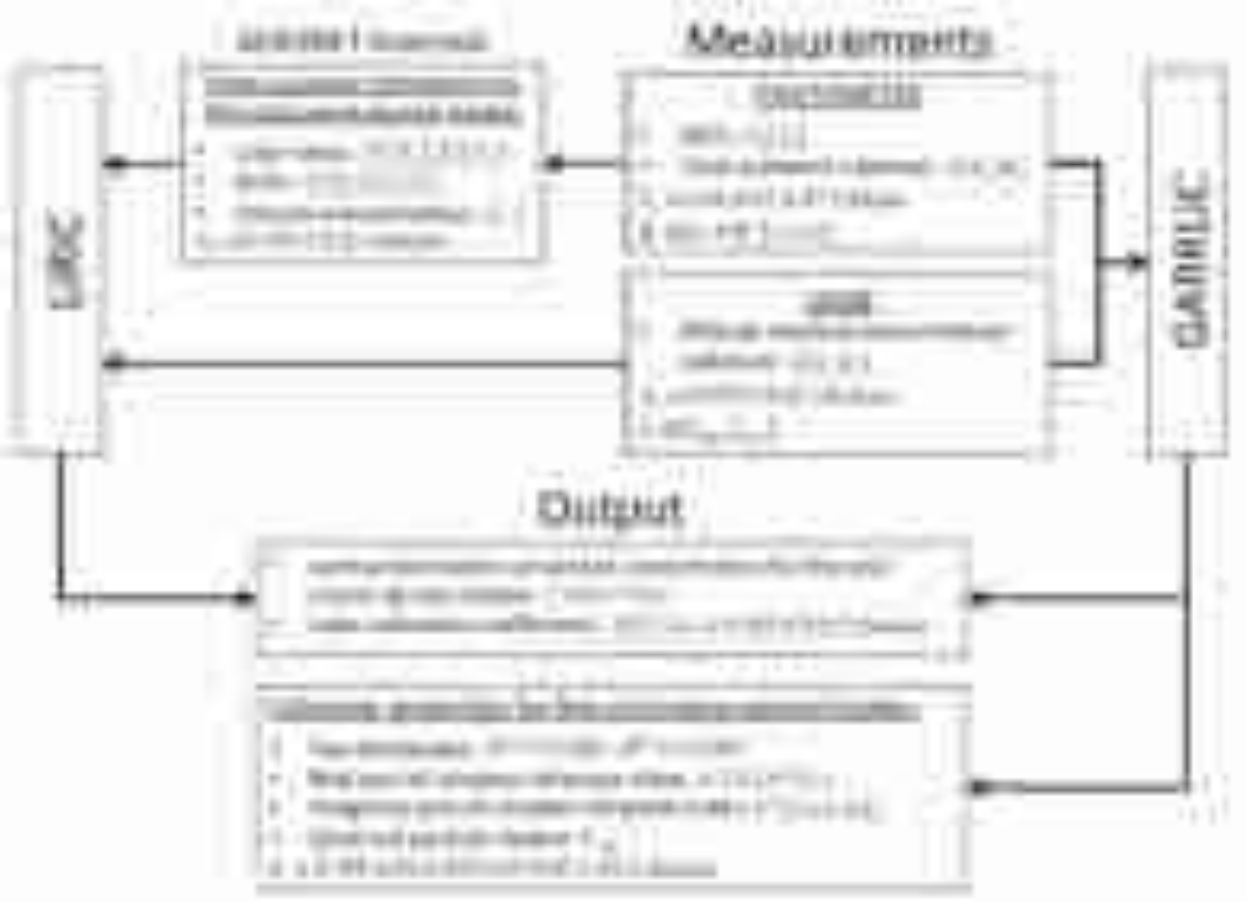


Figure 6.2.1: Comparison of LiRIC and GARRLiC algorithms. This scheme is obtained from Lopatin et al. (2013).

A more cost-effective alternative to multiwavelength lidar systems is provided by automatic lidars and ceilometers (ALCs), which generally operate at lower laser powers and use a single wavelength while providing continuous measurements. Among these instruments, ceilometers are particularly widespread. They were originally designed to determine cloud-base height using low-power pulsed near-infrared lasers. However, advances in instrument technology have enabled modern ceilometers to detect aerosol layers and provide vertically resolved information on aerosol distributions, in addition to their primary cloud-monitoring function. Their ability to operate continuously and unattended, together with their relatively low cost and widespread deployment, makes them particularly valuable for aerosol monitoring. For example, the E-PROFILE network, operated within EUMETNET, brings together a large number of automatic

lidars and ceilometers across Europe, providing extensive spatial coverage of atmospheric aerosol and cloud observations (https://e-profile.eu).

Synergies between ceilometers and sun photometers have been used, for example, to retrieve aerosol extinction and backscatter profiles by applying the aforementioned Klett–Fernald–Sasano inversion method (e.g., Wiegner et al., 2014; Cazorla et al., 2017). Alternatively, the GRASP algorithm can be used to jointly invert sun-photometer AOD and sky radiance measurements together with ceilometer range-corrected signal profiles, following a synergistic retrieval approach similar to GARRLiC. This approach was implemented by Román et al. (2018), who introduced the GRASPpac methodology, with “pac” standing for “photometer and ceilometer”. The GRASPpac method combines AERONET AOD and sky radiance measurements at four wavelengths with ceilometer RCS measurements at 1064 nm to retrieve vertically resolved aerosol properties, including aerosol volume concentration profiles. The authors evaluated the retrievals using airborne in-situ measurements collected during two research flights over Granada (see Figure 6.2.2), as well as in-situ observations from a high-altitude mountain station (see Figure 6.2.3). The retrieved volume concentration profiles showed good agreement with the independent measurements, demonstrating the potential of this approach for aerosol profiling using widely deployed, continuously operating ceilometers.

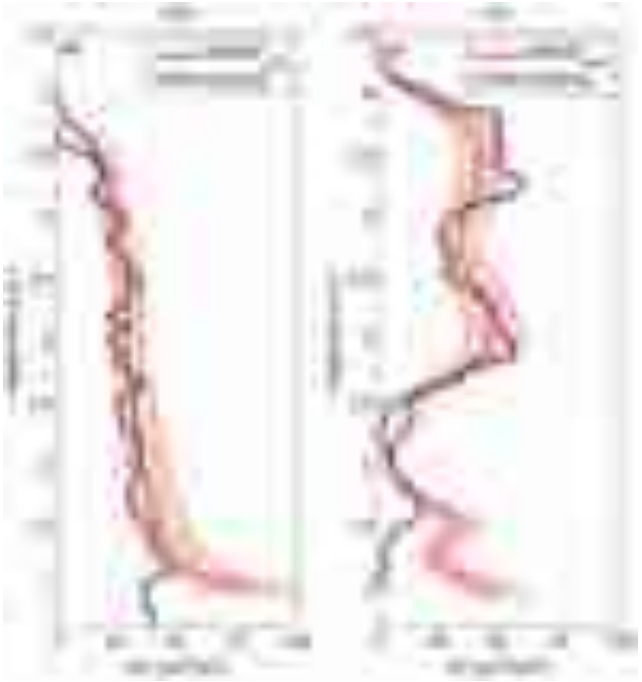


Figure 6.2.2: Profiles of aerosol volume concentration (VC) obtained by airborne instrumentation (black line) and GRASPpac (red line) at the flights F30 (panel a) and F31 (panel b) during the ChArMEx/ADRIMED campaign over Granada city on 16th and 17th June 2013, respectively. Shadow band represents uncertainty in the GRASPpac retrieval. This figure is obtained from Román et al. (2018).

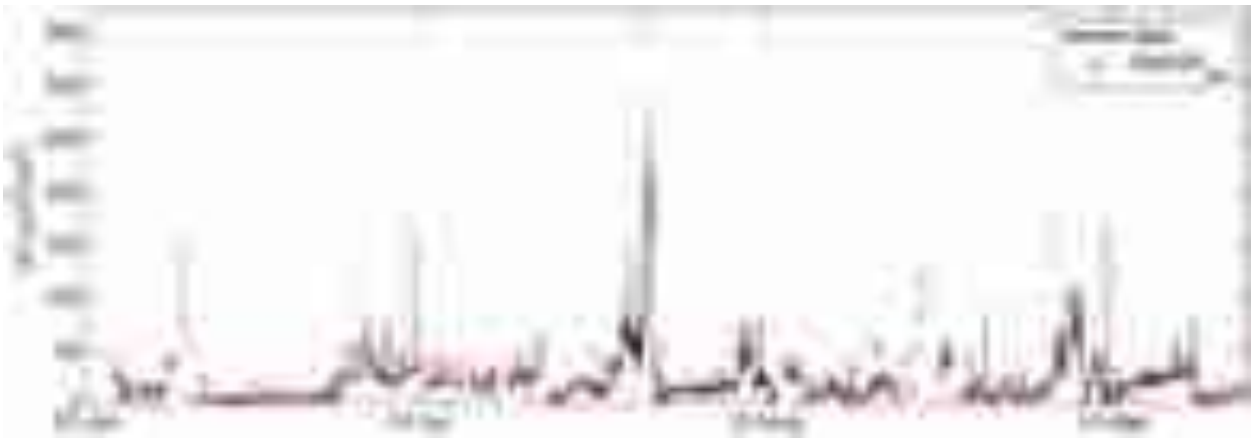


Figure 6.2.3: Temporal evolution of the aerosol volume concentration (VC) measured at the Sierra Nevada Station (SNS; high-altitude mountain station) and retrieved by GRASPpac at the same altitude during the SLOPE I campaign in Granada in summer 2016. This figure is obtained from Román et al. (2018).

The GRASPpac methodology has subsequently been applied in several studies to investigate aerosol properties under different atmospheric conditions. For instance, Titos et al. (2019) conducted a three-year evaluation of aerosol optical properties and volume concentration retrieved at the Montsec mountain station (southern Pyrenees), comparing the results with independent in-situ measurements. Their findings showed good agreement for scattering and extinction coefficients, while the performance of volume concentration retrievals depended on the relative contribution of fine and coarse particles. Herreras et al. (2019) evaluated aerosol extinction profiles retrieved over Granada (Spain) by comparing the integrated extinction within different atmospheric layers against estimates derived from AOD measurements at three AERONET stations located at different altitudes. Bazo et al. (2023) used GRASPpac retrievals to investigate the vertically resolved aerosol radiative effect in both the shortwave (see Figure 6.2.4) and longwave spectral ranges, examining its seasonal variability and its dependence on aerosol extinction. More recently, Muñiz-Rosado et al. (2026) evaluated aerosol profile retrieval approaches based on ceilometer measurements at three European stations, using GRASPpac products alongside sun–sky photometer and balloon-borne in-situ observations to assess retrieval performance under different aerosol conditions. Furthermore, the GRASPpac methodology has been integrated into CAECENET (Herrero del Barrio et al., 2024), an automated system to retrieve column-integrated and vertically resolved aerosol properties in near real time that is explained below.

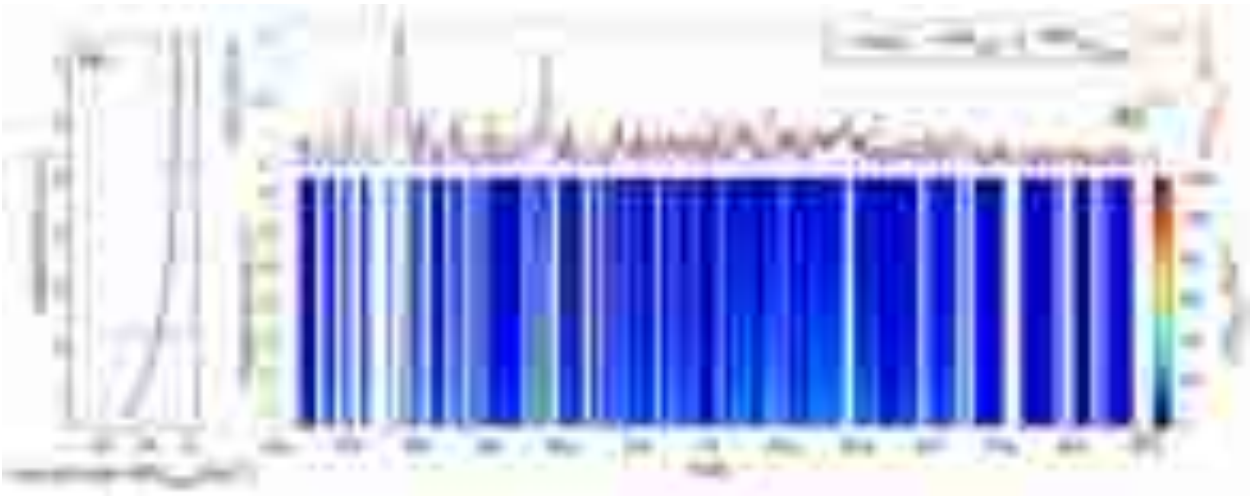


Figure 6.2.4: Annual mean ARE_{sw} (Aerosol Radiative Effect on shortwave solar radiation) profile, error bars show the standard deviation. (b) Time series of the AOD at 1064 nm and the ARE_{sw} at the surface. Black markers denote the monthly average of the ARE_{sw} at the surface, with the standard deviation as error bars. (c) Times series of the ARE_{sw} vertical profiles. These results correspond to Granada (Spain). This figure is obtained from Bazo et al. (2023).

Beyond ceilometers, GRASP has also been used to combine sun–sky photometer measurements with observations from other types of ALCs, including micro-pulse lidars (MPLs) instruments. For example, López-Cayuela et al. (2022) investigated the retrieval of column-integrated and vertically resolved optical and microphysical properties of Saharan dust by combining AERONET sun–sky photometer measurements with MPL observations at 532 nm at El Arenosillo (Huelva, Spain). More recently, Lopatin et al. (2024) compared aerosol properties retrieved using GRASP and MPL measurements at the KAUST site in Saudi Arabia over the 2019–2022 period. The authors also investigated the influence of incorporating volume depolarization measurements on retrieval performance and examined the diurnal and seasonal variability of aerosol properties. These studies demonstrate the versatility of GRASP in exploiting synergies between passive photometric measurements and different types of active remote-sensing systems.

6.2.2 CAECENET Study: a photometer - ceilometer synergy

CAECENET (Photometer–ceilometer network, based on CÆLIS-ICENET, Herrero del Barrio et al., 2024) is an example of how the synergy between photometers and ceilometers can be exploited to obtain vertically resolved aerosol properties. The system uses the GRASPpac algorithm (Román et al., 2018), with aerosol optical depth (AOD) and sky radiance measurements from sun/sky photometers in the CÆLIS database (Fuertes et al., 2018) and range-corrected signal profiles from ceilometers in the ICENET database (Iberian Ceilometer Network; Cazorla et

al., 2017) as input. The algorithm runs automatically and continuously at every station that is part of the network, all of which have a collocated photometer and ceilometer. Each time a new sky radiance measurement is available, CAECENET looks for a coincident cloud free ceilometer profile and AOD measurement, runs the retrieval and stores the columnar and vertical products (with their uncertainties) in a database. This network makes it possible to follow how an aerosol event propagates (its arrival time and speed), how the altitude of the aerosol layers changes, which processes (such as deposition or mixing into the boundary layer) modify its concentration, and how all this affects the aerosol optical properties. This was illustrated in Herrero del Barrio et al., 2024 analysing two events over the Iberian Peninsula. Firstly, a Saharan dust outbreak from 3 to 5 October 2022, when AOD at 440 nm reached 1.55 in Granada and between 0.6 and 0.8 in Madrid and Valladolid, with Ångström exponent values below 0.2. The retrieved size distributions were dominated by the coarse mode, and the single scattering albedo was above 0.98 except at 440 nm, as expected for mineral dust. The profiles placed the dust layer at about 3 km a.s.l. in central Spain (volume concentration peaks of 130 to 180 $\mu m^3/cm^3$) and between 1.5 and 4 km a.s.l. in Granada (up to 325 $\mu m^3/cm^3$). In the second event, smoke from the Canadian wildfires reached the Peninsula between 26 and 29 June 2023, with AOD at 440 nm up to 2.22 in Badajoz and 1.83 in Madrid. In this case the fine mode was dominant, with a modal radius of about 0.23 µm, typical of aged smoke. CAECENET showed thin layers between 3 and 8 km a.s.l. reaching the five stations one after another, with volume concentrations above 100 $\mu m^3/cm^3$. In both cases HYSPLIT back trajectories confirmed the origin of the air masses, and the results show how the combination of both networks allows regional aerosol events to be monitored in near real time.

6.2.3 Validation of ceilometers with help of Photometers and radiosoundings AOD measurements synergy study:

Ceilometer networks such as E-Profile (more than 400 stations), ICENET and ALICENET provide dense, continuous coverage of aerosol layers in the lower troposphere. One of their limitations is that a single-wavelength elastic signal at 1064 nm cannot separate backscatter from extinction, so the lidar ratio must be assumed. The classical Klett-Fernald backward inversion calibrates each profile by assuming an aerosol-free reference altitude aloft, which is hard to find in daytime, when the signal-to-noise ratio is low and elevated layers are present; errors then propagate downward.

Two alternatives to the backward inversion are available. The first relies on instrumental synergy: $GRASP_{pac}$ (Román et al., 2018) jointly inverts AERONET AOD and sky radiances with the 1064 nm ceilometer signal to retrieve backscatter and extinction profiles (250-7000 m), together with optical and microphysical properties. The lidar ratio is estimated within the inversion rather than prescribed. The second is the forward iterative method (Li et al., 2021), which integrates upward from the lowest points of the profile and therefore does not require an aerosol-free reference altitude. Instead, it relies on an independent calibration constant CL, which E-Profile derives from at least 3 h of cloud-free nighttime signal and then applies to daytime profiles.

Muñiz-Rosado et al. (2026) compare the two standalone ceilometer retrievals, the Klett–Fernald backward inversion and the forward iterative method, both assuming a lidar ratio of 50 sr, at three E-Profile stations (Granada, Payerne and Lindenberg) over 2019-2020. Each retrieval is

evaluated against three reference datasets: in situ backscatter profiles from COBALD balloon-borne sondes, synergistic $GRASP_{pac}$ profiles, and integrated-column AOD from AERONET.

Two nighttime COBALD soundings provide direct backscatter at 940 nm. During a Saharan dust event at Payerne (25 June 2019), both methods correlate with the sonde (r = 0.94 forward, 0.95 backward), but the forward retrieval gives RMSE = 0.15 versus 0.29 Mm^{-1} sr^{-1} and a slope of 0.92 versus 0.66, as the backward profile underestimates backscatter throughout the dust layer. At Lindenberg (27 August 2020), where no aerosol-free reference exists aloft, the backward profile agrees poorly (r = 0.51, RMSE = 2.11 Mm^{-1} sr^{-1}), whereas the forward profile matches the sonde (r = 0.97, RMSE = 0.06 Mm^{-1} sr^{-1}).

The $GRASP_{pac}$ comparison covers the full record (2064, 1524 and 1000 profiles at Granada, Payerne and Lindenberg), grouped by aerosol load (high: AOD440 ≥ 0.2) and dominant mode (coarse: AE ≤ 0.8; fine: AE ≥ 1.2) (Figure 6.2.5). The forward retrieval agrees more closely at all sites (r = 0.97, 0.90 and 0.96, against 0.82, 0.72 and 0.82), with slopes close to unity; at Granada, the RMSE falls from 0.19 to 0.08 Mm^{-1} sr^{-1}.

The methods differ most under coarse-mode conditions, where the backward RMSE is more than twice the forward one at Granada (0.58 versus 0.26 Mm^{-1} sr^{-1}) and Payerne (0.50 versus 0.27 Mm^{-1} sr^{-1}). The backward deviations also vary with altitude (Figures 6.2.5 a-c), consistent with error propagation from a contaminated reference altitude, a trend the forward retrieval largely removes. Under fine-mode conditions, the gap narrows (0.29 versus 0.17 Mm^{-1} sr^{-1} at Granada).

Integrating extinction up to 5 km gives a column AOD that can be compared with daytime AERONET Level 2.0 observations (Fig. 6.2.6). The forward retrieval agrees closely with AERONET (r = 0.88–0.94, RMSE = 0.010–0.013, slopes close to unity), with a near-zero bias and RMSE values comparable to, or lower than, recent GRASP–MPLNET intercomparisons (Lopatin et al., 2024), whereas the backward method performs considerably worse (r ≤ 0.54, slopes ≤ 0.47). Under coarse-mode conditions, the backward mean deviations reach −0.116 to −0.184, and at Granada the forward retrieval halves them (−0.070 versus −0.147).

To test whether the residual AOD deviations differ from the fixed lidar ratio, the comparison with AERONET was repeated using 30, 50 and 70 sr and a daily IFS-CAMS estimate. For the full dataset, 50 sr and the CAMS-based value give the lowest RMSE, whereas 30 and 70 sr introduce negative and positive biases. Under coarse-mode conditions, the CAMS-based value lowers the forward RMSE from 0.085 to 0.053 at Granada and from 0.062 to 0.048 at Payerne. The backward deviations remain large and negative in all configurations, indicating that their main limitation is the reference altitude rather than the lidar ratio.

Overall, the forward retrieval gives a more vertically consistent representation of aerosol backscatter and extinction, mainly because a single, independent nighttime calibration replaces the profile by profile search for an aerosol-free reference altitude. GRASPpac provides both the profile solid comparison and a retrieved lidar ratio, and its agreement with the forward retrieval shows that calibrated single-wavelength ceilometers reproduce the main features of the synergistic solution. The results support integrating forward retrievals into networks such as E-Profile and ICENET as a cost-effective complement to multi-wavelength lidars.

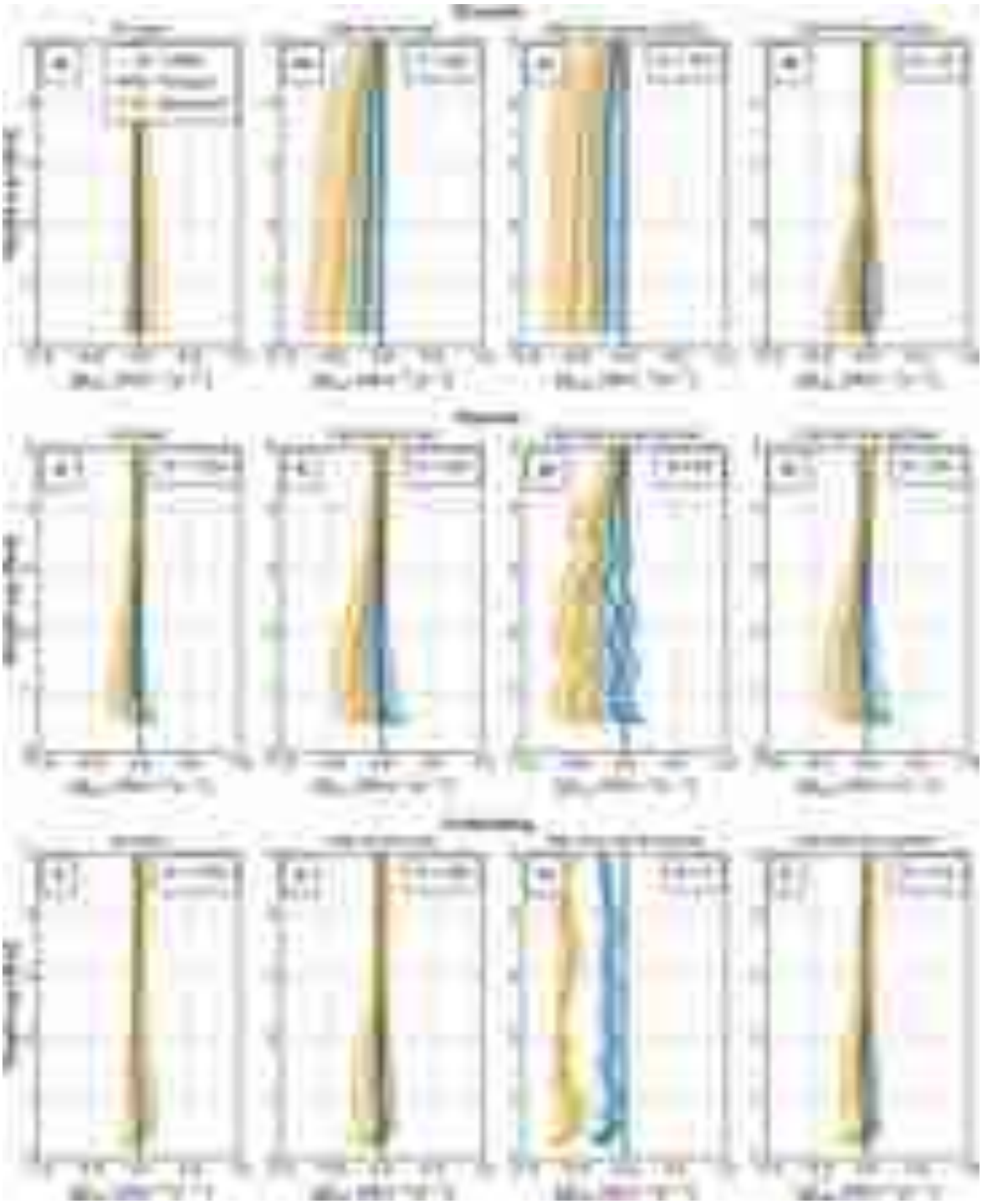


Figure 6.2.5: Backscatter deviation profiles (ceilometer minus GRASPpac) for the backward (orange) and forward (blue) retrievals, by site and aerosol regime. Source: Figure 5 of Muñiz-Rosado et al. (2026).

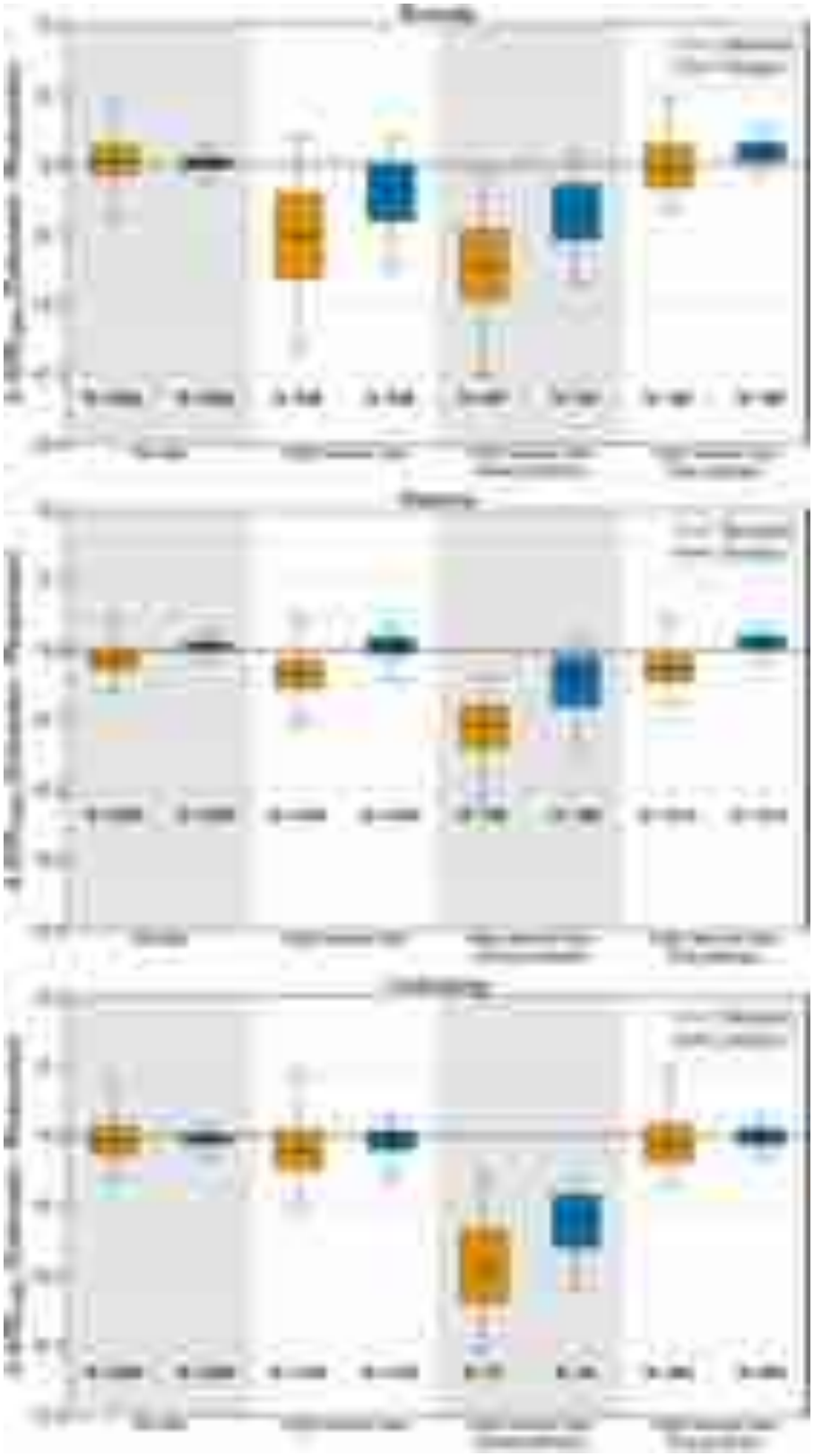


Figure 6.2.6: Ceilometer minus AERONET AOD at 1064 nm for the backward (yellow) and forward (blue) retrievals, by site and aerosol regime. Source: Figure 7 of Muñiz-Rosado et al. (2026).

6.3. Synergies Stellar - Lidar: AWIPEV Station at Ny-Ålesund

AWIPEV station in Ny-Ålesund (W coast of Spitsbergen, 78.9°N, 11.9°E) is equipped with a Raman Lidar, a star photometer and, operated by University Valladolid, a CIMEL 318. Hence during Polar night comparisons between lidar and stellar AOD measurements can be performed. However, both the lidar and the star photometer need to be switched on manually by an operator. Therefore, the data coverage is incomplete.

Still, few case studies of joint measurements do exist. As obviously star photometer - Lidar comparisons in the Arctic are restricted to winter months, Polar Stratospheric Clouds (PSCs) are one obvious target. One example is shown in Figure 6.3.1. In the upper left the lidar backscatter is plotted (at 532nm). The evening hours from UT 20 to 24 show quite constant conditions which are favorable for the comparison of instruments which measure in different directions: Next to some aerosol in the lower troposphere a slightly polluted lower stratosphere and a PSC which in the evening is located at 15 to 20km altitude can be seen. In the upper right the integrated backscatter from lidar is depicted.

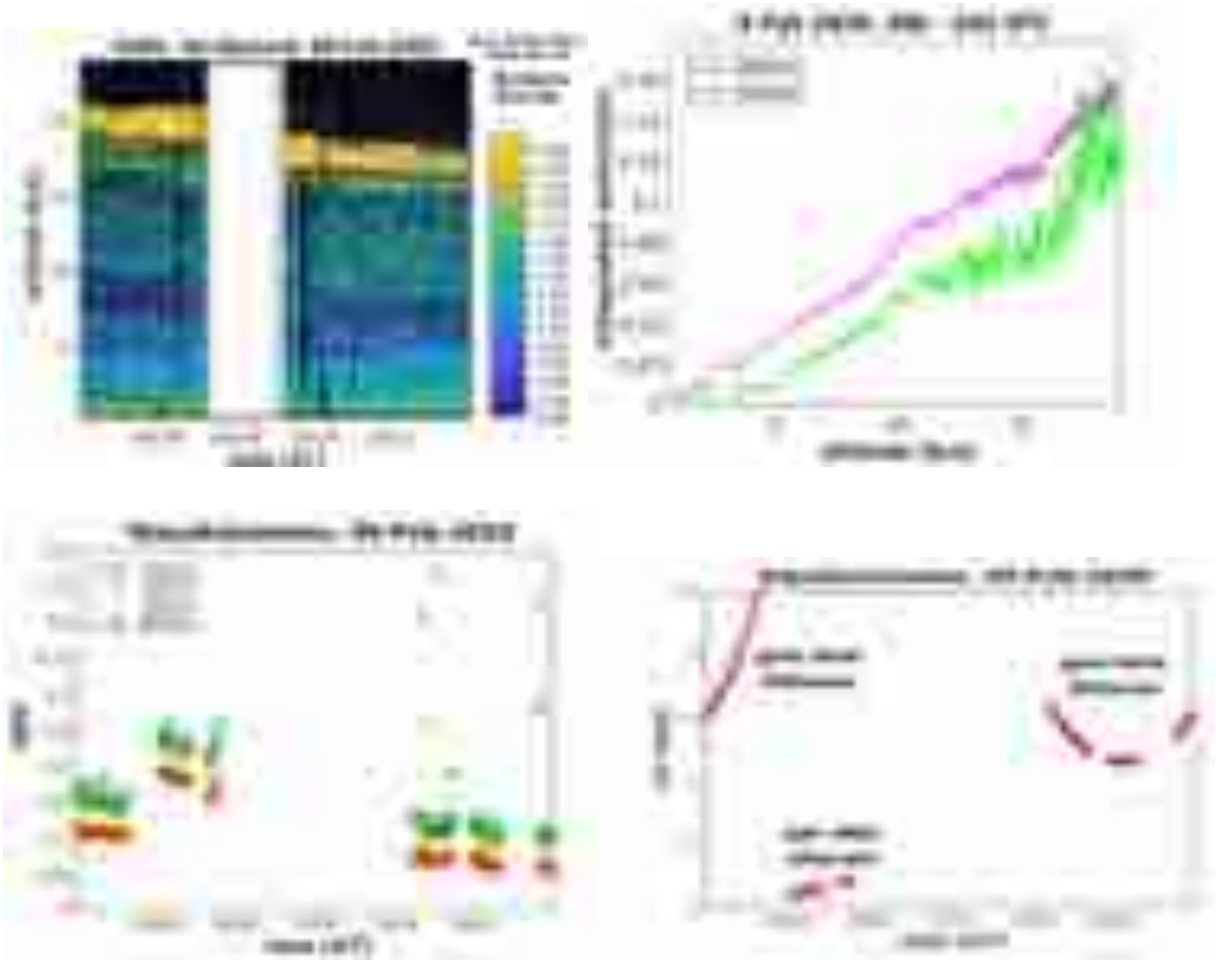


Fig 6.3.1: example of a PSC measurement from 9 Feb 2020. A) Lidar backscatter at 532nm b) Lidar AOD profile for UT 20 - 24, c) star photometer d) selected stars with their air mass.

Without the PSC the AOD would be around 0.08 at 532nm and 0.12 for the UV. The PSC increases the AOD of about 0.04 in both wavelengths. In total, the lidar AOD fairly agrees in both instruments. Some sporadic outliers, different wavelengths at different times, in the star photometer can be explained by very high wind speeds that introduced vibrations in the mount of the instrument. Of course, misalignments will lead to a reduced photo current which translates into too high AOD values.

Aside from possible PSCs the Arctic atmosphere is generally quite clean. For this reason it is unlikely to find different aerosol classes in various altitudes. Hence a comparison between (star-) photometer and lidar might be easier than over polluted areas. During several observations in Feb 2020 the agreement in AOD between star photometer and lidar was indeed generally good. Exceptions were mainly due to different timing of passing thin clouds, Figure 6.3.2 left. During evening hours the star Alhena (γ Gem) is about 30° altitude in the Southern direction, while the lidar looks into the zenith. However, during one day of the campaign (8 Feb, Figure 6.3.3 right) the AOD was clearly higher in the star photometer. Further the temporal variations are completely uncorrelated. Given that a lidar does not cover the whole atmosphere, a higher AOD in the photometer seems surprising. However, the site Ny-Ålesund is located in a fjord with mountains in the southern direction. Local mist formation due to orographic effects around the summits might be an explanation why this deviation in AOD has been found for one case out of five intensive measurement days.
The Figures in this section refer to yet unpublished material from a winter campaign in 2020. Some further aspects of a comparison star photometer to lidar is briefly described in Graßl et al. 2024.

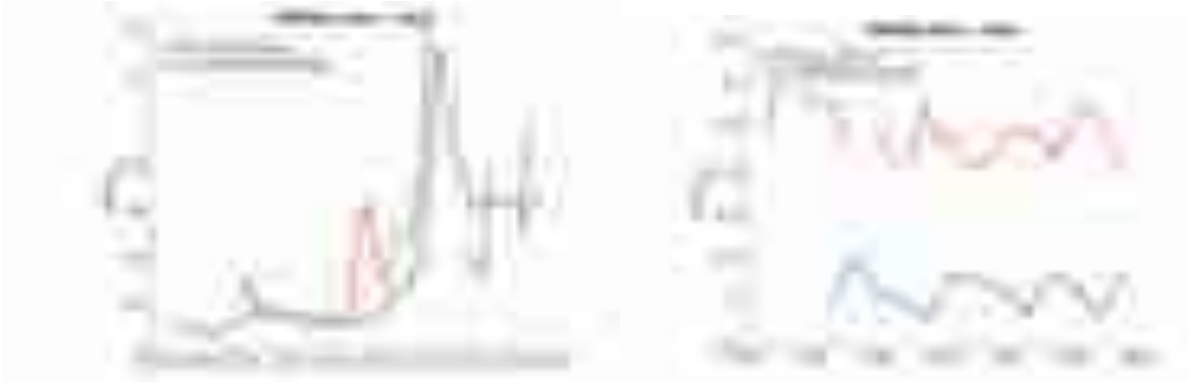


Fig 6.3.2: Comparison of AOD between lidar and star photometer for two different days.

7. From today to tomorrow: Recent innovations in the systems

After discussing the past and present, let us turn to the future of aerosol remote sensing in general, and AOD in particular. Here, we present two innovative and promising approaches to AOD measurement. The first is multi-star photometry—observing many stars simultaneously with all-sky cameras at night (section 7.1). The second is a complementary product developed by astronomers, who need to know AOD to correct for atmospheric effects in their observations. In section 7.2, we present work by a group of astronomers in Prague, Czech Republic, who retrieve AOD from measurements made with wide-field telescopes.

7.1 AOD retrieval from the stars with all-sky cameras

AOD at night-time can be partially obtained with moon photometry, but it is not enough to fill the gap since the Moon is visible just about the half time of night. This is even less since moon photometers only make measurements between the first and third Moon quarters. Star photometry can fill this gap when the Moon is not visible.

Traditional star photometers make accurate and precise measurements of AOD at nighttime. However, they present some weak points like: they need a big dome to protect them from environmental conditions such as rain; they are not fully automatic; they are expensive; they scan stars one by one; and until we know, there are only seven star photometers at five stations in the world being operative: two at Sherbrooke, Canada, one at Eureka, North-West Canada, one at Ny-Ålesund, Svalbard, one at Lindenberg, Germany and one mobile starphotometer mainly based in Granada, Spain. This last one named EXCALIBUR (section 2.2.2), obtained the star direct irradiance from the star image captured by a CCD sensor; the star direct irradiance was obtained from the pixels identified as the star. Unfortunately, this instrument is not working anymore. Nowadays in the world we only have four working operative instruments at three stations: Sherbrooke: Two starphotometers, Ny-Ålesund: One and Eureka: One.

The all-sky cameras are also instruments that take images of the sky. A typical all-sky camera is formed by a glass dome, to protect the optics to the environmental conditions, a fisheye lens to focus the sky light in a sensor, usually a CMOS. These instruments are designed to take images of the full sky, usually to detect cloud cover, but at night-time they can take images like the one observed in Figure 7.1.1, where a lot of stars can be identified. This suggests that perhaps the direct irradiance from the stars could be obtained from these all-sky camera images. This is what was proposed by Román et al. (2025).

These cameras are less accurate since there are less pixels looking at one star: On the other hand, they perfectly operate outdoors without the need of big domes, they are fully automatic and cheaper, they scan all stars in one shot, and there are a lot of all-sky cameras around the world.

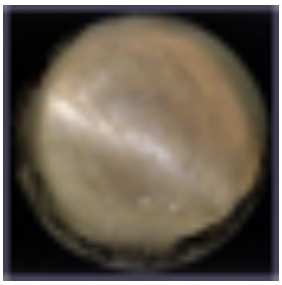


Figure 7.1.1: High Dynamic Range all-sky image at nighttime captured by an OMEA-3C-TF all-sky camera installed in the Spanish Antarctic base "Base Juan Carlos I". This camera belongs to the Group of Atmospheric Optics of the University of Valladolid (GOA-UVa), which provided the image shown.

7.1.1 Main principles

Román et al. (2025) used a total of eight all-sky cameras installed at the nine different sites shown in the map of Figure 7.1.2. All these all-sky cameras were the OMEA-3C model from Alcor System (see Figure 7.1.3). These cameras have a RGB Bayer color filter, that allows to estimate images at four color channels: red, green, blue and gray. One of the cameras has an additional filter that reduces the width of the spectral response; this model is named OMEA-3C-TF and it looks equal as the one shown in Figure 7.1.3. All cameras were configured to take raw images with 14 bits depth resolution, 2000 by 2000 pixel size. In addition, the cameras were configured to take every two minutes a sequence of raw images with different exposure times following the guidelines of the GOA-SCAN network (Román et al., 2025; Herrero del Barrio, 2026).

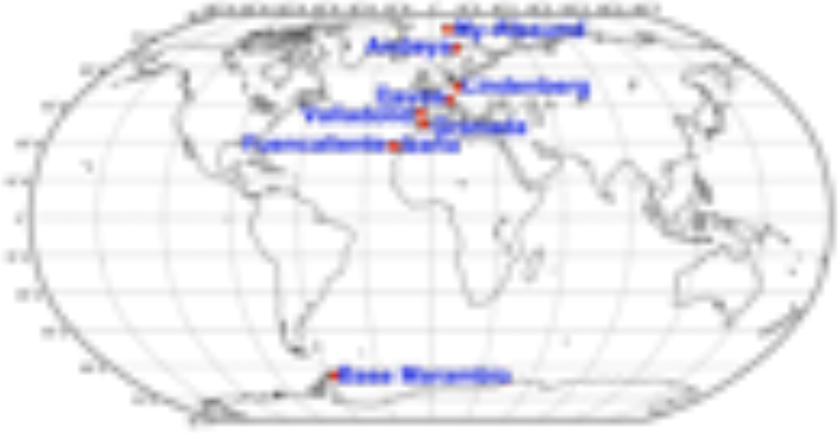


Figure 7.1.2: Geographical locations of the nine stations utilized in Román et al. 2025 (obtained from Figure 2 of Román et al. 2025).



Figure 7.1.3: OMEA-3C-TF camera installed in the Science Faculty of Valladolid. This camera model looks identical to the OMEA-3C model.

To extract the star light from each image, it is needed first to remove the background light (the skyglow). It can be done as is explained in the scheme of Figure 7.1.4 for the green component of one image. When zooming in, the big dipper can be appreciated in the raw image, where the background is not zero. The background can be calculated for each color image using some filters. The original image minus the background corresponds to the image background corrected as is shown in the right side of Figure 7.1.4.

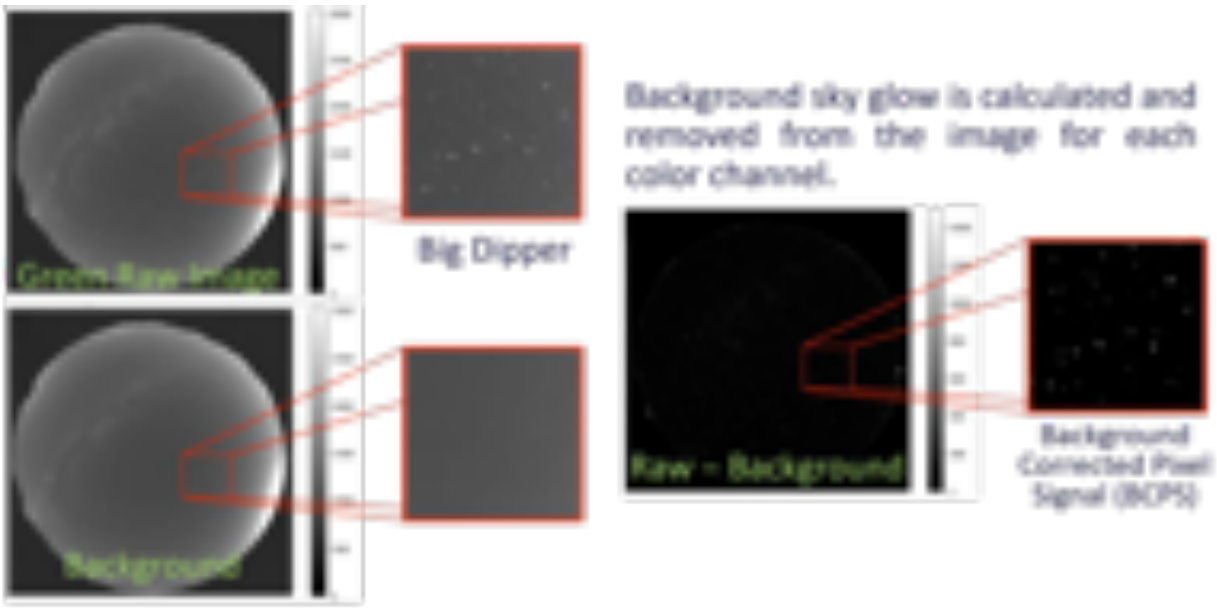


Figure 7.1.4: Scheme about background calculation and removal to calculate background corrected pixel signal (BCPS) in the green component of a raw example image.

All the cameras were geometrically calibrated by ORION app (Antuña-Sánchez et al., 2022), knowing the azimuth and zenith viewed by each pixel; therefore, any star can be located in the

images. With this, the next method for all color channels and a list of 50 stars was applied to extract the star irradiance (Figure 7.1.5 shows an example for Alnilam): 1) A eighty by eighty pixel box centered in the chosen star is selected and the identified segment closest to the center of the box (yellow segment in Figure 7.1.5b), is assumed as the star; 2) the integrated BCPS signal in a five pixel circular aperture centered in the star (white circle of Figure 7.1.5b) is calculated; and 3) this integrated signal divided by the time exposure is assumed as an uncalibrated star signal (USI).

This USI signal is too noisy, then some filters are applied to smooth this signal. This smoothed signal is used to make Langley plots every night, obtaining the calibration constant for each color channel and star. For one specific date, color and star, the value of this calibration constant is assumed as the median within plus minus 6 months window. With this value and the recorded USI value, the total optical depth can be calculated by Beer's law.

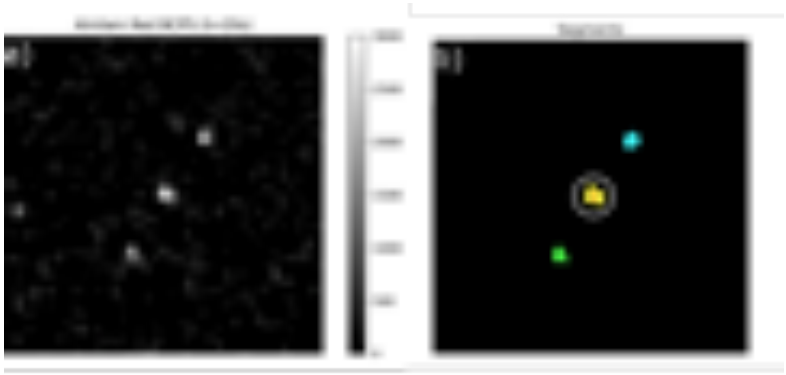


Figure 7.1.5: a) Background-corrected pixel signal (BCPS), in digital counts (DCs), for a subimage within a selected 80 × 80 pixel box, centered on the Alnilam star, derived from the red channel of the raw image recorded in Valladolid on 19 January 2024 at 23:40 UTC (with an exposure time of 20 s). Segments identified as stars are marked in color in panel b), where the yellow segment corresponds to Alnilam, the red cross indicates its centroid, and the white circle denotes the region used to extract the star's BCPS. Source: Figure 4 of Román et al. (2025).

However to obtain the aerosol optical depth it is necessary to remove the Rayleigh and gases absorption. To this end, it is needed to take into account the spectral response of the cameras. The spectral direct irradiance of each star was calculated with a radiative transfer model for different gases and pressures amounts. The optical depths were obtained convoluting these simulations with the camera response, and a linear relationship was found between optical depth and the gas concentration/pressure. Then, the gases amounts and pressure are obtained from ERA5 reanalysis, and with these values and the obtained linear relationships, the Rayleigh and gases optical depth are calculated and subtracted from TOD to obtain AOD. A similar method

was done to obtain the effective wavelengths of the camera, being 591, 534, 466 and 537 nm for red, green, blue and gray for the OMEA-3C model (614, 538, 472, and 548 nm for OMEA-3C-TF). Once the AOD for each star and channel is obtained, they are quality assurance and cloud filtered. The filtered AOD values from all stars are averaged in 5 minute windows. After that, another cloud and quality-assurance filter is applied. Finally, one AOD value and its propagated uncertainty is obtained per channel every 5 minutes.

As a result, Figure 7.1.6 shows in blue the retrieved AOD at Izaña (Spain) in the green channel during 20 days in summer 2022. The values correlate with those obtained by lunar photometer, and perfectly fits with the values obtained at daytime. These results point out the potential of all-sky cameras to continuously monitor the AOD during the Polar night in Arctic and Antarctic stations. A direct comparison of the camera AOD against the corrected lunar values for the eight cameras used by Román et al. (2025), revealed a high correlation in most cases, with the worst results in the high latitude places. Regarding the differences between both databases (camera minus lunar values), the mean was about 0.02 and the standard deviation about 0.03 and 0.04. The OMEA-3C-TF was one of the cameras showing better results.



Figure 7.1.6: AOD at 534 nm (AOD534) at Izaña (Tenerife, Spain) for 20 days in July 2022. Blue error bars represent the nighttime camera AOD ± its associated error. The red crosses and green dots correspond to the AOD data from the Sun–sky–Moon photometer during daytime and nighttime, respectively.

7.1.2 Stations and status

The methodology described in the previous section was applied by Román et al. (2025) to the eight cameras installed in the nine locations of Figure 7.1.2, and nowadays it is extended to all the cameras of the GOA-SCAN network (see Sites & Measurements tab of https://goa.uva.es). The station of Fuencaliente is not already equipped with an all-sky camera, since it was temporarily installed to monitor the Tajogaite volcano eruption (Barreto et al., 2026), but the remaining eight stations of Figure 7.1.2 are still active. In addition, nowadays there are another 25 active all-sky cameras in GOA-SCAN. Two of them are in Antarctica: Base Juan Carlos I (Spanish base; -62.66ºN; -60.38ºE) and Dome Concordia (Italian base; -75.10ºN; 123.32ºE). 20 of the mentioned cameras, all OMEA-3C-TF, are installed in different sites of Valladolid city (Spain) and surroundings; more info about these GOA-SCAN cameras is available in Herrero del Barrio et al. (2026) and in this link: https://goa.uva.es/proyecto-presente. Finally, three OMEA-

3C-TF cameras are additionally installed in the region of Lindenberg, participating nowadays in the C3SAR campaign (https://c3sar.de/campaign).

The AOD at nighttime is retrieved for all these GOA-SCAN cameras in near-real time by the GOA-UVa. This network is designed to add all-sky cameras from other groups (this is the case of the all-sky camera in Davos, which belongs to PMOD/WRC) in order to process, among others, the AOD at nighttime. All-sky cameras could help to fill the gap of AOD at nighttime on a global scale due to their low-cost and automatic work.

7.2 AOD retrieval with wide-field stellar photometry

The use of stars for atmospheric monitoring (both cloud detection and AOD retrieval) has been proposed at the Pierre Auger Observatory in Argentina more than 20 years ago and a robotic telescope FRAM (F/Photometric Robotic Atmospheric Telescope) has been operated at the Los Leones site of the Fluorescence detector (FD) of the Observatory continuously since 2005. The original concept used a photoelectric detector to precisely measure the apparent brightness of individual bright stars in different filters in order to measure the wavelength dependence of the aerosol extinction in real time (the Ångström exponent). Additionally, a small CCD camera with a telephoto lens has been added, primarily used to detect clouds along the trajectories of interesting cosmic-ray showers based on a rapid-response trigger system. The rapid follow-up system has been later upgraded with a larger camera and better optics and has become the primary contribution of the FRAM project to the Pierre Auger Observatory, with a second FRAM being installed in 2021 at the Cohuieco FD station in order to expand the coverage to more cosmic-ray showers.
The use of the photoelectric photometer was eventually abandoned as the precision of the measurements was insufficient for the purpose. Similarly, attempts to extract precise aerosols in different filters from measurements of specific stellar fields with a CCD camera on the 30-cm main telescope have never been successful. Eventually, it was realized that a more precise AOD retrieval is actually possible using the data taken during the rapid follow-ups of cosmic-ray showers with the wide-field system, as these cover a large span of air mass and thus can be used to extract the AOD from a fit of extinction as a function of air mass, independently of the absolute calibration of the instrument and detection chain. Obviously, such data can be also obtained without the motivation from a cosmic-ray shower, thus a generally applicable method of AOD retrieval from wide-field photometry has been developed.

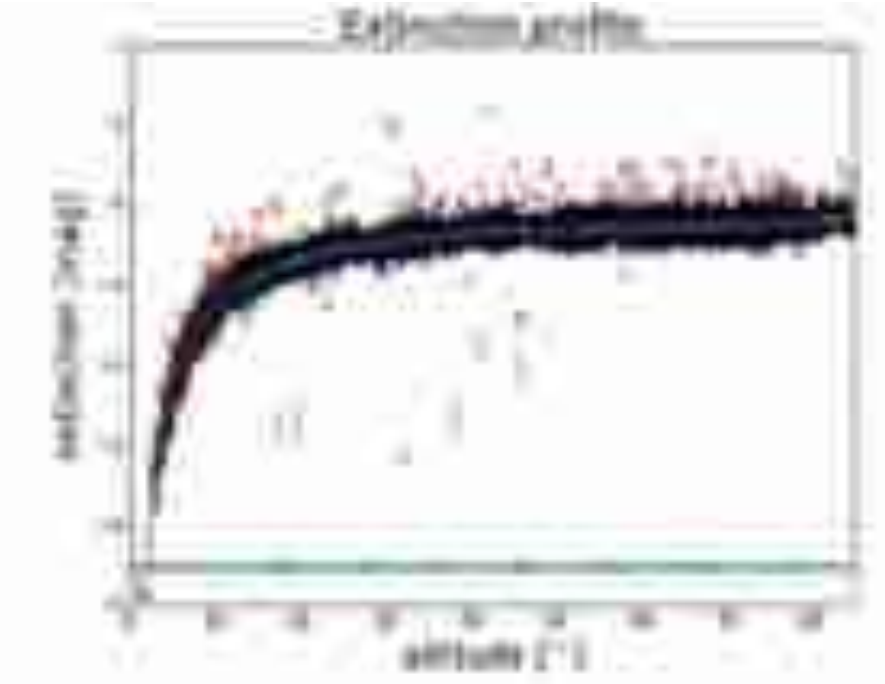


Figure 7.2.1: An example of an extinction profile obtained by scanning over a large span of air mass. This profile is not affected by clouds and can be used to fit AOD.

At the Pierre Auger Observatory, AOD is regularly retrieved using a bi-static LIDAR system, where the detector is the Fluorescence detector itself, as well as several elastic and Raman LIDAR systems. All the LIDAR systems provide the full vertical profile of AOD, while the FRAM method only measures the integral value across the entire atmosphere. The FRAM AOD measurements are thus only complementary - they can be used to study horizontal inhomogeneity of aerosols and fast temporal changes, as the LIDAR measurements are limited in volume to limit the disturbance to the FD observations. Based on the Auger experience, the method has been successfully proposed to the upcoming Cherenkov Telescope Array Observatory (CTAO). There, FRAM measurements will be an integral part of the atmospheric monitoring system, providing interpolation with high temporal resolution between LIDAR measurements of the vertical AOD profiles. In this scheme, sufficient variations in the total AOD detected by the FRAM can trigger a new profile measurement by the LIDAR (which requires an interruption of the gamma-ray observations).

7.2.1 Main principles

The method for aerosol retrieval with wide-field photometry is described in great detail in Ebr et al. 2021. The main idea is that when assuming horizontally homogeneous (stratified) aerosols in the vicinity of the FRAM, the apparent brightness of any given star can be predicted from its catalog brightness with only two free parameters that can potentially differ from one air mass scan to the other- the vertical AOD and the calibration constant of the system. This constant (usually expressed in magnitudes as a zeropoint) depends on the hardware parameters of the detector -

optics, its cleanness, camera, its internal and external temperature, optical alignment and focusing state - as well as on the exact parameters of the software pipeline used to convert the signal in the camera pixels into the instrumental brightness. Further parameters are needed for accurate prediction of the instrumental brightness, such as correction for position of the image on the camera and for the color index of the star, but those mostly do not vary on short time-scales and can be considered part of the fixed system response.



Figure 7.2.2: A simplified schema of the data processing pipeline. The selection of scans unaffected by clouds still requires human input as there is a large variety of possible effects.

A principle, AOD could be extracted from just a few stars measured at two different air masses. The wide-field method with a continuous coverage over a large range of air masses however has the major advantage of providing a smooth profile, from which any presence of clouds is immediately detectable - cloud-affected scans are discarded, because the fit would be skewed by the clouds being only at specific airmass. The vast amount of stars measured during a single scan provide such great statistics that uncertainties in AOD determination are purely systematics, even though the measurement of a single star with such a small aperture is often dominated by Poisson fluctuations. As any systematics related to the overall sensitivity cancel out, the dominant source of uncertainty are any effects that have any air mass dependence and can thus bias the fit. A major discovery was that the cameras used to not exhibit a perfectly linear dependence over the large dynamic range used in the analysis and thus the sensitivity is affected by the extinction. This major systematics (at the level of 0.02) was removed by laboratory measurements of the

linearity of all the cameras in use. Further laboratory measurements were needed to obtain precise spectral response of the system, which is necessary mainly for precise subtraction of the molecular extinction which varies very fast with wavelength. After all considerations, the maximal uncertainty in vertical AOD is estimated at 0.006 correlated and 0.005 uncorrelated.



Figure 7.2.3: Overview of the current FRAM network.

7.2.2 Stations current status, results, comparisons, validations

Currently, 5 FRAMs are operated: two at the Pierre Auger Observatory, and three at or near the future CTAO sites - two near Cerro Paranal in Chile and one at Observatorio Roque de los Muchachos, Canary islands, Spain. The Auger FRAMs do primarily rapid-follow ups of cosmic-ray showers with anomalous profiles to determine whether the anomaly is intrinsic to the shower or caused by interference from the clouds. Furthermore, they do regular scans in airmass independently of cosmic-ray triggers for AOD retrieval. CTAO FRAMs are designated as “CTA Pathfinders” and provide aerosol climatology for the sites through frequent air mass scans. This data will provide the baseline for knowing the range of possible conditions at the sites so that an appropriate range of simulations is prepared in advance for data analysis once CTAO is operational. At the northern site, there is already one CTAO Large-size Telescope (LST) operational, with three more in commissioning, as well as the MAGIC telescope, which has been operated there for many years. The FRAM thus also provides those telescopes with real-time

data on AOD directly in their respective fields of view. For this mode, where a fit in air mass is not possible, due to the fixed direction of the field of view, the absolute calibration is tracked by the results of the fit from the regular air mass scans (Dominis Prester et al. 2024).
All of the FRAMs include a wide-field system (and some also a narrow-field telescope not regularly used for AOD retrieval). All the wide-field systems are based on G4 CCD or C4 CMOS cameras from Moravian Instruments, with 36x36 mm chips at 4k times 4k pixels. Auger FRAMs use 300/2.8 Nikon and Canon lenses (giving FoV 7 degrees) while CTAO FRAMs use Zeiss and Samyang 135/2 lenses (15 degrees FoV). All FRAMs are fully robotic and can work autonomously for potentially unlimited time. For safety reasons however they are checked every evening for issues by a human observer, remotely from the Czech Republic. At the claimed precision better than 0.01 in AOD, it is surprisingly difficult to validate the FRAM data, as sources of sufficiently precise measurements that would be directly comparable at the relevant sites are surprisingly scarce. The most convincing validation is the correlation with night-time Sun/Moon Photometer measurements (Ebr et al. 2021).

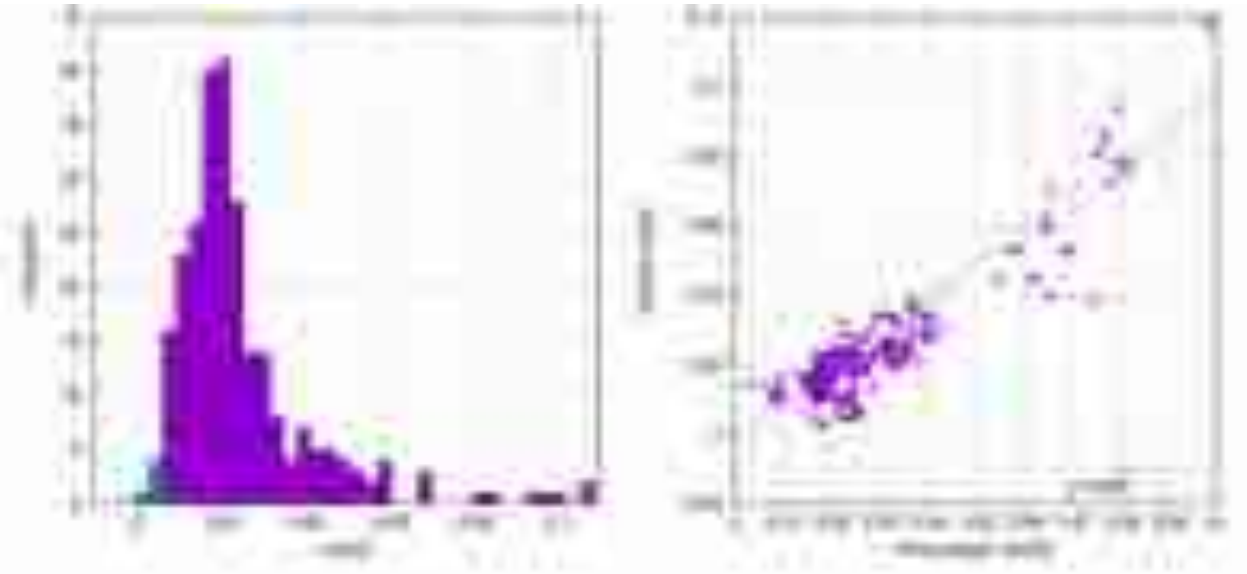


Figure 7.2.4: Distribution of vertical AODs from a sample of measurements at all CTAO sites (left) and correlation between FRAM and Moon Photometer at La Palma (right) from (Ebr et al. 2021).

It is interesting to note that a 0.01 precision in AOD is generally not sufficient for the determination of the Ångström coefficient in the prevailing conditions on the Auger and CTAO sites, where the absolute AOD values are generally way below 0.1. However it turns out that on top of the already correlated uncertainties, even some of the technically uncorrelated uncertainties cancel out when images are taken in quick succession in different filters but in the same position on the sky. For a site with stable conditions, all the correlated uncertainties then can be removed using the requirement that the linear correlation between AOD in different filters passes through zero (a paper detailing this method will be submitted soon).

8. Summary

In this final deliverable of Working Group 1 of the COST Action HARMONIA, we have sought to provide an overview of photometry in Europe through time: its distant past, recent past, present and future, while showing how COST Action HARMONIA has contributed to this rich history.

In Part 2, we reviewed the different types of photometry (solar, stellar and lunar) and their histories—reaching back to the seventeenth-century mathematicians Bouguer and Lambert, the nineteenth- and twentieth-century astronomers Beer and Langley, and the early twentieth-century Ångström family, pioneers in measuring solar radiation through the atmosphere. We traced the basic principles and history of solar, stellar and lunar photometry, and took stock of where the field stands today.

In Part 3, we discussed the three major measurement networks—AERONET, GAW-PFR and SKYNET—and their respective instruments (CIMEL, PFR and Prede), tracing the early development of the instruments and the first steps of each network. We saw that these major advances were built on human interaction: people with different skills, backgrounds and nationalities who met—sometimes by chance—and worked together to develop ambitious instruments and, eventually, large-scale measurement networks. It would have been easier to foster exchanges and travel if HARMONIA had existed in the 1990s! Today's HARMONIA community builds on the work of those scientists, engineers, researchers and technicians, as well as their successors in instrument-manufacturing companies, university research laboratories and government institutions. Above all, it continues their spirit of international—and especially European—collaboration: the pleasure of meeting at workshops, field campaigns and conferences across Europe, and of exchanging ideas formally and informally, in presentations, beside posters, by setting up instruments, over icebreakers or at dinner.

In Part 4, we travelled across Europe and through time to visit the laboratories, observatories and company workshops where instruments and ideas were born, and where some of the longest measurement series began. We explored the places that helped establish European photometry and continue to advance it today. We also saw how HARMONIA has built on foundations laid over several decades, helping new branches of photometry flourish by supporting the students, doctoral researchers and postdoctoral fellows who may become tomorrow's researchers and inventors of instruments and networks. We discussed the summer, spring and winter schools, and the workshops HARMONIA was able to hold at historic and remarkable observatories such as Izaña, Lindenberg and Davos.

In Part 5, we travelled to the poles to understand the importance of making high-quality aerosol and aerosol optical depth (AOD) measurements at as many stations as possible. We explored how photometry groups across Europe—from the Nordic countries to Italy, France, Germany, Switzerland and Spain—have contributed to this effort, how the stations' network has evolved over time, and where it stands today.

In Part 6, we presented the essence of HARMONIA: harmonising different approaches and fostering synergies among measurement techniques. We showed that the work of HARMONIA members extends beyond sun photometers and AOD measurements, forming part of a broader effort to measure and characterise aerosols.

Finally, in Part 7, we presented two innovative and promising techniques for measuring aerosols. The camera-based method (section 7.1) for retrieving AOD by observing many stars simultaneously is one of HARMONIA's legacies: the study began thanks to the connections fostered by HARMONIA and may become one of its most distinctive contributions.

This deliverable has told the story of photometry in Europe—yesterday, today and tomorrow; solar, stellar and lunar. HARMONIA is now drawing to a close, but it has become part of that story and has enabled many memorable scientific and human journeys.

We conclude with a photo (Figure 8.1) of the core group, HARMONIA's early-career researchers and a few invited experts, all HARMON..ized in HARMONIA T-shirts at this year's retreat in Astypalea, Greece.

We hope to meet again soon beyond HARMONIA, while carrying forward its wonderful spirit of openness, creativity and friendship across borders.



Figure 8.1: Farewell picture of HARMONIA at the retreat of Astypalea (Greece), July 2026, with core group members, young and invited scientist; Standing behind from left to right: Dimitra

Kouklaki (NOA & NKUA), Africa Barreto (AEMET), Pavla Dagson Waldhauserhova (LBHI), Yeşer Aslanoğlu (Hacettepe Univ.), Stelios Kazadzis (PMOD/WRC), Stavros Solomos (RCAPC), Carlos Toledano (UVa), Pablo González Sicilia (AEMET), Lionel Doppler (DWD), Roberto Román (UVa), Luca Egli (PMOD/WRC), Alberto Redondas (AEMET), Ilias Fountoulakis and Nikolaos Papadimitriou (RCAPC), Panos Raptis (NOA), Victor Estellés (UVEG), Peter Hrabcák (SHMI), Anca Nemuc (INOE); Sitting in the first rank: Gaurav Kumar (UVEG), Georgia Charalambous (ECoE), Monica Campanelli (ISAC-CNR), Kathrin Anhorn and Eliane Tobler (PMOD/WRC), Benjamin Torres (LOA), Meritxell Garcia Suñer (UVEG), Henri Diémoz (ARPA).

References

1. Aaltonen, V., E. Rodriguez, S. Kazadzis, et al. On the variation of aerosol properties over Finland based on the optical columnar measurements. Atmos. Res., 116, 46–55, doi:https://doi.org/10.1016/j.atmosres.2011.07.014, 2012.
2. Alados-Arboledas, L., D. Müller, J. L. Guerrero-Rascado, F. Navas-Guzmán, D. Pérez-Ramírez, and F. J. Olmo: Optical and microphysical properties of fresh biomass burning aerosol retrieved by Raman lidar, and star-and sun-photometry, Geophys. Res. Lett., 38, L01807, https://doi.org/10.1029/2010GL045999, 2011.
3. Alekseeva, G. A., Arkharov, A. A., Galkin, V. D., et al.: The Pulkovo Spectrophotometric Catalog of Bright Stars in the Range from 320 TO 1080 NM, Balt. Astron., 5, 603–838, available at: http://adsabs.harvard.edu/abs/1997BaltA...6..481A (last access: 21 September 2021),1996.
4. Ångström, A., On the atmospheric transmission of sun radiation and on dust in the air, *Geografiska Annaler, 2*, 156-166. https://doi.org/10.2307/519399, 1929.
5. Ångström, A. K.: Techniques of Determinig the Turbidity of the Atmosphere[1]. *Tellus*, *13*(2), 214–223. https://doi.org/10.3402/tellusa.v13i2.9493, 1961.
6. Ångström, A. K.: "On determinations of the atmospheric turbidity and their relation to pyrheliometric measurements", Adv. In Geophys., 14, 269, https://www.sciencedirect.com/science/chapter/bookseries/abs/pii/S0065268708601594?via%3Dihub, 1970.
7. Ansmann, A., Wagner, F., Müller, et al.: European pollution outbreaks during ACE 2: Optical particle properties inferred from multiwavelength lidar and star-Sun photometry, J. Geophys. Res.-Atmos., 107, AAC 8-1–AAC 8-14, https://doi.org/10.1029/2001JD001109, 2002.
8. Antuña-Sánchez, J.C., R. Román., J.L. Bosch et al.: ORION software tool for the geometrical calibration of all-sky cameras. PLoS ONE 17(3): e0265959, https://doi.org/10.1371/journal.pone.0265959 , 2022.

9. Barreto, A., Cuevas, E., Damiri, B., et al.: A new method for nocturnal aerosol measurements with a lunar photometer prototype, Atmos. Meas. Tech., 6, 585–598, https://doi.org/10.5194/amt-6-585-2013, 2013.
10. Barreto, A., Cuevas, E., Pallé, P., et al.: Recovering long-term aerosol optical depth series (1976–2012) from an astronomical potassium-based resonance scattering spectrometer, Atmos. Meas. Tech., 7, 4103–4116, https://doi.org/10.5194/amt-7-4103-2014, 2014.
11. Barreto, Á., Cuevas, E., Granados-Muñoz, M.-J., et al.: The new sun-sky-lunar Cimel CE318-T multiband photometer – a comprehensive performance evaluation, Atmos. Meas. Tech., 9, 631–654, https://doi.org/10.5194/amt-9-631-2016, 2016.
12. Barreto, Á., Román, R., Cuevas, E., et al.: Assessment of nocturnal aerosol optical depth from lunar photometry at the Izaña high mountain observatory. Atmospheric Measurement Techniques, 10(8), 3007-3019. doi:https://doi.org/10.5194/amt-10-3007-2017, 2017.
13. Barreto, A., Román, R., Cuevas, E., et al.: Evaluation of night-time aerosols measurements and lunar irradiance models in the frame of the first multi-instrument nocturnal intercomparison campaign. Atmospheric environment, 202, pp.190-211, https://doi.org/10.1016/j.atmosenv.2019.01.006, 2019.
14. Barreto, A., F. Quirós, O.E. García et al., Volcanic plume height during the 2021 Tajogaite eruption (La Palma) from two complementary monitoring methods – implications for satellite-based products, Atmos. Meas. Tech., 19 (4), 1385–1406, https://doi.org/10.5194/amt-19-1385-2026, 2026.
15. Barrie, L., and C. Wehrli: WMO/GAW Experts Workshop on a Global Surface-Based Network for Long Term Observations of Column Aerosol Optical Properties, GAW Report No. 162, WMO/TD-No. 1287, https://library.wmo.int/idurl/4/41246, 2004.
16. Bates, T. S., Huebert, B. J., Gras, J. L., Griffiths, F. B., & Durkee, P. A. International Global Atmospheric Chemistry (IGAC) Project's First Aerosol Characterization Experiment (ACE 1): Overview. Journal of Geophysical Research: Atmospheres, 103(D13), 16297–16318. https://doi.org/10.1029/97JD03741, 1998.
17. Bazo, E., Granados-Muñoz, M. J., Román, R., et al.: Evaluation of the vertically-resolved aerosol radiative effect on shortwave and longwave ranges using sun-sky photometer and ceilometer measurements, Atmos. Res., 282, 106517, https://doi.org/10.1016/j.atmosres.2022.106517, 2023.
18. Becker, R., Doppler, L., Weber, S. and Baum, W.: 35 Jahre AOD-Messungen am MOL, MOL-RAO aktuell 01/2021, https://www.dwd.de/DE/forschung/atmosphaerenbeob/lindenbergersaeule/rao_download/aktuell_2021_01.pdf?__blob=publicationFile&v=2, 2021.
19. Benavent-Oltra, J. A., Román, R., Granados-Muñoz, M. J., et al.: Comparative assessment of GRASP algorithm for a dust event over Granada (Spain) during ChArMEx-ADRIMED 2013 campaign, Atmos. Meas. Tech., 10, 4439–4457, https://doi.org/10.5194/amt-10-4439-2017, 2017.

20. Benavent-Oltra, J. A., Román, R., Casquero-Vera, J. A., et al.: Different strategies to retrieve aerosol properties at night-time with the GRASP algorithm, Atmos. Chem. Phys., 19, 14149–14171, https://doi.org/10.5194/acp-19-14149-2019, 2019.
21. Benavent-Oltra, J. A., Casquero-Vera, J. A., Román, et al.: Overview of the SLOPE I and II campaigns: aerosol properties retrieved with lidar and sun–sky photometer measurements, Atmos. Chem. Phys., 21, 9269–9287, https://doi.org/10.5194/acp-21-9269-2021, 2021.
22. Boichu, M., et al.: Growth and Global Persistence of Stratospheric Sulfate Aerosols From the 2022 Hunga Tonga–Hunga Ha'apai Volcanic Eruption. Journal of Geophysical Research: Atmospheres, 128, https://doi.org/10.1029/2023JD039010, 2023.
23. Campanelli, M., Estellés, V., et al.: COST-HARMONIA WG2, Deliverable D2.2: List of possible improvements on the quality of solar, lunar and stellar photometry: https://harmonia-cost.eu/wp-content/uploads/2024/11/D22_v1.pdf, 2024.
24. Cazorla, A., Casquero-Vera, J. A., Román, R., et al.: Near-real-time processing of a ceilometer network assisted with sun-photometer data: monitoring a dust outbreak over the Iberian Peninsula, Atmos. Chem. Phys., 17, 11861–11876, https://doi.org/10.5194/acp-17-11861-2017, 2017.
25. Chaikovsky, A., Dubovik, O., Holben, B., et al.: Lidar-Radiometer Inversion Code (LIRIC) for the retrieval of vertical aerosol properties from combined lidar/radiometer data: development and distribution in EARLINET, Atmos. Meas. Tech., 9, 1181–1205, https://doi.org/10.5194/amt-9-1181-2016, 2016.
26. Chen, Y.-C., Hamre, B., Frette, Ø., et al.: Aerosol optical properties in Northern Norway and Svalbard. Applied Optics, 55(4), 660–672. DOI: https://doi.org/10.1364/AO.55.000660, 2016.
27. Cuevas, E., Romero-Campos, P. M., Kouremeti, N., et al.: Aerosol optical depth comparison between GAW-PFR and AERONET-CIMEL radiometers from long-term (2005–2015) 1 min synchronous measurements, Atmos. Meas. Tech., 12, 4309–4337, https://doi.org/10.5194/amt-12-4309-2019, 2019.
28. De Ory Ajamil, F.: El Centenario del Observatorio de Izaña: La apasionante historia de un Observatorio de montaña en una remota isla del Atlántico Norte. Agencia Estatal de Meteorología. https://repositorio.aemet.es/handle/20.500.11765/1820, 2016.
29. Devaux, C., Vermeulen, A., Deuzé, J. L., et al.: Retrieval of aerosol single-scattering albedo from ground-based measurements: Application to observational data. Journal of Geophysical Research, 103, 8753–8761. https://doi.org/10.1029/98JD00276, 1998.
30. Di Carmine, C., Campanelli, M., Nakajima, T., Tomasi, C., & Vitale, V. Retrievals of Antarctic aerosol characteristics using a Sun-sky radiometer during the 2001–2002 austral summer campaign. Journal of Geophysical Research: Atmospheres, 110, D13202. https://doi.org/10.1029/2004JD005280, 2005.
31. Dominis Prester, D. et al: Characterisation of the Atmosphere in Very High Energy Gamma-Astronomy for Imaging Atmospheric Cherenkov Telescopes, Universe, Volume 10, Issue 9, id.349, 2024.
32. Doppler, L., Masoom, A., and Karanikolas, A.: COST-HARMONIA WG1, Deliverable D1.1: Create a list of existing and foreseen campaigns or experiments needed for night and day aerosol

measurements and report on the data collection and analysis of the data/measurements, https://harmonia-cost.eu/wp-content/uploads/2023/10/COST_CA21119_HARMONIA-WG1_Deliverable-D11.pdf, 2023.
33. Doppler, L., Akriti Masoom, et al.: COST-HARMONIA WG1, Deliverable D1.2: Differences and harmonisation possibilities in AOD retrieval methods, https://harmonia-cost.eu/wp-content/uploads/2024/12/Harmonia_D1.2_ver2.pdf, 2024.
34. Doppler, L., Karanikolas, A., Garcia Suñer, M., et al.: Differences and harmonization possibilities in AOD retrieval methods, COST ACTION, COST-EUROPEAN COOPERATION IN SCIENCE AND TECHNOLOGY, Brussels, Belgium, COST CA21119 HARMONIA-WG1 Deliverable-D1.3, https://harmonia-cost.eu/wp-content/uploads/2026/10/HARMONIA-WG1_D1.3_Harmonised-AOD-Retrievals_V03-1.pdf, 2026.
35. Dubovik, O., and M. D. King, A flexible inversion algorithm for retrieval of aerosol optical properties from Sun and sky radiance measurements, J. Geophys. Res., 105 (D16), 20673–20696, https://doi.org/10.1029/2000JD900282, 2000.
36. Dubovik, O., et al.: GRASP: a versatile algorithm for characterizing the atmosphere. SPIE Newsroom, 19 September 2014. https://doi.org/10.1117/2.1201408.005558, 2014.
37. Dubovik, O., Fuertes, D., Litvinov, P., et al.: A Comprehensive Description of Multi-Term LSM for Applying Multiple a Priori Constraints in Problems of Atmospheric Remote Sensing: GRASP Algorithm, Concept, and Applications, Frontiers in Remote Sensing, 2, https://doi.org/10.3389/frsen.2021.706851, 2021.
38. Durkee, P. A., Nielsen, K. E., Smith, P. J., et al.: Regional aerosol optical depth characteristics from satellite observations: ACE-1, TARFOX and ACE-2 results. Tellus B, 52(2), 484–497. https://doi.org/10.1034/j.1600-0889.2000.00040.x, 2000.
39. Ebr, J. et al: A New Method for Aerosol Measurement Using Wide-field Photometry, The Astronomical Journal, Volume 162, Issue 1, id.6, 2021.
40. Fedarenka, A., et al.: Utilization of AERONET polarimetric measurements for improving retrieval of aerosol microphysics: GSFC, Beijing and Dakar data analysis. Journal of Quantitative Spectroscopy and Radiative Transfer, 179, 72–97. https://doi.org/10.1016/j.jqsrt.2016.03.021, 2016.
41. Fiddes, S. L., Protat, A., Mallet, et al: Southern Ocean cloud and shortwave radiation biases in a nudged climate model simulation: does the model ever get it right?. Atmospheric Chemistry and Physics, 22(22), 14603-14630, https://doi.org/10.5194/acp-22-14603-2022, 2022
42. Freud, E., Krejci, R., Tunved, P., et al.: Pan-Arctic aerosol number size distributions: seasonality and transport patterns. Atmospheric Chemistry and Physics, 17(13), 8101-8128, https://doi.org/10.5194/acp-17-8101-2017, 2017.
43. Fröhlich, C.: Determination of aerosol optical depth from ground measurements, Advances in Space Research, Volume 2, Issue 5, Pages 139-145, ISSN 0273-1177, https://doi.org/10.1016/0273-1177(82)90341-6., 1983.
44. Fu, Y. J., Huang, G. H., Huang, et al.: Is the cloud absorption of solar radiation still underestimated notably by current model-based reanalyses?. Advances in Climate Change Research, 17(1), 12-24. https://doi.org/10.1016/j.accre.2025.10.003, 2026.

45. Fuertes, D., Toledano, C., González, R., et al.: CÆLIS: software for assimilation, management and processing data of an atmospheric measurement network, Geosci. Instrum. Method. Data Syst., 7, 67–81, https://doi.org/10.5194/gi-7-67-2018, 2018.
46. Giles, D. M., Sinyuk, A., Sorokin, M. G., et al.: Advancements in the Aerosol Robotic Network (AERONET) Version 3 database – automated near-real-time quality control algorithm with improved cloud screening for Sun photometer aerosol optical depth (AOD) measurements, Atmos. Meas. Tech., 12, 169–209, https://doi.org/10.5194/amt-12-169-2019, 2019.
47. González, R., Toledano, C., Román, R., et al.: Daytime and nighttime aerosol optical depth implementation in CÆLIS, Geosci. Instrum. Method. Data Syst., 9, 417–433, https://doi.org/10.5194/gi-9-417-2020, 2020.
48. González-Fernández, D., Román, R., Mateos, D., et al.: Retrieval of Solar Shortwave Irradiance from All-Sky Camera Images. Remote Sens. 2024, 16, 3821. https://doi.org/10.3390/rs16203821, 2024
49. Graßl, S., and Ritter, C.: Properties of Arctic Aerosol Based on Sun Photometer Long-Term Measurements in Ny-Ålesund, Svalbard. Remote Sensing, 11(11), 1362. https://doi.org/10.3390/rs11111362, 2019
50. Graßl, S., Ritter, C., Wilsch, J., et al. : From Polar Day to Polar Night: A Comprehensive Sun and Star Photometer Study of Trends in Arctic Aerosol Properties in Ny-Ålesund, Svalbard. Remote Sensing, 16(19), p.3725., https://doi.org/10.3390/rs16193725, 2024.
51. Graßl, Sandra: Arctic Aerosols: From the Boundary Layer to the Stratosphere, PhD Thesis of the Universität Potsdam, https://doi.org/10.25932/publishup-68054, 2025: https://publishup.uni-potsdam.de/opus4-ubp/frontdoor/deliver/index/docId/68054/file/grassl_diss.pdf, 2025.
52. Griesche, H. J., Barrientos-Velasco, C., Deneke, H., et al.: Low-level Arctic clouds: a blind zone in our knowledge of the radiation budget. Atmospheric Chemistry and Physics, 24(1), 597-612. https://doi.org/10.5194/acp-24-597-2024, 2024 .
53. Gueymard, C: Turbidity determination from broadband irradiance measurements: A detailed multicoefficient approach, Journal of Applied Meteorology, Vol. 37, pp 414-435. https://doi.org/10.1175/1520-0450(1998)037<0414:TDFBIM>2.0.CO;2, 1998.
54. Hansen, G., K. Aspmo, T. Berg, et al.: Atmospheric Monitoring at the Norwegian Antarctic Station Troll: Measurement Programme and First Results, Polar Research, 28, 353-363, https://doi.org/10.1111/j.1751-8369.2009.00134.x, 2009.
55. Harrison, L., Michalsky, J., and Berndt, J.: Automated multifilter rotating shadow-band radiometer: an instrument for optical depth and radiation measurements, Appl. Opt., 33, 5118–5125, https://doi.org/10.1364/AO.33.005118, 1994.
56. Heimo, A., Fröhlich, C. Influence of the El Chichon eruption in Central Europe determined as change in atmospheric transparency at Davos, Switzerland. Theor Appl Climatol 40, 3–7 . https://doi.org/10.1007/BF00867787, 1989.
57. Herber, A., L.W. Thomason, H. Gernandt, et al., Continuous day and night aerosol optical depth observations in the Arctic between 1991 and 1999, J. Geophys. Res., 107(D10), 4097, https://agupubs.onlinelibrary.wiley.com/doi/pdfdirect/10.1029/2001JD000536, 2002.

58. Herman, M., Balois, J. Y., Gonzalez, L., et al.: Stratospheric aerosol observations from a balloon-borne polarimetric experiment. Applied Optics, 25, 3573–3584. https://doi.org/10.1364/AO.25.003573, 1986.
59. Herman, M., Deuzé, J. L., Devaux, C., et al.: Remote sensing of aerosols over land surfaces including polarization measurements and application to POLDER measurements. Journal of Geophysical Research, 102, 17039–17049. https://doi.org/10.1029/96JD02109, 1997.
60. Herman, J., Cede, A., Spinei, E., et al.: NO2 column amounts from ground-based Pandora and MFDOAS spectrometers using the direct-sun DOAS technique: Intercomparisons and application to OMI validation, J. Geophys. Res., 114, D13307, https://doi.org/10.1029/2009JD011848, 2009.
61. Herreras, M., Román, R., Cazorla, A., et al. M.: Evaluation of retrieved aerosol extinction profiles using as reference the aerosol optical depth differences between various heights, Atmos. Res., 230, 104625, https://doi.org/10.1016/j.atmosres.2019.104625, 2019.
62. Herrero-Anta, S., Eckhardt, S., Evangeliou, N., et al.: Exceptional high AOD over Svalbard in summer 2019: a multi-instrumental approach, Atmos. Chem. Phys., 26, 1435–1457, https://doi.org/10.5194/acp-26-1435-2026, 2026.
63. Herrero del Barrio C, Román R, González R, et al.: CAECENET: An automatic system processing photometer and ceilometer data from different networks to provide columnar and vertically-resolved aerosol properties. PLoS ONE 19(12): e0311990. https://doi.org/10.1371/journal.pone.0311990, 2024.
64. Herrero del Barrio, C., R. Román, Herrero-Anta, S, et al., Cloud height mapping using multi simultaneous sky images from an all-sky camera network, Atmos. Meas. Tech., 19, 5785–5814. https://doi.org/10.5194/amt-19-5785-2026, 2026.
65. Hirsikko, A., O'Connor, E. J., Komppula, M., et al.: Observing wind, aerosol particles, cloud and precipitation: Finland's new ground-based remote-sensing network, Atmos. Meas. Tech., 7, 1351–1375, https://doi.org/10.5194/amt-7-1351-2014, 2014.
66. Holben, B. E., Slutsker, T., et al.: . Multi-band automatic sun and sky scanning radiometer system for measurement of aerosols., https://ntrs.nasa.gov/citations/19950010576, 1994.
67. Holben, B. N., Eck, T. F., Slutsker, I., et al.: AERONET– A federated instrument network and data archive for aerosol characterization, Remote Sens. Environ., 66, 1–16, https://doi.org/10.1016/S0034-4257(98)00031-5., 1998.
68. Holben, B. N., AERONET: Thirty Years of Observations and Research., AERONET Science and Application Exchange, Sep 17-19, 2024, in College Park, Maryland, USA, 2024.
69. Hoyt, D.V., Fröhlich, C. Atmospheric transmission at Davos, Switzerland 1909–1979. Climatic Change 5, 61–71. https://doi.org/10.1007/BF00144680, 1990
70. IPCC, 2021: Climate Change 2021: The Physical Science Basis. Contribution of Working Group I to the Sixth Assessment Report of the Intergovernmental Panel on Climate Change. Cambridge University Press, Cambridge, United Kingdom and New York, NY, USA, In press, https://doi.org/10.1017/9781009157896, 2021.

71. Ivănescu, L., Baibakov, K., O'Neill, N. T., Blanchet, J.-P., and Schulz, K.-H.: Accuracy in starphotometry, Atmos. Meas. Tech., 14, 6561–6599, https://doi.org/10.5194/amt-14-6561-2021, 2021.
72. Karanikolas, A., Kouremeti, N., Gröbner, J., et al..: Sensitivity of aerosol optical depth trends using long-term measurements of different sun photometers, Atmos. Meas. Tech., 15, 5667–5680, https://doi.org/10.5194/amt-15-5667-2022, 2022.
73. Karanikolas, A., Doppler, L., Hrabcák, P., and Anyfanti, K.:COST-HARMONIA WG1, Deliverable D1.4: Spectral AOD and AOD in the UV, COST ACTION, COST-EUROPEAN COOPERATION IN SCIENCE AND TECHNOLOGY, Brussels, Belgium, COST CA21119 HARMONIA-WG1 Deliverable-D1.4, https://harmonia-cost.eu/wp-content/uploads/2026/10/WG1-D1.4-Spectral-and-UV-AODHARMONIAtemplate.pdf, 2026.
74. Karl, T., Gohm, A., Rotach, M. W., et al., and Staudinger, M.: Studying urban climate and air quality in the Alps: The Innsbruck Atmospheric Observatory, Bull. Amer. Meteor. Soc., 101, E488–E507, https://doi.org/10.1175/BAMS-D-19-0270.1, 2020.
75. Karol, Y., Tanré, D., Goloub, P., Vervaerde, C., Balois, J. Y., Blarel, L., Podvin, T., Mortier, A., and Chaikovsky, A.: Airborne sun photometer PLASMA: concept, measurements, comparison of aerosol extinction vertical profile with lidar, Atmos. Meas. Tech., 6, 2383–2389, https://doi.org/10.5194/amt-6-2383-2013, 2013.
76. Kazadzis, S., Kouremeti, N., Diémoz, H., et al.: Results from the Fourth WMO Filter Radiometer Comparison for aerosol optical depth measurements, Atmos. Chem. Phys., 18, 3185–3201, https://doi.org/10.5194/acp-18-3185-2018, 2018a.
77. Kazadzis, S., Kouremeti, N., Nyeki, S., Gröbner, J., and Wehrli, C.: The World Optical Depth Research and Calibration Center (WORCC) quality assurance and quality control of GAW-PFR AOD measurements, Geosci. Instrum. Method. Data Syst., 7, 39–53, https://doi.org/10.5194/gi-7-39-2018, 2018b.
78. Kazadzis, S., Kouremeti, N., and Gröbner, J.: Fifth WMO Filter Radiometer Comparison (FRC-V) 27 September to 25 October 2021, Davos, Switzerland, WMO GAW report 280, https://library.wmo.int/records/item/66263-fifth-wmo-filter-radiometer-comparison-frc-v?offset=5, 2023.
79. Kieffer, H. H. and Stone, T. C.: The spectral irradiance of the moon, Astron. J., 129, 2887–2901, https://iopscience.iop.org/article/10.1086/430185/pdf, 2005.
80. Kreuter, A., Zangerl, M., Schwarzmann, M., and Blumthaler, M.: All-sky imaging: a simple, versatile system for atmospheric research, Appl. Opt., 48, 1091–1097, https://doi.org/10.1364/AO.48.001091, 2009.
81. Kudo, R., Diémoz, H., Estellés, V., Campanelli, M., et al.: Optimal use of the Prede POM sky radiometer for aerosol, water vapor, and ozone retrievals, Atmos. Meas. Tech., 14, 3395–3426, https://doi.org/10.5194/amt-14-3395-2021, 2021.
82. Lachat, D., Wehrli, C.: A century of apparent atmospheric transmission over Davos, Switzerland. Theor Appl Climatol 110, 539–547. https://doi.org/10.1007/s00704-012-0685-z, 2012.

83. Leiterer, U., and Weller, M.: BAS—The project of an earth-atmosphere spectrophotometer for basic research, Acta Astronautica, Volume 12, Issue 6, Pages 419-429,ISSN 0094-5765, https://doi.org/10.1016/0094-5765(85)90048-7, 1985.
84. Leiterer, U., Weller, M.: Sun photometer BAS/ABAS for atmospheric research. In: Instruments and Observing Methods Report No. 33, Papers presented at the WMO Technical Conference on Instruments and Methods of Observation (TECO-1988); WMO TD No. 222,21-26., pp. 21-26, https://library.wmo.int/idurl/4/41668, 1988.
85. Leiterer, U, Naebert, A, Naebert, T, and Alekseeva, G.: A new star photometer developed for spectral aerosol optical thickness measurements in Lindenberg. Contributions to Atmospheric Physics; Vol. 68;2,. https://www.osti.gov/etdeweb/biblio/178652, 1995.
86. Li, L., Dubovik, O., Derimian, Y., Schuster, G. L., et al.: Retrieval of aerosol components directly from satellite and ground-based measurements, Atmos. Chem. Phys., 19, 13409–13443, https://doi.org/10.5194/acp-19-13409-2019, 2019.
87. Li, Z., Goloub, P., Devaux, C., Gu, X., Deuzé, J. L., Qiao, Y., and Zhao, F.: Retrieval of aerosol optical and physical properties from ground-based spectral, multi-angular, and polarized sun-photometer measurements. Remote Sensing of Environment, 101, 519–533. https://doi.org/10.1016/j.rse.2006.01.012, 2006.
88. Li, Z., Blarel, L., Podvin, T., Goloub, P., Buis, J. P., and Morel, J. P.: Transferring the calibration of direct solar irradiance to diffuse-sky radiance measurements for CIMEL Sun–sky radiometers. Applied Optics, 47, 1368–1377. https://doi.org/10.1364/AO.47.001368, 2008.
89. Li, Z., Blarel, L., Podvin, T., Goloub, P., and Chen, L.: Calibration of the degree of linear polarization measurement of polarized radiometer using solar light. Applied Optics, 49, 1249–1256. https://doi.org/10.1364/AO.49.001249, 2010.
90. Li, Z., Li, K., Li, D., Yang, J., Xu, H., Goloub, P., and Victori, S.: Simple transfer calibration method for a Cimel Sun–Moon photometer: calculating lunar calibration coefficients from Sun calibration constants. Applied Optics, 55, 7624–7630. https://doi.org/10.1364/AO.55.007624, 2016.
91. Li, Z., et al.: Comprehensive Study of Optical, Physical, Chemical, and Radiative Properties of Total Columnar Atmospheric Aerosols over China: An Overview of Sun-Sky Radiometer Observation Network (SONET) Measurements. Bulletin of the American Meteorological Society, 99, 739–755. https://doi.org/10.1175/BAMS-D-17-0133.1, 2018.
92. Longarela, B., Román, R., Buitrago, F., et al., Continuous day-and-night Cloud Cover estimation from all-sky images with neural networks. Atmospheric Research, https://doi.org/10.1016/j.atmosres.2026.109403, 2026
93. Lopatin, A., Dubovik, O., Chaikovsky, A., et al.: Enhancement of aerosol characterization using synergy of lidar and sun-photometer coincident observations: the GARRLiC algorithm, Atmos. Meas. Tech., 6, 2065–2088, https://doi.org/10.5194/amt-6-2065-2013, 2013.
94. Lopatin, A., Dubovik, O., Stenchikov, G., et al.: Comparison of diurnal aerosol products retrieved from combinations of micro-pulse lidar and sun photometer observations over the KAUST observation site, Atmos. Meas. Tech., 17, 4445–4470, https://doi.org/10.5194/amt-17-4445-2024, 2024.

95. López-Cayuela, M.-Á., Herreras-Giralda, M., Córdoba-Jabonero, C., et al.: Vertical assessment of the mineral dust optical and microphysical properties as retrieved from the synergy between polarized micro-pulse lidar and sun/sky photometer observations using GRASP code, Atmos. Res., 264, 105818, https://doi.org/10.1016/j.atmosres.2021.105818, 2022.
96. Mateos, D., Toledano, C., Calle, A., et al.: Saharan and Arabian dust optical properties registered by sun photometry during A-LIFE field experiment in Cyprus, Atmos. Chem. Phys., 26, 1993–2005, https://doi.org/10.5194/acp-26-1993-2026, 2026.
97. Mazzola, M., Stone, R. S., Herber, A., et al.: Evaluation of sun photometer capabilities for retrievals of aerosol optical depth at high latitudes: The POLAR-AOD intercomparison campaigns. Atmospheric Environment, 52:4–17. https://doi.org/10.1016/j.atmosenv.2011.07.042, 2012.
98. Mazzola, M., Stone, R. S., Kouremeti, N., et al.: Monitoring aerosol optical depth during the Arctic night: Instrument development and first results. Atmospheric Research, 311:107667, https://doi.org/10.1016/j.atmosres.2024.107667, 2024.
99. Mélin, F., Zibordi, G., Carlund, T. et al.: Validation of SeaWiFS and MODIS Aqua/Terra aerosol products in coastal regions of European marginal seas. Oceanologia 2013, no. 55(1), pp. 27-51. doi:10.5697/oc.55-1.027, https://www.sciencedirect.com/science/article/pii/S0078323413500029, 2013.
100. Mielonen, T., Levy, R. C., Aaltonen, V., et al.: Evaluating the assumptions of surface reflectance and aerosol type selection within the MODIS aerosol retrieval over land: the problem of dust type selection, Atmos. Meas. Tech., 4, 201–214, https://doi.org/10.5194/amt-4-201-2011, 2011.
101. Mitev, V. M., Grigorov, I. V., and Simeonov, V. B.: Lidar measurement of atmospheric aerosol extinction profiles: a comparison between two techniques – Klett inversion and pure rotational Raman scattering methods, Appl. Opt., 31, 6469–6474, https://doi.org/10.1364/AO.31.006469, 1992.
102. Mortier, A., Goloub, P., Derimian, Y., et al.: Climatology of aerosol properties and clear-sky shortwave radiative effects using Lidar and Sun photometer observations in the Dakar site. Journal of Geophysical Research: Atmospheres. https://doi.org/10.1002/2015JD024588, 2016.
103. Muñiz-Rosado, J., Cazorla, A., Sauvageat, E., et al.: Validation of ceilometer aerosol profile retrievals using sun–sky photometer and balloon-borne in situ measurements, Atmos. Chem. Phys., 26, 10255–10285, https://doi.org/10.5194/acp-26-10255-2026, 2026.
104. Nakajima, T., Tanaka, M., & Yamauchi, T.:Retrieval of the optical properties of aerosols from aureole and extinction data. Applied Optics, 22(19), 2951–2959. DOI: 10.1364/AO.22.002951, 1983.
105. Nakajima, T., Tanaka, M., Hayasaka, T., et al.: Airborne measurements of the optical stratification of aerosols in turbid atmospheres. Applied Optics, 25(23), 4374–4381.DOI: 10.1364/AO.25.004374, 1986.
106. Nakajima, T., Tonna, G., Rao, R., Boi, P., Kaufman, Y., & Holben, B.: Use of sky brightness measurements from ground for remote sensing of particulate polydispersions. Applied Optics, 35(15), 2672–2686. DOI: 10.1364/AO.35.002672. 1996.

107. Nakajima, T., S.-C. Yoon, V. Ramanathan, et al.: Overview of the Atmospheric Brown Cloud East Asian Regional Experiment 2005 and a study of the aerosol direct radiative forcing in east Asia, J. Geophys. Res., 112, D24S91, doi:10.1029/2007JD009009, 2007.
108. Nakajima, T., Campanelli, M., Che, H., Estellés, et al..: An overview of and issues with sky radiometer technology and SKYNET, Atmos. Meas. Tech., 13, 4195–4218, https://doi.org/10.5194/amt-13-4195-2020, 2020.
109. Nyeki, S., L. Vuilleumier, J. Morland, et al.: A 10-year integrated atmospheric water vapor record using precision filter radiometers at two high-alpine sites, Geophys. Res. Lett., 32, L23803, https://doi.org/10.1029/2005GL024079, 2005
110. Nyeki, S., C. H. Halios, W. Baum, et al.: Ground-based aerosol optical depth trends at three high-altitude sites in Switzerland and southern Germany from 1995 to 2010, J. Geophys. Res., 117, D18202, https://doi.org/10.1029/2012JD017493, 2012.
111. Nyeki, S., C. H. Halios, W. Baum, et al.: Ground-based aerosol optical depth trends at three high-altitude sites in Switzerland and southern Germany from 1995 to 2010, J. Geophys. Res., 117, D18202, https://doi.org/10.1029/2012JD017493, 2015.
112. Pérez, C., Nickovic, S., Baldasano, et al.: A long Saharan dust event over the western Mediterranean: Lidar, Sun photometer observations, and regional dust modeling, J. Geophys. Res.-Atmos., 111, D15214, https://doi.org/10.1029/2005JD006579, 2006.
113. Pérez-Ramírez, D., Aceituno, J., Ruiz, B., Olmo, F. J., and Alados-Arboledas, L.:. Development and calibration of a star photometer to measure the aerosol optical depth: Smoke observations at a high mountain site, Atmos. Environ., 42, 2733–2738, https://doi.org/10.1016/j.atmosenv.2007.06.009, 2008a.
114. Pérez-Ramírez,, D., Ruiz, B., Aceituno, J., Olmo, F. J., and Alados-Arboledas, L.: Sun/star photometry to derive the aerosol optical depth, Int. J. Remote Sens., 29, 5113–5132, https://do.org/:10.1080/01431160802036425, 2008b.
115. Pérez-Ramírez,, D., Lyamani, H., Olmo, F. J., and Alados-Arboledas, L.: Improvements in star photometry for aerosol characterizations, J. Aerosol Sci., 42, 737–745, https://doi.org/10.1016/j.jaerosci.2011.06.010, 2011.
116. Pérez-Ramírez, D., Lyamani, H., Olmo, F. J., et al.: Cloud screening and quality control algorithm for star photometer data: assessment with lidar measurements and with all-sky images, Atmos. Meas. Tech., 5, 1585–1599, https://doi.org/10.5194/amt-5-1585-2012, 2012.
117. Persson, T.: Solar radiation climate in Sweden, Physics and chemistry of the Earth (B), Vol. 24, No. 3, pp 275-279. https://doi.org/10.1016/S1464-1909(98)00050-1, 1999.
118. Platt, S.M., Svendby, T., Hermansen, O., Lunder, C., Duflot, V., Schmidbauer, N., Stebel, K.: Monitoring of greenhouse gases and aerosols at Svalbard and Birkenes in 2024. Annual report (NILU report 22/2025), https://hdl.handle.net/11250/5330700, 2025.
119. Polar-AOD (2026). Website https://bo.isp.cnr.it/geonetwork/polaraod/eng/catalog.search#/home (accessed 21 October 2026).
120. Popovici, I. E., Goloub, P., Podvin, et al.: Description and applications of a mobile system performing on-road aerosol remote sensing and in situ measurements, Atmos. Meas. Tech., 11, 4671–4691, https://doi.org/10.5194/amt-11-4671-2018, 2018.

121. Popovici, I. E., Deng, Z., Goloub, P., et al.: Mobile On-Road Measurements of Aerosol Optical Properties during MOABAI Campaign in the North China Plain, Atmosphere, 13, 21, https://doi.org/10.3390/atmos13010021, 2022.
122. Prodi, F., and Tomasi, C.: Sahara dust program—I. The Italian network of sun-photometers. Extinction models based on multimodal particle size distributions. Journal of Aerosol Science, 14(4), 517–527. https://doi.org/10.1016/0021-8502(83)90008-3, 1983.
123. Pulimeno, S., Lupi, A., Vitale, V.,et al.: Recent advances in aerosol optical depth measurements in polar regions: insights from the Polar-AOD Program. Atmospheric Chemistry and Physics, 26(3), 1809-1846, https://doi.org/10.5194/acp-26-1809-2026, 2026
124. Pulimeno, Simone: Improving long-term aerosol observing capabilities in polar areas, PhD Thesis of the Università Ca'Foscari Venezia, https://iris.unive.it/bitstream/10278/5113409/2/PhD_thesis_compressed.pdf, 2026.
125. Quinn, P. K., Shaw, G., Andrews, E., et al.: Arctic haze: current trends and knowledge gaps. Tellus B, 59(1), 99-114, https://doi.org/10.1111/j.1600-0889.2006.00226.x, 2007.
126. Raes, F., Bates, T. S., McGovern, F., & Van Liedekerke, M.: The 2nd Aerosol Characterization Experiment (ACE-2): General overview and main results. Tellus B, 52(2), 111–125. https://doi.org/10.3402/tellusb.v52i2.16088, 2000.
127. Rodríguez, E., Toledano, C., Cachorro, V. E., et al.: Comparison of aerosol optical properties at the sub-arctic stations ALOMAR-Andenes, Abisko and Sodankylä in late spring and summer 2007. Atmospheric Research, 107, 20–30. DOI: 10.1016/j.atmosres.2011.12.003, 2012.
128. Rodríguez, E., C. Toledano, V. E. Cachorro, et al.: Aerosol characterization at the sub-Arctic site Andenes (69°N, 16°E), by the analysis of columnar optical properties, Quarterly J. Royal Meteorological Society, Q. J. R. Meteorol. Soc. 138: 471–482, https://doi.org/10.1002/qj.921, 2012b.
129. Román, R., Torres, B., Fuertes, D., et al.: Remote sensing of lunar aureole with a sky camera: Adding information in the nocturnal retrieval of aerosol properties with GRASP code, Remote Sens. Environ., 196, 238–252, https://doi.org/10.1016/j.rse.2017.05.013, 2017.
130. Román, R., Benavent-Oltra J.A., Casquero-Vera, J.A. et al. Retrieval of aerosol profiles combining sunphotometer and ceilometer measurements in GRASP code, Atmospheric Research, Vol. 204, ISSN 0169-8095, https://doi.org/10.1016/j.atmosres.2018.01.021., 2018
131. Román, R., González, R., Toledano, C., et al.: Correction of a lunar-irradiance model for aerosol optical depth retrieval and comparison with a star photometer, Atmos. Meas. Tech., 13, 6293–6310, https://doi.org/10.5194/amt-13-6293-2020, 2020.
132. Román, R., González-Fernández, D., and Antuña-Sánchez, J. C.: CNN-CC model (Convolutional Neural Network for Cloud Cover) [Software]. https://doi.org/10.5281/ZENODO.10817550, 2024
133. Román, R., González-Fernández, D., Antuña-Sánchez, J. C., et al.: Star photometry with all-sky cameras to retrieve aerosol optical depth at nighttime, Atmos. Meas. Tech., 18, 2847–2875, https://doi.org/10.5194/amt-18-2847-2025, 2025.

134. Ruyneau de Saint-George, P., Boichu, M., et al.: Record growth of stratospheric aerosols from 2019 Raikoke eruption with sulfate-coating of submicronic ash. Scientific Reports. https://www.nature.com/articles/s41598-026-52949-y.pdf, 2026.
135. Sanchez Barrero, M. F., Popovici, I. E., Goloub, P., et al.: Enhancing mobile aerosol monitoring with CE376 dual-wavelength depolarization lidar, Atmos. Meas. Tech., 17, 3121–3146, https://doi.org/10.5194/amt-17-3121-2024, 2024.
136. Sanchez-Barrero, M. F., Goloub, P., Blarel, L., et al.: Aerosol variability over oceans using micro-pulse lidar and photometer: insights from TRANSAMA ship-based campaign, Atmos. Meas. Tech., 19, 507–528, https://doi.org/10.5194/amt-19-507-2026, 2026a.
137. Sanchez-Barrero, M. F., Torres, B., Blarel, L., et al.: Automatic Ship-Based Photometers for Enhanced Aerosol Characterization Over the Open Ocean: Towards a Global Network, EGU General Assembly 2026, Vienna, Austria, 3–8 May 2026, EGU26-20297, https://doi.org/10.5194/egusphere-egu26-20297, 2026b.
138. Schafer, J., Eck, T. F., Slutsker, I., Gupta, P., Sorokin, M., Sinyuk, A., and Smirnov, A.: An assessment of lunar photometry in AERONET, Atmos. Meas. Tech., 19, 6487–6502, https://doi.org/10.5194/amt-19-6487-2026, 2026.
139. Schmale, J., Zieger, P. & Ekman, A.M.L. Aerosols in current and future Arctic climate. Nat. Clim. Chang. 11, 95–105. https://doi.org/10.1038/s41558-020-00969-5, 2021.
140. Schmale, J., Sharma, S., Decesari, S., Pernov, J., et al.: Pan-Arctic seasonal cycles and long-term trends of aerosol properties from 10 observatories, Atmos. Chem. Phys., 22, 3067–3096, https://doi.org/10.5194/acp-22-3067-2022, 2022.
141. Schmid, B. and Wehrli, C.: Comparison of sun photometer calibration by use of the Langley technique and the standard lamp, Applied Optics, Vol. 34, No. 21, pp. 4500-4512. https://doi.org/10.1364/AO.34.004500, 1995.
142. Shaw, G. E., Reagan, J. A., & Herman, B. M.: Investigations of atmospheric extinction using direct solar radiation measurements made with a multiple wavelength radiometer. Journal of Applied Meteorology and Climatology, 12(2), 374-380. https://doi.org/10.1175/1520-0450(1973)012<0374:IOAEUD>2.0.CO;2, 1973.
143. Shaw, G. E., Sun photometry. Bull. Am. Meteorol. Soc. 64:4–11., https://doi.org/10.1175/1520-0477(1983)064<0004:SP>2.0.CO;2 , 1983.
144. Shaw, G. E.: The Arctic haze phenomenon. Bulletin of the American Meteorological Society, 76(12), 2403-2414, https://doi.org/10.1175/1520-0477(1995)076<2403:TAHP>2.0.CO;2, 1995.
145. Shaw, G.E.: Genesis of sun photometry. J. Appl. Remote Sens. 1 (1), 1–13. https://doi.org/10.1117/1.2712483, 2007.
146. Stock, M., C. Ritter, V. Aaltonen, W. Aas, D. Handorff, A. Herber, R. Treffeisen and K. Dethloff. Where does the optically detectable aerosol in the European Arctic come from? Tellus B 2014, 66, 21450, http://dx.doi.org/10.3402/tellusb.v66.21450, 2014.
147. Stohl, A. Characteristics of atmospheric transport into the Arctic troposphere. Journal of Geophysical Research: Atmospheres, 111(D11), https://doi.org/10.1111/j.1600-0889.2006.00226.x, 2006.

148. Stone, R. S., et al.: A three-dimensional characterization of Arctic aerosols from airborne Sun photometer observations: PAM-ARCMIP, April 2009. Journal of Geophysical Research: Atmospheres, 115, D13203. https://doi.org/10.1029/2009JD013605, 2010.
149. Tanré, D., Devaux, C., Herman, M., Santer, R., and Gac, J. Y.: Radiative properties of desert aerosols by optical ground-based measurements at solar wavelengths. Journal of Geophysical Research, 93, 14223–14231. https://doi.org/10.1029/JD093iD11p14223, 1988.
150. Tanré, D., Bréon, F. M., Deuzé, J. L., et al.: Remote sensing of aerosols by using polarized, directional and spectral measurements within the A-Train: the PARASOL mission, Atmos. Meas. Tech., 4, 1383–1395, https://doi.org/10.5194/amt-4-1383-2011, 2011.
151. Takamura, T., T. Nakajima, and and SKYNET community group: Overview of SKYNET and its activities. Opt. Pura Apl., 37, 3303–3308, 2004.
152. Titos, G., Ealo, M., Román, R., Cazorla, A., et al.: Retrieval of aerosol properties from ceilometer and photometer measurements: long-term evaluation with in situ data and statistical analysis at Montsec (southern Pyrenees), Atmos. Meas. Tech., 12, 3255–3267, https://doi.org/10.5194/amt-12-3255-2019, 2019.
153. Toledano, C., Cachorro, V. E., Berjón, A., Sorribas, M., Vergaz, R., de Frutos, A., Antón, M., & Gausa, M.: Aerosol optical depth at ALOMAR Observatory (Andøya, Norway) in summer 2002 and 2003. Tellus B, 58(3), 218–228. DOI: 10.1111/j.1600-0889-2006.00184, https://ui.adsabs.harvard.edu/scan/manifest/2006TellB..58..218T, 2006.
154. Toledano, C., Cachorro, A. Berjón, A., et al.: RIMA-AERONET network: long term monitoring of aerosol properties. Opt. Pura Apl, 44, 629-633, https://sedoptica.es/Menu_Volumenes/Pdfs/OPA44-4-629.pdf, 2011.
155. Toledano, C., Cachorro, V., Gausa, M., et al.: Overview of sun photometer measurements of aerosol properties in Scandinavia and Svalbard. Atmospheric Environment, 52:18–28.,https://doi.org/10.1016/j.atmosenv.2011.10.022, 2012.
156. Toledano, C., González, R., Fuertes, D., et al.: Assessment of Sun photometer Langley calibration at the high-elevation sites Mauna Loa and Izaña, Atmos. Chem. Phys., 18, 14555–14567, https://doi.org/10.5194/acp-18-14555-2018, 2018.
157. Toledano, C., González, Mateos, D., et al.: Sun photometers - Chapter 7 of book: Field Measurements for Passive Environmental Remote Sensing, Elsevier (2023), Pages 121-138,ISBN 9780128239537, https://doi.org/10.1016/B978-0-12-823953-7.00005-8., 2023.
158. Toledano, C., Taylor, S., Barreto, Á., et al.: LIME: Lunar Irradiance Model of ESA, a new tool for absolute radiometric calibration using the Moon, Atmos. Chem. Phys., 24, 3649–3671, https://doi.org/10.5194/acp-24-3649-2024, 2024.
159. Tomasi, C.: Features of the scale height for particulate extinction in hazy atmospheres. Journal of Applied Meteorology, 21(7), 931–944. https://doi.org/10.1175/1520-0450(1982)021%3C0931:FOTSHF%3E2.0.CO;2, 1982.
160. Tomasi, C., & Prodi, F.: Measurements of atmospheric turbidity and vertical mass loading of particulate matter in the Po Valley area. Journal of Applied Meteorology and Climatology, 21 (11), 1589–1597, https://sci-hub.ru/10.1029/jc087ic02p01279, 1982.

161. Tomasi, C., Guzzi, R., & Vitale, V.: Sun photometric measurements of atmospheric aerosol optical depth at thermal infrared wavelengths. Applied Optics, 22 (23), 3769–3770, 1983.
162. Tomasi, C., Prodi, F., Sentimenti, M., & Cesari, G.: Multiwavelength sun-photometers for accurate measurements of atmospheric extinction in the visible and near-IR spectral range. Applied Optics, 22(4), 622–630. https://doi.org/10.1364/AO.22.000622, 1983.
163. Tomasi, C., Marani, S., Vitale, V., Wagner, F., Cacciari, A., & Lupi, A.: Precipitable water evaluations from infrared sun-photometric measurements analyzed using the atmospheric hygrometry technique. Tellus B, 52(2), 734–749. https://doi.org/10.1034/j.1600-0889.2000.00032.x, 2000.
164. Tomasi, C., Vitale, V., Lupi, A. et al. (2007), Aerosols in polar regions: A historical overview based on optical depth and in situ observations, J. Geophys. Res., 112, D16205, doi:10.1029/2007JD008432, https://agupubs.onlinelibrary.wiley.com/doi/pdf/10.1029/2007JD008432, 2007.
165. Tomasi, C., Petkov, B., Stone, R. S., et al.: Characterizing polar atmospheres and their effect on Rayleigh-scattering optical depth. Journal of Geophysical Research, 115, D02205. https://doi.org/10.1029/2009JD012852, 2010.
166. Tomasi, C., Lupi, A., Mazzola, et al.: An update on polar aerosol optical properties using POLAR-AOD and other measurements performed during the International Polar Year. Atmospheric Environment, 52:29–47. https://doi.org/10.1016/j.atmosenv.2012.02.055, 2012.
167. Tomasi, C., Kokhanovsky, A. A., Lupi, A., et al.: Aerosol remote sensing in polar regions. Earth-Science Reviews, 140:108–157, https://doi.org/10.1016/j.earscirev.2014.11.001, 2015a.
168. Tomasi, C., et al.: Seasonal variations of the relative optical air mass function for background aerosol and thin cirrus clouds at Arctic and Antarctic sites. Remote Sensing, 7, 7157–7180. https://doi.org/10.3390/rs70607157, 2015b.
169. Torres, B., Dubovik, O., Fuertes, D., et al.: Advanced characterisation of aerosol size properties from measurements of spectral optical depth using the GRASP algorithm, Atmos. Meas. Tech., 10, 3743–3781, https://doi.org/10.5194/amt-10-3743-2017, 2017.
170. Torres, B., Blarel, L., Goloub, P., et al.: Adaptation of the CIMEL-318T to shipborne use: 3 years of automated AERONET-compatible aerosol measurements on board the research vessel Marion Dufresne, Atmos. Meas. Tech., 18, 4809–4838, https://doi.org/10.5194/amt-18-4809-2025, 2025.
171. Tunved, P., Ström, J., & Krejci, R.: Arctic aerosol life cycle: linking aerosol size distributions observed between 2000 and 2010 with air mass transport and precipitation at Zeppelin station, Ny-Ålesund, Svalbard. Atmospheric Chemistry and Physics, 13(7), 3643-3660, https://doi.org/10.5194/acp-13-3643-2013, 2013.
172. Uchiyama, A., Shiobara, M., Kobayashi, H., et al.: Nocturnal aerosol optical depth measurements with modified sky radiometer POM-02 using the moon as a light source, Atmos. Meas. Tech., 12, 6465–6488, https://doi.org/10.5194/amt-12-6465-2019, 2019.

173. Vermeulen, A., Devaux, C., and Herman, M.: Retrieval of the scattering and microphysical properties of aerosols from ground-based optical measurements including polarization. I. Method. Applied Optics, 39, 6207–6220. https://doi.org/10.1364/AO.39.006207, 2000.
174. Vitale, V., & Tomasi, C.: Atmospheric turbidity measurements at Terra Nova Bay with a multiwavelength sunphotometer. Nuovo Cimento C, 13 (2), 463–474, https://iris.cnr.it/handle/20.500.14243/220526, 1990.
175. Vitale, V., Tomasi, C., Lupi, A., Cacciari, A., & Marani, S.: Retrieval of columnar aerosol size distributions and radiative-forcing evaluations from sun-photometric measurements taken during the CLEARCOLUMN (ACE 2) experiment. Atmospheric Environment, 34(29–30), 5095–5105. https://doi.org/10.1016/S1352-2310(00)00269-7, 2000a.
176. Vitale, V., Tomasi, C., von Hoyningen-Huene, W., et al.: Spectral measurements of aerosol particle extinction in the 0.4–3.7 μm wavelength range, performed at Sagres with the IR-RAD sun-radiometer. Tellus B, 52(2), 716–733. https://doi.org/10.1034/j.1600-0889.2000.00028.x, 2000b.
177. Wagner, J., Ubele, A. A., Schenzinger, V., and Kreuter, A.: Extended aerosol optical depth (AOD) time series analysis in an Alpine valley: a comparative study from 2007 to 2023, Aerosol Research, 2, 153–159, https://doi.org/10.5194/ar-2-153-2024, 2024.
178. Wagner, F., Mattis, I., and W. Thomas: Sonnenphotometrie auf dem Hohen Peißenberg, GAW BRIEF DES DWD (GAW Letter of Deutscher Wetterdienst), Nr. 87, https://www.dwd.de/DE/forschung/atmosphaerenbeob/zusammensetzung_atmosphaere/hohenpeissenberg/download/gaw_briefe/gaw_brief_087_de_pdf.pdf?__blob=publicationFile&v=2, 2026.
179. Warneke, C., Schwarz, J. P., Dibb, J., et al.: The FIREX-AQ Science Team: Fire Influence on Regional to Global Environments and Air Quality (FIREX-AQ), J. Geophys. Res.-Atmos., 128, https://doi.org/10.1029/2022JD037758, 2023.
180. Wehrli, Ch.: Calibrations of filter radiometers for determination of atmospheric optical depth, Metrologia, 37 419-422. https://doi.org/10.1088/0026-1394/37/5/16, 2000
181. Wehrli, C.: Aufbau eines neuen Messnetzes für Aerosol Optische Dicke, GAW BRIEF DES DWD (GAW Letter of Deutscher Wetterdienst), Nr. 9, https://www.dwd.de/DE/forschung/atmosphaerenbeob/zusammensetzung_atmosphaere/hohenpeissenberg/download/gaw_briefe/gaw_brief_009_de_pdf.pdf?__blob=publicationFile&v=2, 2002.
182. Wehrli, C.: GAWPFR: A network of aerosol optical depth observations with precision filter radiometers, GLOBAL ATMOSPHERE WATCH, p. 36, 2005.
183. Wehrli, C.: Remote Sensing of Aerosol Optical Depth in a global surface network, PhD Thesis of the ETH Zürich, https://doi.org/https://doi.org/10.3929/ethz-a-005659798, 2008.
184. Wehrli, C.: Precision Filter Radiometer Documentation (PFR Manual V4.1), PMOD/WRC, 2009

185. Weller, M., Plessing, P., Rentsch, H., et al.: Regional differences of column-related aerosol parameters in Germany, Atmospheric Environment, Volume 34, Issues 29–30, https://doi.org/10.1016/S1352-2310(00)00351-4., 2000
186. Weller, M., and Gericke, K.. Long-term observations of aerosol optical depths at the Meteorological Observatory Lindenberg. Meteorologische Zeitschrift, 14(5), 651-662. DOI: 10.1127/0941-2948/2005/0070,https://www.schweizerbart.de/content/papers/download/54350, 2005.
187. Wiegner, M., Madonna, F., Binietoglou, I., et al.: What is the benefit of ceilometers for aerosol remote sensing? An answer from EARLINET, Atmos. Meas. Tech., 7, 1979–1997, https://doi.org/10.5194/amt-7-1979-2014, 2014.
188. WMO: Recent Progress in Sunphotometry, Determination of the aerosol optical depth, Environmental Pollution Monitoring and Research Programme, No. 43, 21 pp., https://library.wmo.int/idurl/4/40934, 1986.
189. WMO/GAW: report No. 101, Report of the WMO workshop on the measurement of atmospheric optical depth and turbidity, (WMO TD No. 659), Chapter 4: Working Group Discussions – Sunphotometry, 4–5, 1993.
190. World Meteorological Organization: Report of the WMO Workshop on the Measurement of Atmospheric Optical Depth and Turbidity, Silver Spring, USA, 6–10 December 1993, Global Atmospheric Watch Technical Note No. 101, WMO TD No. 659, https://library.wmo.int/idurl/4/41034, 1994
191. WMO: Aerosol measurement procedures, guidelines and recommendations, GAW Report No. 153, WMO TD No. 1178, avaible at: https://library.wmo.int/pmb_ged/wmo-td_1178.pdf , 2003.
192. WMO: WMO/GAW Experts Workshop on a Global Surface-Based Network for Long Term Observations of Column Aerosol Optical Properties, GAW Report No. 162, WMO TD No. 1287, available at: https://library.wmo.int/pmb_ged/wmo-td_1287.pdf (last access: 1 September 2018), 2005.
193. WMO: Abridged final report with resolutions and recommendations, GAW Report WMO TD No. 1019, WMO-CIMO Fourteenth session Geneva 7–14 December 2006, 2007.
194. WMO: Commission for Instruments and Methods of Observation, Sixteenth session WMO no.1138, Saint Petersburg, Secretariat of the World Meteorological Organization, https://library.wmo.int/idurl/4/53076, 2014.
195. WMO/GAW: report No. 227, WMO/GAW Aerosol Measurement Procedures, Guidelines and Recommendations, 2nd Edn., WMO- No. 1177, ISBN 978-92-63-11177-7, (WMO/TD- No. 1177), ISBN 978-92-63-11177-7, Chapter 7: Aerosol Optical Depth 60–67, 2016.
196. Wuttke, S., Kreuter, A., and Blumthaler, M.: Aerosol climatology in an Alpine valley, J. Geophys. Res., 117, D20202, https://doi.org/10.1029/2012JD017854, 2012.
197. Zhang, Z., Zhou, L., & Zhang, M.: A progress review of black carbon deposition on Arctic snow and ice and its impact on climate change. Adv. Polar Sci, 35(2), 178-191. doi: 10.12429/j.advps.2023.0024, 2024.

Table of acronyms

3MI	Multi-Viewing, Multi-Channel, Multi-Polarisation Imager (instrument)
ABAS	*Automatisches Boden-Atmosphäre Spektralfotometer* (Automatic Earth - Atmosphere Spectrophotometer)
ACE	Aerosol Characterization Experiment
ACTRIS	Aerosol, Clouds and Trace Gases Research Infrastructure
AE	Ångström Exponents (α, β): characterize AOD spectral variation
AEMET	*Agencia Estatal de Meteorología* (Spain meteorological service)
AERONET	AErosol RObotic NETwork: AOD and aerosol properties measurements network using CIMEL CE-318 photometer
AGORA	Aerosol and Gas Optical Remote Analysis Laboratory
ALC	Automatic Lidars and Ceilometers
ALICENET	Automated LIdar-CEilometer NETwork
ALOMAR	Arctic Lidar Observatory for Middle Atmosphere Research, Andenes, Andøya island,Vesterålen archipelago, Norway
AOD	Aerosol Optical Depth (also known as AOT: Aerosol Optical Thickness): Main parameter used to characterise aerosol amount and aerosol impact on radiation in the atmosphere. AOD is also the main parameter measured with photometers.
APRS	Asian-Pacific Radiation Symposium
AR	Assessment Report (referred to IPCC)
ARE_{SW}	Aerosol Radiative Effect on Shortwave solar radiation
ARPA-VDA	*Agenzia regionale per la protezione ambientale -Valle d'Aosta* (Regional Environmental Protection Agency - Aosta Valley), Saint-Christophe (Aosta), Italy
ASI	All-Sky Imager
AWI	*Alfred-Wegener-Institut* (German Polar Institute)
AWIPEV	AWI and IPEV joint station at Ny-Ålesund, Spitsbergen (Svalbard)
BAPMoN	Background Air Pollution Monitoring Network
BAQUNIN	Boundary-layer Air Quality analysis Using Network of Instruments
BAS	*Boden-Atmosphäre Spektralfotometer* (Earth - Atmosphere Spectrophotometer)
BC	Black Carbon
BCPS	Background-Corrected Pixel Signal
BfS	*Bundesamt für Strahlenschutz,* Federal Office for Radiation Protection
BSRN	Baseline Surface Radiation Network
BTS	*BiTec Sensor Spektralradiometer*: Array spectroradiometer manufactured by GHO

C3SAR	Cloud 3D Structure And Radiation campaign at Lindenberg
CAECENET	Photometer–ceilometer network, based on CÆLIS-ICENET
CALINET	CALItoo-NETwork
CARS	Center of Aerosol Remote Sensing, related to ACTRIS
CAS	Czech Academy of Sciences, Prague, Czech Republic
CCD	Charge-Coupled Device
CF	Central Facility
ChArMEx/ADRIMED	Chemistry-Aerosol Mediterranean Experiment / Aerosol Direct Radiative Impact on the regional climate in the MEDiterranean region
CIMO	Commission for Instruments and Methods of Observation (WMO)
CMOS	Complementary Metal-Oxide-Semiconductor
CNES	*Centre National d'Études Spatiales*
CNR	*Consiglio Nazionale delle Ricerche* (Italian national research council)
COBALD	Compact Optical Backscatter Aerosol Detector
COST	European COoperation in Science and Technology: funding organisation for research and innovation networks.
CREGARS	Centre for REactive trace GAses Remote Sensing
CSEM	*Centre Suisse d'Electronique et de Microtechnique,* Swiss centre of electronics and microtechnique
CTAO	Cherenkov Telescope Array Observatory
DHI	Diffuse Horizontal Irradiance
DNI	Direct Normal Irradiance
DWD	*Deutscher Wetterdienst* (German meteorological service)
E-PROFILE	EUMETNET profiling network
EBAS	European dataBASe hosting observation data of atmospheric chemical composition and physical properties, developed and operated by the Norwegian Institute for Air Research (NILU).
ECoE	ERATOSTHENES Centre of Excellence, Limassol, Cyprus
EMEP	European Monitoring and Evaluation Programme
EMPIR	European Metrology Programme for Innovation And Research
ERA5	ECMWF Reanalysis v5
ESA	European Space Agency
ESR	European SKYNET radiometers network
EU	European Union
EUMETNET	Network of European Meteorological Services
EUMETSAT	European Organisation for the Exploitation of Meteorological Satellites
EURAMET	EURopean Association of national METrology institutes

EXCALIBUR	EXtinction CAmera and LumInance BackgroUnd Register, Astronomica S.L. (Starphotometer of University of Granada, Spain)
FD	Fluorescence detector
FISBAT-CNR	Institute for the Study of Microphysics and Radiation of the Lower and Upper Atmosphere, former CNR institution, Bologna, Italy
FMI	Finnish Meteorological Institute
FoV	Field of View
FRAM	F/Photometric Robotic Atmospheric Monitor
FRC	Filter Radiometer Campaign: WMO campaigns scheduled in Davos at PMOD/WRC, every five years
FRC-IV	Fourth WMO Filter Radiometer Campaign: WMO campaign organised in Davos at PMOD/WRC, September/October 2015
FU	*Freie Universität,* Berlin, Germany
FUB	*Freie Universität Berlin,* Berlin, Berlin, Germany
FWHM	Full Widths at Half Maximum
FZU	*Fyzikální ústav Akademie věd České republiky:* Institute of Physics of the Czech Academy of Sciences, Prague
GARRLiC	Generalized Aerosol Retrieval from Radiometer and Lidar Combined data
GAW	Global Atmosphere Watch: WMO Programme of trends monitoring of the atmosphere
GAW-PFR	Global Atmosphere Watch - Precision Filter Radiometer network: AOD measurement network of WMO/GAW Programm
GFAT-UGR	*Grupo de investigación de Física de la ATmósfera - Universidad de GRanada*: Group of of Atmospheric Physics of the University of Granada
GHI	Global Horizontal Irradiance
GHO	*Gigahertz-Optik*, instrument manufacturer based in Türkenfeld, Germany
GLI	GLobal Imager (JAXA mission)
GOA (GOA-UVa)	*Grupo de Óptica Atmosférica - Universidad de Valladolid* (Group of Atmospheric Optics)), Valladolid, Spain
GOA-SCAN	All-sky camera network of GOA
GRASP	Generalised Retrieval of Atmosphere and Surface Properties: Company based in Lille, France
GRASPpac	GRASP photometer and ceilometer
GSFC	NASA Goddard Space Flight Center, Greenbelt (Maryland)
HARMONIA	International network for harmonisation of atmospheric aerosol retrievals from ground based photometers: Name of the COST action
HYSPLIT	Hybrid Single-Particle Lagrangian Integrated Trajectory model
IAO (IAO-MUI)	Innsbruck Atmospheric Observatory, belongs MUI university, Innsbruck, Austria
IARC	Izaña Atmospheric Research Center: AEMET observatory at Izaña (Tenerife)

ICENET	Iberian CEilometer NETwor
IFS-CAMS	Integrated Forecasting System - Copernicus Atmosphere Monitoring Service
IGAC	International Global Atmospheric Chemistry program
IGY	International Geophysical Year
IISTA-CEAMA	*Instituto Interuniversitario de Investigación del Sistema Tierra en Andalucía - CEntro Andaluz de Medio Ambiente*: Andalusian Institute for Earth System Research
INOE	*Institutul Național de Cercetare-Dezvoltare pentru Optoelectronică* (National Institute of Research and Development for Optoelectronics), Măgurele (Bucaresti), Romania
INSU	*Institut National des Sciences de l'Univers*
IPCC	Intergovernmental Panel on Climate Change
IPEV	*Institut Paul Émile Victor* (French Polar Institute)
IPY	International Polar Year (2007-2008)
IR	Infrared
ISAC (ISAC-CNR)	*Istituto di Scienze dell'Atmosfera e del Clima*, CNR (Institute of Atmospheric Sciences and Climate), Rome, Italy
ISAO-CNR	Institute for Atmospheric and Oceanic Sciences,. Former CNR institution, Bologna, Italy
ISDC	International SKYNET Data Center
ISP (ISP-CNR)	*Istituto di Scienze Polari*, CNR (Institute of polar science), Bologna, Italy
JAXA	Japan Aerospace eXploration Agency
KAUST	King Abdullah University of Science and Technology
KIT	*Karlsruhe Institute of Technology*, Karlsruhe and Garmisch-Patenkirchen, Germany
LBHI	Landbúnaðarháskóli Íslands (Agricultural University of Iceland), Hvanneyri, Iceland
LIDAR	LIght Detection And Ranging
LIME	Lunar Irradiance Model of ESA
LIRIC	LIdar-Radiometer Inversion Code
LISA	*Laboratoire Interuniversitaire des Systèmes Atmosphériques*
LOA	*Laboratoire d'Optique Atmosphérique* (Laboratory of Atmospheric Optics), Université de Lille-I, Villeneuve d'Ascq (Lille), France
LST	Large-size Telescope
LuftBlick	Internationally operating science and engineering company founded in 2012 that is located in Innsbruck, Austria.
MAMS	Mobile Aerosol Monitoring System
MAP-IO	Marion Dufresne Atmospheric Program – Indian Ocean
MAPP	Metrology of Aerosol Optical Properties: EURAMET/EMPIR project campaign at Izaña (Tenerife, Spain), September 2022
MD-GDR	*Meteorologischer Dienst* of German Democratic Republic

MFR-SR	Multi-Filter Rotating Shadowband Radiometer
MOHP	*Meteorologisches Observatorium Hohenberg, Deutscher Wetterdienst* (DWD observatory of Hohenpeißenberg), Hohenpeißenberg, Germany
MOL-RAO	*Meteorologisches Observatorium Lindenberg - Richard Aßmann Observatorium, Deutscher Wetterdienst* (DWD observatory of Lindenberg), Lindenberg (Tauche), Germany
MPL	Micro-Pulse Lidar
MPLNET	Micro-Pulse Lidar Network
MS	Motor Ship
MUI	Medical University of Innsbruck, Innsbruck, Austria
NASA	National Aeronautics and Space Administration (USA space administration)
NF	National Facility
NIER	National Institute of Environmental Research (Korea)
NILU	*Norsk institutt for luftforskning,* Norwegian Institute for Air Research (Norway meteorological service)
NIPR	国立極地研究所 (National Institute of Polar Research), Tokyo, Japan
NKUA	National and Kapodistrian University of Athens, Athens, Greece
NOA	National Observatory of Athens, Athens Greece
NOAA	US National Oceanic and Atmospheric Administration
OHP	*Observatoire de Haute-Provence,* Haute-Provence Observatory
ORION	All-sky camera calibration tool
OSM	One Star Method for stellar photometry with *Schulz und Partner* starphotometer
PAM-ARCMIP	Polar Airborne Measurements-Arctic Regional Climate Model sImulation Project
PARASOL	Polarization and Anisotropy of Reflectances for Atmospheric Science coupled with Observations from a Lidar (mission)
PEARL	Polar Environment Atmospheric Research Laboratory, Eureka (Nunavut), Canada
PFR	Precision FilterRadiometer: Photometer manufactured by PMOD/WRC
PGN	Pandonia Global Network
PHOTONS	PHOtométrie pour le Traitement Opérationnel de Normalisation Satellitaire
PM	Particle Matter; Example: PM10 are particles having a diameter below 10 μm
PML	Plymouth Marine Laboratory
PMOD/WRC	*Physikalisch-Meteorologisches Observatorium* Davos /and World Radiation Center
PNRA	*Programma Nazionale di Ricerche in Antartide,* National Antarctic Research Programme (Italy)
POLDER	POLarization and Directionality of the Earth's Reflectances instrument
POM	Precise design Of Meteorological and scientific instrument: Photometer manufactured by Prede and used in the network SKYNET. Originally: Prede “Oreole” Meter (Prede Aureole Meter)
PSC	Polar Stratospheric Clouds

PSR	Precision Spectroradiometer
RCAPC	Research Centre for Atmospheric Physics and Climatology (Academy of Athens), Athens, Greece
RCF	RIMO Correction Factor
RCS	Range-Corrected Signal
RGB	Red-Green-Blue
RIMA	*Red Ibérica de Medida Fotométrica de Aerosoles*, Iberian Aerosol Photometric Measurement Network
RIMO	ROLO Implementation for Moon photometry Observation: open lunar reflectance model developed by GOA-UVa and AEMET/IARC
RMSE	Root Mean Square Error
ROBAS	Robotic - BAS spectrophotometer
ROLO	Robotic Lunar Observatory: lunar reflectance model of USGS
RSDC	Regional SKYNET Data Center
RV	Research Vessel
SCILLA	Summer Campaign for Intercomparison of Lunar measurements of Lindenberg's Aerosol: Campaign at DWD/MOL-RAO in Lindenberg (Tauche, Germany), August/September 2020
SEM	Star Extraterrestrial Magnitude (a specificity of star photometry TSM method)
SEMI	Star Extraterrestrial Magnitude Instrumental (a specificity of star photometry TSM method)
SHMI	Slovak Hydrometeorological Institute, Gánovce (observatory), Slovakia
SIOS	Svalbard Integrated Arctic Earth Observing System
SKYNET	SKY Measurements NETwork: AOD and aerosol properties measurements network using Prede-POM instrument
SLOPE	Sierra Nevada Lidar aerOsol Profiling Experiment
SMHI	Swedish Meteorological and Hydrological Institute
SMN	*Servicio Meteorológico Nacional*: Argentinian Weather Service
SNS	*Sierra Nevada Station*
SONET	Sun-sky radiometer Observation NETwork (China)
SORBETTO	Solar radiation based established techniques for atmospheric observations, schools organised by ISAC-CNR Rome about photometry.
SPST	Schulz und Partner Sternphotometer: starphotometer developed by the company *Dr Schulz und Partner GmbH*, Germany
SSA	Single-Scattering Albedo
STSM	Short Term Scientific Mission: Grant possibility of a COST Action (including a visit to another institute)
TOD	Total Optical Depth
TRANSAMA	Transit to AMARYLLIS-AMAGAS: ship campaign carried out by the vessel Marion Dufresne

	II
TSM	Two Star Method for stellar photometry with *Schulz und Partner* starphotometer
UBA	*Umweltbundesamt,* German Environment Agency
UNEP	United Nations Environment Programme
USGS	United States Geological Survey, Flagstaff (AZ), USA
USI	Uncalibrated Star Irradiance
UT/UTC	Universal Time / Coordinated Universal Time
UV	Ultraviolet
UVa	*Universidad de Valladolid* (University of Valladolid), Valladolid, Spain
UVEG	*Universitat de València Estudi General* (University of Valencia), Burjassot (Valencia), Spain
VC	Volume Concentration
VM	Virtual Mobility: grant possibility of a COST action.
WG	Working Group
WMO	World Meteorological Organisation
WORCC	World Optical Depth Research Calibration Center
Zu-Zi Trasse	Zugspitze - Zingst Trail (DWD network of AOD and radiation measurements)

Acknowledgements

We would like to thank all our current colleagues and predecessors across the institutions, companies, laboratories and universities who have brought our stations, our three major measurement networks and their instruments to where they are today—and made it possible for us to build on their achievements.
Of course, we would also like to thank the entire HARMONIA community and all its members for their hard work, wonderful energy and good humour.
Finally, a very special thank-you to Stelios Kazadzis for your boundless commitment as Chair (the COST Action's lead) and for making everything we had hoped for possible.

As lead author, I (Lionel Doppler) would especially like to thank my colleagues Roberto Roman (University of Valladolid) and Monica Campanelli (ISAC-CNR, Rome) for sharing the initiative that began on a rainy day in October 2018 in Lindenberg: "What if we launched a COST Action on photometers?" My thanks also go to Stelios Kazadzis (PMOD/WRC, Davos), who joined us and championed the proposal with such dedication, experience and insight.
Thank you all for your hard work and courage. Our efforts paid off: we were able to share this unique experience and enjoy so many successful moments over the past four years.
And I'll leave my final word to you Stelios as a great COST action leader, in the caption below our photo:



Σε ευχαριστώ, Στέλιο! … Pour ta patience, ta générosité, ta gentillesse… Et pour ton amitié !